Utah State University
DigitalCommons@USU

All Graduate Theses and Dissertations | Graduate Studies

5-1985

Chemical Weathering of Pyrite in Soils

Aaron D. Brown
Utah State University

Follow this and additional works at: https://digitalcommons.usu.edu/etd

Part of the Soil Science Commons

Recommended Citation

Brown, Aaron D., "Chemical Weathering of Pyrite in Soils" (1985). *All Graduate Theses and Dissertations*. 4345.
https://digitalcommons.usu.edu/etd/4345

This Dissertation is brought to you for free and open access by the Graduate Studies at DigitalCommons@USU. It has been accepted for inclusion in All Graduate Theses and Dissertations by an authorized administrator of DigitalCommons@USU. For more information, please contact digitalcommons@usu.edu.

CHEMICAL WEATHERING OF PYRITE IN SOILS

By

Aaron D. Brown

A dissertation submitted in partial fulfillment
of the requirements for the degree
of
DOCTOR OF PHILOSOPHY
in
Soil Science and Biometeorology
with emphasis in
Soil Chemistry

Approved:

UTAH STATE UNIVERSITY
Logan, Utah

1985

PREFACE

> In training a child to the activity of thought, above all things we must beware of what I will call "inert ideas"--that is to say, ideas that are merely received into the mind without being utilized, or tested, or thrown into fresh combinations.
>
> In the history of education, the most striking phenomenon is that schools of learning, which at one epoc are alive with a ferment of genius, in a succeeding generation exhibit merely pedantry and routine. The reason is, that they are overladen with inert ideas. Education with inert ideas is not only useless: it is, above all things, harmful--*Corruptio optimi, pessima*.
>
> Alfred North Whitehead (1967, p. 1-2)

Much has been written on the nature and properties of the mineral pyrite. It would seem that little more remains to be described, qualitatively or quantitatively. However, as Whitehead implies, one of the most satisfying aspects of the applied sciences is the opportunity to use the wealth of ideas available from various other fields in new ways. There were several problems in the field of soil science which served to motivate my choice of pyrite oxidation as a topic for study.

Oxidation and reduction processes in soils are very complex and, thus, difficult to study. It could be argued, however, that in some cases they are the most important processes in the maintenance of soil fertility. Consider,

for example, that the majority of the world's population prefers paddy rice as the dietary staple. Rice generally requires continuous flooding for growth; conditions which lead to anaerobic, chemically reduced soils. In contrast, an important step in preparation of fields for replanting of rice is a dry, aerobic, chemically oxidizing fallow period of a few days or weeks. Perhaps the chemistry of pyrite oxidation can serve to illuminate the chemistry of this reduction-oxidation cycle found in soils.

The mineral composition of soil has long been used by agricultural chemists as an index of fertility. One of the many theoretical tools available for the analysis of mineral composition is chemical thermodynamics as applied to solutions at equilibrium with soils. This has been a sucessful approach in the case of minerals which simply dissolve, however, it has been difficult to analyze situations where minerals are oxidized or reduced. Lindsay (1979) has proposed a rather novel method of interpretation (pe+pH), for which pyrite oxidation may be a suitably well defined test case.

The oil crises of the 1970's forced the United States to reconsider the utility of its vast reserves of coal as an energy source. A large portion of this coal is located in shallow deposits in the intermountain region and pyritic or other acid-forming materials are found in association. In order to reclaim for perpetual use land which has been

mined, acid-forming materials must be identified and neutralized or otherwise specially treated. What is unique about this region is the presence of calcareous and sodic soils and overburden in the same areas, even the same strata, in which mining is taking place. These alkaline materials could, in principle, eliminate the need for special treatment practices in some cases. Unfortunately, the methods used for characterization of the acid and base contents of soil and overburden have been found to be inaccurate for this region. This study of the oxidation of pyrite under alkaline conditions may prove useful in the interpretation of the behavior of soil and overburden during reclamation.

Many people have inspired and guided me to this point. Niwat Hirunburana, Chavalit Chalothorn and Tadesse Kibreab of Chiang Mai University helped me see the opportunities in soil science. Frank Schnitzer and Dennis Fransway of the Wyoming Department of Environmental Quality provided hard questions and hard data on the significance of acid-forming materials in coal mining in this region. Fred Bender of AMAX Research and Development, Golden, Colorado, was a great help in providing references and a sample of pyrite. Willard Lindsay has been very generous in giving suggestions and consenting to review this manuscript at Colorado State University. I am grateful for the timely advice and assistance of Peter Kolesar of the Geology Department and Neal Langerman, formerly of the Department of Chemistry and

Biochemistry. I also acknowledge the the continuing guidance of the rest of my committee members and the special help of Lynn Dudley. I thank Mrs. Betty Smith for her eleventh hour help with the production of the printed product.

I owe many thanks to Jerry Jurinak, my major professor, for providing unconditional support and for confidence in my work. He has been a worthy example both as a professional and as a person.

I am indebted to my many friends in Logan, who gave me much joy, put up with me sometimes and celebrated with me when it was time. Al Stevenson and Catherine Sharpsteen were particularly important as the generous hosts of weekly gatherings. One of my fellow graduate students, Christopher Amrhein, made innumerable contributions, tangible and intangible to the development of this dissertation, including: the drawing on page 48, the construction of the pyrite electrodes and showing me how to cross-country ski. Thanks, Chris.

This work is dedicated to my parents. Thanks for being patient.

Aaron D. Brown

Aaron D. Brown
Riverside, California

TABLE OF CONTENTS

	Page
PREFACE	ii
LIST OF TABLES	ix
LIST OF FIGURES	xi
ABSTRACT	xiv
INTRODUCTION	1
LITERATURE REVIEW	4
Thermodynamics of Redox Reactions	6
Electrochemistry of Pyrite Oxidation	7
The Kinetics of Oxidation Reactions	9
Microbial Catalysis of Pyrite Oxidation	10
THEORY	12
Thermodynamic Theory: The Phase Rule	12
Application of the Phase Rule to Pyrite Dissolution/Oxidation	15
Thermodynamic Variables of State in Redox Reactions	17
Application of Single Ion Activities to Phase Analysis of Pyrite Oxidation	20
Application of State Variables pe and pH to Phase Dynamics in Oxidation of Pyrite	22
Thermodynamics of Electrochemical Reactions	31
Kinetics of Oxidation	36
Kinetics and Mechanisms of Homogeneous Oxidation of Aqueous Iron(II)	36
The Kinetic Salt Effect	39
Kinetics of Heterogeneous Oxidation of Aqueous Iron(II)	41
Kinetics of Pyrite Oxidation-Dissolution	43
Structural Chemistry of Pyrite	47
Structural Chemistry of Soluble Reduced Sulfur Compounds	49
Mechanisms of Aqueous Sulfur Oxidation	53
Thermodynamics of Reduced Sulfur Compounds	58
Kinetics of Aqueous Sulfur Oxidation	63
Microbial Catalysis of Pyrite Oxidation	65

TABLE OF CONTENTS (Continued)

Page

Pyrite Oxidation in Soils and Overburden . . . 69
Pyrite Oxidation and Soil Development . . . 73
Effect of Reduced Sulfur Compounds on Plant Growth 75
Summary 77

METHODS 80

Characterization of the Minerals Used . . . 80
Batch Experiments I: Long Term Studies . . . 81
Controlled pH Experiments 83
Batch Experiments II: Comprehensive Studies . 84
Pyrite Electrodes 86
Column Study 87

RESULTS AND DISCUSSION 89

Characterization of the Minerals Used . . . 89
Long Term Oxidation of Pyrite 92
Oxidation of Pyrite at Constant pH and Ionic Strength 105
The Effect of Surface Area on Pyrite Oxidation Rates 107
Reaction Order for Pyrite Oxidation Expressed as Iron Oxidation Products . . 109
The Effect of Ionic Strength on Pyrite Oxidation 116
Sulfur Oxidation 120
Effect of Reduced Sulfur Compounds on Pyrite Oxidation Rate 130
The Effect of DTPA on Pyrite Oxidation . . . 134
The Efects of Other Specific Ions, Ion Exchange and Specific Minerals on Pyrite Oxidation 146
Thermodynamics of Pyrite Oxidation 150
Column Studies: The Influence of Calcium Carbonate on Pyrite Oxidation Products . 156
Implications for Reclamation of Mine Spoils and Tailings 161

CONCLUSIONS 163

Analytical Chemistry 163
Thermodynamics 164
Pyrite Electrochemistry 165
Kinetics 165
Implications 167

TABLE OF CONTENTS (Continued)

Page

LITERATURE CITED 168

APPENDICES 180

Appendix A. Solid Phase Analysis for Oxidized Iron 181

Appendix B. Calibration of Platinum Redox Electrodes 183

Appendix C. Photometric Determination of Sulfate 186

VITA 190

LIST OF TABLES

Table | Page

1. Experimental treatments used in longterm studies . 82
2. Selective dissolution of standard pyrite . . . 90
3. Analysis of HF washed pyrite 90
4. Paricle size analysis for pyrite standard . . . 91
5. Rates of oxidation of pyrite in long term experiments (5040 h) 95
6. Redox data for long term pyrite oxidation experiment 101
7. Solution composition after 5040 h pyrite oxidation 102
8. Thermodynamic phase analysis of long term pyrite oxidation experiment 103
9. Oxidation of pyrite at controlled pH 107
10. Effect of surface area on pyrite oxidation rate at constant ionic strength ($I = 10$ mol m^{-3}) . . 109
11. Kinetic data for pyrite oxidation at pH 3.5 expressed as iron oxidized 110
12. Kinetic data for pyrite oxidation at pH 8.2 expressed as iron oxidized 112
13. Kinetic data for pyrite oxidation at pH 9 expressed as iron 114
14. Effect of specific salts and ionic strength on kinetics of pyrite oxidation using the modified Brønsted equation 117
15. Effect of ionic strength on pyrite oxidation (as $NaClO_4$) 123
16. Effect of ionic strength on pyrite oxidation (as NaCl) 124

LIST OF TABLES (Continued)

Table Page

17. Effect of ionic strength on disulfane disulfonate oxidation (Initial concentration 0.1 mol($K_2S_4O_6$) m^{-3} in $NaClO_4$) 126

18. Effect of ionic strength on thiosulfate oxidation (Initial concentration 0.1 mol($Na_2S_2O_3$) m^{-3} in $NaClO_4$) 126

19. Effect of reduced sulfur compounds on pyrite oxidation rate (I = 500 mol m^{-3} as $NaClO_4$) . . . 130

20. Effect of reduced sulfur compounds on pyrite oxidation in the presence and absence of $CaCO_3$ 132

21. Effect of oxidation of reduced sulfur compounds on pH in the presence of pyrite and $CaCO_3$ (I = 500 mol m^{-3} as $NaClO_4$) 133

22. Effect of DTPA on pyrite oxidation (I = 10 mol m^{-3}) 135

23. Calculations of solution equilibria in the presence of DTPA and pyrite using GEOCHEM (at pH 3.4) . . 137

24. Calculations of solution equilibria in the presence of DTPA, $CaCO_3$ and pyrite using GEOCHEM (pH 7.9) 141

25. Effect of solution calcium on pyrite oxidation . 146

26. Effect of calcium-containing minerals $CaCO_3$, $CaSO_4$ and exchange resin on pyrite oxidation . . 147

27. Effect of anion and cation exchange on pyrite oxidation 148

28. Rates of production of soluble sulfur compounds in column effluent (Ionic strength = 500 mol($NaClO_4$) m^{-1}) 160

29. Ratio of reduced sulfur compounds to total sulfur in column effluent 161

LIST OF FIGURES

Figure | Page

1a. Redox (pe) stability diagram for water as a function of pH 26

1b. Transformed redox (pe+pH) stability diagram for water as a function of pH 26

2. Redox (pe) stability diagram for aqueous oxidation of pyrite as a function of pH. Assumed activities of $Fe^{2+} = 10^{-4}$ M, $SO_4^{2-} = 10^{-3}$ M; sulfur oxidation is ignored 28

3. Transformed redox (pe+pH) stability diagram for aqueous oxidation of pyrite as a function of pH. Assumed activities of $Fe^{2+} = 10^{-4}$ M, $SO_4^{2-} = 10^{-3}$ M; sulfur oxidation is ignored 29

4. Pyrite crystal structure (redrawn from Wyckoff, 1948). Small spheres represent iron. Large spheres represent sulfur 48

5. Thiosulfate 50

6. Monosulfane disulfonate (redrawn from Ferrari et al., 1977) 50

7. Disulfane disulfonate (Foss and Hordvik, 1964) . 51

8. Trisulfane trisulfonate (Marøy, 1971) 51

9. Tetrasulfane disulfonate (Marøy, 1973) 52

10. Sites (at arrows) for nucleophilic displacement of thiosulfate from trisulfane disulfonate . . . 56

11. Relative abundance of aqueous sulfur species (as S) produced during short-term experiments as a function of pH. Partial pressure of oxygen 0.2 (Goldhaber, 1980) 59

12. Redox (pe) stability diagram for reduced sulfur compounds as a function of pH. Assumed total sulfur concentration 10^{-3} M 61

13. Transformed redox (pe+pH) stability diagram for reduced sulfur as a function of pH. Assumed total sulfur concentration 10^{-3} M 62

LIST OF FIGURES (Continued)

Figure Page

14. The distribution of sulfite species in water as a function of pH. Assumed total sulfite activity of 10^{-3} M 76

15. Effect of calcium carbonate an pyrite oxidation kinetics measured as conductivity 93

16. Effect of increased surface area on the rate of pyrite oxidation measured as solution conductivity 96

17. Long term pyrite oxidation: pH and redox changes with time 97

18. Long term pyrite oxidation in the presence of calcium carbonate: pH and redox changes with time 98

19. Pyrite oxidation in the presence of calcium saturated bentonite: changes in pH and redox . . 99

20. Sulfur products of pyrite oxidation at pH 6 . . 106

21. Effect of surface area on pyrite oxidation rate measured as production of sulfate and iron(III) . 108

22. Pyrite oxidation kinetics at pH 3.5. Background electrolyte 10 mol($NaClO_4$) m^{-3}. Zero order rate constant 27 pmol(Fe) m^{-2} s^{-1} 111

23. Pyrite oxidation kinetics at pH 8.2 in the presence of calcium carbonate. Background electrolyte 10 mol($NaClO_4$) m^{-3}. Zero order rate constant 45 pmol(Fe) m^{-2} s^{-1} 113

24. Pyrite oxidation kinetics at pH 9. Background electrolyte 10 mol($NaHCO_3$) m^{-3}. Zero order rate constant 119 pmol(Fe) m^{-3} s^{-1} 115

25. pH dependence of pyrite oxidation rate as pmol(Fe) m^{-2} s^{-1} 121

26. pH dependence of pyrite oxidation rate as pmol(SO_4^{2-}) m^{-2} s^{-1} 122

LIST OF FIGURES (Continued)

Figure Page

27. Distribution of pyritic sulfur oxidation products sulfate, sulfane disulfonate and thiosulfate between pH 7.5 and 9 125

28. The effect of ionic strength on thiosulfate oxidation measured as disulfane disulfonate (background electrolyte, $NaClO_4$) 128

29. Distribution of thiosulfate oxidation products in the presence and absence of pyrite 129

30. Redox equilibrium diagram: measured pe+pH and pH of all batch experiments 151

31. Comparison of measured pe and pH with calculated iron(III) hydroxide and hydronium jarosite redox equilibria 152

32. Pyrite and platinum electrode pe measurements versus the glass electrode pH 154

33. Comparison of measured thiosulfate, disulfane disulfonate, Fe^{2+} and pH with redox equilibria for reduced sulfur compounds and iron(III) hydroxide 155

34. Accumulation of sulfate in the effluents of three columns containing pyrite and calcium carbonate in different sequences 157

ABSTRACT

Chemical Weathering of

Pyrite in Soils

by

Aaron D. Brown, Doctor of Philosophy

Utah State University, 1985

Major Professor: Dr. J. J. Jurinak
Department: Soil Science and Biometeorology

The products of pyrite oxidation, including solution phase Fe^{2+}, Fe^{3+}, $S_2O_3^{2-}$, $S_4O_6^{2-}$, SO_3^{2-} and SO_4^{2-} and solid phase $Fe(OH)_3$, were measured under controlled conditions in order to investigate the behavior of pyrite in calcareous and alkaline soils.

The distribution of sulfur oxidation products is pH dependent and can be interpreted in terms of a metastable equilibrium among thiosulfate, disulfane disulfonate and sulfite. Thiosulfate and sulfite predominate in the pH range greater than about pH 7 or 8. Sulfane disulfonates are more predominant at more acid pH.

Solution concentration data were consistent with the presence of $Fe(OH)_3$. Concentrations of thiosulfate and sulfane disulfonate were consistent with a redox equilibrium among solution iron and sulfur species at pH 6 to 9.

Linear or zero-order kinetics were found to be

sufficient for description of pyrite oxidation in this study. Linear kinetics were observed as electrical conductivity, solution sulfur products and solution plus solid phase iron products. The measurement of solution iron plus solid-phase iron oxide is a more rigorous approach to the extent of reaction than the measurement of sulfate.

The rate of pyrite oxidation is pH dependent, increasing from 10 - 20 pmol(Fe) m^{-2} s^{-1} to 40 - 60 pmol(Fe) m^{-2} s^{-1} between pH 5 and 9. This is consistent with an oxidation mechanism involving the reoxidation of solution Fe^{2+} via a reaction between an iron hydroxide complex and hydrated oxygen as the rate-determining step. The effect of background electrolytes on oxidation rates at low pH also supports this interpretation.

Pyrite oxidation rates in the presence of calcium carbonate, sodium bicarbonate, sodium thiosulfate and calcium-saturated bentonite can be related to the pH effect. Sodium thiosulfate and DTPA appeared to have specific inhibitory effects.

Column studies show that the disposal of pyritic mine spoils or tailings by mixing with calcareous material may produce thiosulfate, a good reducing agent for toxic metals. Burial of lime below pyritic materials may protect groundwater quality more effectively than application of lime to the surface.

(206 pages)

INTRODUCTION

Pyrite oxidation and dissolution have been studied extensively for both metallurgical and environmental reasons. In metallurgy, pyrite is a persistent and unwanted contaminant of ore minerals such as copper sulfides. Historically, pyrite was a commercial source of sulfuric acid, but it is now mainly a by-product of the mining industry. Its presence in waste dumps and abandoned mines has caused significant environmental problems as a result of the sulfuric acid produced during natural oxidation processes.

The rising cost of disposal of pyritic materials in an environmentally sound manner has also promoted interest in alternative uses, particularly in agriculture. The acid producing properties of pyrite could be used to reduce the pH of alkaline soils and promote the aggregation and drainage of sodic calcareous soils. Iron, sulfur and perhaps other micronutrient elements associated with pyrite may be useful in adjustment of soil fertility.

It is ironic that the chemical transformations of a material with such a long commercial history and such distinct properties would still be so poorly understood. The precise mechanism of oxidation of pyrite remains unknown in spite of considerable progress in electrochemistry. The mode

of action of the Thiobacilli, bacteria known to catalyze pyrite oxidation under certain conditions, cannot be assesed accurately without a better understanding of the chemistry of oxidation. Oxidation and weathering of minerals in soils are processes difficult to measure and predict. Such an incomplete understanding of the basic chemistry of a mineral only compounds this difficulty.

Sato (1960b) summarized four basic techniques used in the analysis of pyrite oxidation: analytical, mineralogical, kinetic and electrochemical. The analytical approach centers on the stoichiometry of the reaction and the identity of the reactants and the products. The mineralogical approach is similar, except that the properties of the solid phase reactants and products are studied exclusively. Both the analytical and mineralogical properties of pyrite oxidation are easily and appropriately described by the theories of chemical thermodynamics. The kinetics of pyrite oxidation cannot be explained by the same theories, but depend, likewise, on an accurate knowledge of the reactants and products. The kinetic approach can be used to help identify the possible mechanisms of oxidation at the molecular level. The electrochemistry of oxidation combines knowledge of the stoichiometry of the reaction, physical properties of the mineral reactants and products and the thermodynamics of the reaction in order to identify the steady state reaction mechanism. To this list should be added the microbiological approach, most favored in recent years, which simply assumes

that the kinetics of pyrite oxidation are entirely dependent on the viability of microbial populations. This approach also requires information concerning the stoichiometry of the reaction, mineralogical properties, kinetics and thermodynamics of the reaction to to be accurately applied (e.g. Hoffmann et al., 1981).

The purpose of this study was to unravel the complexity of the pyrite oxidation reaction, particularly as it might apply to the chemistry of neutral to alkaline soils and analysis of the acid production potential of pyritic overburden. Previous assumptions concerning the analytical chemistry and kinetics of non-biological oxidation were reevaluated in order to identify more accurately the mechanism of pyrite oxidation. In order to accomplish this task all of the classical techniques categorized by Sato (1960b) were employed. On the basis of the work of others (Arkesteyn, 1980) further study of the microbiology of pyrite oxidation was considered to be unnecessary for the applications of concern. However, the information gained from this study of the chemistry of pyrite oxidation should definitely be applied in future microbiological studies.

LITERATURE REVIEW

Pyrite is a persistent mineral because of the slowness of the oxidation-dissolution reaction in spite of the extreme oxidizing conditions of the atmosphere. It is thermodynamically unstable in the presence of oxygen as indicated by the negative free energy change calculated for the overall reaction:

$$FeS_2 + 15/4\ O_2 + 7/2\ H_2O = Fe(OH)_3 + 2\ H_2SO_4 \qquad [1]$$

$$G^o = -1.21\ MJ\ mol^{-1}.$$

The kinetic constraints on this reaction are only beginning to be understood. One of the most recent and extensive reviews on pyrite oxidation is that of Lowson (1982).

There are three mechanisms advanced for the oxidation of pyrite: (a) microbiological catalysis, (b) dissolution followed by homogeneous oxidation or (c) electrochemical (heterogeneous) oxidation followed by dissolution and further homogeneous oxidation. These mechanisms are not mutually exclusive, however, the relative importance of one mechanism over another may be determined by other factors such as pH, pe, oxygen pressure or moisture. A major difficulty in distinguishing among the possible mechanisms is that the oxidation reaction probably never follows the stoichiometry of equation [1] exactly. Elemental sulfur is also a common and relatively inert reaction product of

pyrite oxidation. It has been proposed instead that at least two main reactions must be occurring (McKay and Halpern, 1958), for example:

$$FeS_2 + 2\ O_2 = FeSO_4 + S \qquad [2a]$$

$$2\ FeS_2 + 7\ O_2 + 2\ H_2O = 2\ FeSO_4 + 2\ H_2SO_4 \qquad [2b]$$

Oxidation of the iron(II) follows separately. Stokes (1901) attempted to use this property to analytically distinguish between pyrite and marcasite since each mineral produced different sulfate to elemental sulfur ratios under standardized, anoxic conditions.

The stoichiometry problem, while critical for kinetic studies, has rarely been treated adequately in pyrite oxidation. Usually only one or two components of equation [1] are actually measured during the course of the reaction. Commonly, oxygen consumed, or sulfate (or even H^+) produced is the only measure of oxidation used (Ainsworth and Blanchar, 1984, Pugh et al., 1984, Caruccio et al., 1981, Goldhaber, 1980, Geidel, 1980, Vlek and Lindsay, 1978, Smith and Shumate, 1970, McKay and Halpern, 1958). The electrochemical reduction of Fe^{3+} (aq) by pyrite has been used as a means to study the nature of the oxidation reaction (Singer and Stumm, 1970, Garrels and Thompson, 1960, Stokes, 1901). The amount of oxidized iron produced has also been used as a measure of extent of reaction (Goldhaber, 1980, Steger, 1977). Elemental sulfur is rarely measured because it is insoluble in water and difficult to separate from pyritic sulfur. Mishra (1973) determined

sulfur by CS_2 extraction. Others have determined sulfur by difference (Goldhaber and Reynolds, 1977, McKay and Halpern, 1958).

The chemistry of sulfur in the oxidation of pyrite is proving to be complex (Goldhaber, 1980, Steger and Desjardins, 1978, Goldhaber and Reynolds, 1977, Ginzburg, et al., 1961, Sato, 1960a, 1960b). In these investigations, thiosulfate, disulfane disulfonate (or other disulfonate) and sulfite were found as intermediate oxidation products. Not only does the product distribution deviate from the stoichiometry of equation [1], but autocatalytic reactions involving products are also occurring.

Thermodynamics of Redox Reactions

The use of thermodynamics to describe oxidation and reduction processes in soils has met with moderate success in recent years. Baas Becking et al. (1960) made a landmark compilation of redox conditions in natural systems and related them to the chemistry and microbiology of those systems. It was found that the limits of these natural conditions were comparable with the limits of stability of several redox-active minerals and solution species. These included organic compounds under the most oxidizing conditions, sulfides under the most reducing, carbonates in alkaline environments and iron compounds in acidic environments.

The most successful thermodynamic studies of redox processes in soils have been associated with flooded soils in the field or saturated soil/water systems in the laboratory. Ponnamperuma's (1972) monograph and Turner and Patrick's (1968) review of the chemistry of submerged soils illustrate the extent to which thermodynamics is useful in explaining the order of reactions and composition of the soil solution after flooding.

The redox reactions of iron compounds have been the subject of the most study. Huber and Garrels (1953) and Sato (1960a and 1960b) and many others conducted studies of iron minerals of geological interest. Ponnamperuma et al. (1967), Goto and Patrick (1972) and Schwab and Lindsay (1983) have used thermodynamics to show the importance of iron(III) hydroxide, "ferrosic oxide" ($Fe_3(OH)_8$) and iron (II) carbonate in determining the solubility of iron in flooded soils. In acid sulfate soils which have developed as a result of drainage of coastal areas and marshes, the mineral jarosite ($KFe_3(SO_4)_2(OH)_6$) has been identified as contributing to iron solubility and reaction (Vlek et al., 1974). Jarosite has also been identified in mine spoils as a buffer of iron solubility and pH (Miller, 1980). Lindsay (1979) has also placed considerable emphasis on the interpretation of soil reactions as redox equilibria.

Electrochemistry of Pyrite Oxidation

The primary mechanism for pyrite oxidation is

electrochemical. These corrosion reactions have only recently been studied extensively although essentially electrochemical mechanisms for pyrite oxidation were assumed by Stokes (1901), Garrels and Thompson (1960) and Singer and Stumm (1970). Bailey and Peters (1976) used $^{18}O_2$ to confirm that molecular oxygen served only as an electron acceptor in the oxidation of pyrite and does not enter into the product formed. Oxygen is reduced at a cathodic site on the surface of the pyrite, which induces a current. At the anodic site, sulfur is oxidized to either elemental sulfur or sulfate by the reactions:

$$FeS_2 + 8\ H_2O = Fe^{2+} + 2\ SO_4^{2-} + 16\ H^+ + 14\ e^- \qquad [3a]$$

$$FeS_2 = Fe^{2+} + 2\ S^o + 2\ e^- \qquad [3b]$$

No explanation has been offered for the relative production of these reactions. Either O_2 or Fe^{3+} can accept electrons and act as oxidant with equivalent effect. The abundance and ease of adsorption of these oxidants determine their relative importance (Smith and Shumate, 1970). The homogeneous oxidation of Fe^{2+} can thus affect the rate of oxidation under certain conditions (Singer and Stumm, 1970).

Pyrite corrosion products are apparently limited to iron(III), sulfate and elemental sulfur. Peters and Majima (1968), Meyer (1979), Biegler and Swift (1979) and Hamilton and Woods (1981) have shown the principal products to be Fe^{3+} and SO_4^{2-} in the anodic reaction:

$$FeS_2 + 8\ H_2O = Fe^{3+} + 2\ SO_4^{2-} + 16\ H^+ + 15\ e^- \qquad [4]$$

The iron(III) forms a visible layer of iron hydroxides on the pyrite surface which can limit corrosion rates at higher pH (Meyer, 1979).

Biegler and Swift (1979) and Hamilton and Woods (1981) have inferred from electrode studies that elemental sulfur is formed at the surface in the reaction:

$$FeS_2 + 3\ H_2O = Fe(OH)_3 + 2\ S^o + 3\ H^+ + 3\ e^- \qquad [5]$$

Based on rotating electrode studies, the sulfur produced is present only as a monolayer at pH 9.2 and 13, but considerably greater amounts are produced at pH 4.6 (Hamilton and Woods, 1981).

The Kinetics of Oxidation Reactions

The kinetics of redox reactions in soils have been studied to some extent, particularly for nutrient elements such as nitrogen and sulfur, but rate laws are usually empirically, rather than theoretically derived, and highly dependent on the specific experimental conditions. Elemental sulfur and pyrite have received considerable attention due to their utility as amendments for sodic or sulfur-deficient soils and the environmental problems caused by pyrite oxidation in mine spoils (Weir, 1975).

Kinetics of oxidation are usually treated in the same manner as dissolution reactions. Since the solution phase is the most convenient for analytical purposes, it is usually the rate of appearance or disappearance of a solution species which is used to determine reaction rates (eg.

Harvard University, 1970, Smith and Shumate, 1970). This approach is based on the assumption that all reactants and products are known and that their proportions are identical to the stoichiometry of the overall reaction. This is reasonable in the case of simple dissolution; however, the oxidation of sulfur does not result in a simple product distribution. Furthermore, there is a tendency to overlook the nature of the solid phase when kinetics are studied in solution. In the oxidation of pyrite, at least two solid phases are involved and both the homogeneous (solution) reactions and the overall heterogeneous (solid/solution) reactions must be considered.

Microbial Catalysis of Pyrite Oxidation

Pyrite is a thermodynamically unstable mineral when exposed to the atmosphere, hence chemical oxidation of pyrite is spontaneous and requires no net energy input. Sulfur- and iron- oxidizing bacteria, particularly of the genus *Thiobacillus*, are known to increase the rate of pyrite oxidation by many orders of magnitude under the proper conditions (Quispel, et al., 1952, Temple and Delchamps, 1953, Singer and Stumm, 1970, Stumm-Zollinger, 1972, Ivarson, et al., 1982). *Thiobacillus ferrooxidans* is often considered the most important factor in pyrite oxidation, although the mechanisms of interaction between the organism and the mineral environment are poorly understood

(Alexander, 1977, Nordstrom, 1982). A more precise understanding of the nature of the non-biological oxidation of pyrite will enable a more detailed understanding of the biological mechanism.

THEORY

A thermodynamic approach to pyrite oxidation facilitates a discussion of solid and solution phase product distribution based on solution phase measurements. It will also help explain the electrochemical behavior of pyrite. The following review of the thermodynamic theory of phase relations will allow the logical integration of extrathermodynamic variables describing acidity (pH) and electrochemical potential (pe). These variables have proven to be useful in the analysis of redox systems, but their interrelationship is not utilized as effectively as it could be.

Thermodynamic Theory: The Phase Rule

One of the general consequences of thermodynamics is that the description of a system in terms of all of the intensive variables restricts the number of components in the system that may vary independently. This result is known as the phase rule, first derived by Gibbs (1961) and is written:

$$f = c + 2 - p - r \qquad [6]$$

where f is the number of intensive independent variables, c is the number of component substances, p is the number of homogeneous phases and r is the number of reactions which relate the intensive variables of at least two components.

A phase is a homogeneous portion of a system which has a distinct discontinuity with the other phases of the system or the thermodynamic universe external to the system studied. Each phase contains one or more component substances whose masses may be varied independently, defining the composition of the phase at temperature and pressure. The substance may either be a real compound (such as $CaCO_3$ in water) or it may be a hypothetical compound which emphasizes the independent nature of the component (such as CaO in water with CO_2). Each component (j) has a corresponding chemical potential u_j which is the differential of the Gibbs free energy of the phase with respect to the mass of the component of interest, all other variables held constant.

A fundamental thermodynamic relationship between the Gibbs free energy G and a set of independent variables T (temperature), P (pressure) and m_i (mass of component i) for any given phase can be given as an equation of state: $G = f(T, P, m_i)$ or in its complete differential form:

$$dG = -SdT + VdP + u_1dm_1 + u_2dm_2 + \dots + u_ndm_n \qquad [7]$$

where S and V are the entropy and volume of the phase and the chemical potential u of each component i is defined:

$$u_i = \left.\frac{G}{m_i}\right|_{T,\, P,\, m_1,\, m_2 \cdots} \qquad [8]$$

At constant T and P and holding composition constant, integration of equation 8 gives:

$$G = u_1m_1 + u_2m_2 + \dots + u_nm_n. \qquad [9]$$

Differentiating equation [9] and equating it with equation [8] under isobaric and isothermal conditions gives:

$$0 = m_1 du_1 + m_2 du_2 + \ldots + m_n du_n. \qquad [10]$$

This is the Gibbs-Duhem equation, which gives the relationship between the intensive variables u_i of the ith component of the phase.

The above argument indicates that for any phase containing n components the total number of intensive variables describing the phase is n+2. The integer 2 accounts for T and P where u_i is the partial molar free energy as in this example. The Gibbs-Duhem relationship is completely general and can be readily derived using thermodynamic functions U (internal energy), H (enthalpy) or A (Helmholtz free energy) with the constraint that the appropriate set of independent state variables (T, P, V or S) be used with each function.

Each phase of a system has one Gibbs-Duhem equation and n+2 independent variables which describe the state of each phase of the system. In general there are p phases and n_p components of each phase which when summed over all phases yields a total of c components and a total of 2p pressure and temperature terms. This results in c+2p possible independent variables of the system.

If the system temperature and pressure are held constant, then there must be a pair of equations relating these variables for each unique pair of phases. Each pair of equations reduces the number of independent variables by

two, hence the number of independent variables of a system at constant temperature and pressure is c+2. There are also p Gibbs-Duhem equations for the system, each of which reduces the number of independent variables by one to leave c+2-p independent variables.

It is a condition of equilibrium that a component which is present in more than one phase must have the same chemical potential in each phase. Each equilibrium reaction between phases reduces the number of independent variables by one. Also if within the same phase there is a reaction which causes one component to be converted to another, then these components are not independently determined and the number of independent variables must be reduced by one. Considering all reactions r among components within the same and different phases, the original form of the phase rule is now obtained as in equation [6].

Application of the Phase Rule to Pyrite Dissolution/Oxidation

The oxidation of pyrite is described by the balanced chemical equation:

$$FeS_2 + 15/4\ O_2 + 7/2\ H_2O = Fe(OH)_3 + 2\ H_2SO_4. \qquad [11]$$

The oxidation reaction is to the right, forming iron(III) hydroxide and sulfuric acid. The reaction takes place in a four phase system consisting of a gas phase with oxygen, an aqueous phase containing the components water, aqueous oxygen, sulfuric acid, dissolved pyrite and dissolved

iron(III) hydroxide, and two solid phases, pyrite and iron(III) hydroxide. There are thus a potential c+2 or 10 independent variables in the system, for example T, P and the masses of each component. The four Gibbs-Duhem equations are as follows:

$$0 = - S(g)dT + V(g)dP + m(O_2)du(O_2) \qquad [12a]$$

$$0 = - S(aq)dT + V(aq)dP + m(O_2)du(O_2) + m(H_2O)du(H_2O) + m(H_2SO_4)du(H_2SO_4) + m(FeS_2)du(FeS_2) + m(Fe(OH)_3)du(Fe(OH)_3) \qquad [12b]$$

$$0 = - S(FeS_2)dT + V(FeS_2)dP + m(FeS_2)du(FeS_2) \qquad [12c]$$

$$0 = - S(Fe(OH)_3)dT + V(Fe(OH)_3)dP + m(Fe(OH)_3)du(Fe(OH)_3. \qquad [12d]$$

There are also four independent equations as a consequence of the chemical reactions within and between phases. Three of these reactions involve the dissolution of oxygen, pyrite and iron(III) hydroxide in water and the third is the interconversion of pyrite and iron(III) hydroxide which also involves water, oxygen and sulfuric acid:

$$u(O_2, aq) - u(O_2, c) = 0 \qquad [13a]$$

$$u(Fe(OH)_3, aq) - u(Fe(OH)_3, c) = 0 \qquad [13b]$$

$$u(FeS_2, aq) - u(FeS_2, c) = 0 \qquad [13c]$$

$$u(Fe(OH)_3) + 2\ u(H_2SO_4) - u(FeS_2) + - 15/4\ u(O_2) - 7/2\ u(H_2O) = 0. \qquad [13d]$$

These reactions complete the thermodynamic description of the system.

From the ten possible independent variables of the system is deducted four degrees of freedom for each of the four Gibbs-Duhem equations, three degrees of freedom for phase equilibrium reactions and one for the oxidation reaction. Two independent variables remain for the system, hence a judicious selection of variables (for example T and P (which includes O_2) or $u(FeS_2, aq)$ and $u(Fe(OH)_3, aq)$ should completely define the system.

Thermodynamic Variables of State in Redox Reactions

A consequence of the phase rule calculations for pyrite is that at constant T and P, all chemical potentials in the system can be determined by solution of the set of four Gibbs-Duhem equations, three phase equilibrium reactions and the chemical oxidation reaction. The difficulty in thermodynamic analysis of this system is that the aqueous phase is an electrolyte solution which has a more complex behavior than the pure solids or gaseous solution. The chemical potential of an aqueous electrolyte is more conveniently defined in terms of individual ions rather than in terms of a compound or substance. This is analytically more realistic. Ionic species are usually determined in the

laboratory and it would be difficult to logically pair cations and anions as compounds in solution. The treatment of single ions in solution can be generalized in a way which will allow the extension of the phase rule to redox reactions in simple electrolytes.

Sposito (1981) has defined and derived the standard state of an electrolyte in aqueous solution, the thermodynamic activity, mean activity coefficients, standard state chemical potentials and the equilibrium constant. These derivations are not repeated here.

The conditions for equilibrium in any reaction at constant temperature and pressure are derived from the integrated form of the Gibbs-Duhem equation [9]:

$$\sum_{j=1}^{n} v_j u_j = 0 \qquad [14]$$

where u_j is the chemical potential of the jth component, as before, and v_j is the stoichiometric coefficient in the reaction. The standard state of an electrolyte is defined as a hypothetical 1 mol kg^{-1} solution, a solution which obeys Henry's law without deviation. Thermodynamic activity (a) is a measure of the deviation of the chemical potential from its standard state potential u^o thus:

$$u = u^o + RT \log_e a \qquad [15]$$

where R and T are the gas constant and temperature. By substituting equation [15] for each component in equation [14], the condition for equilibrium is transformed to a function of standard chemical potentials and the activity of

the component in the phase:

$$_j\, v_j u_j^o + RT\ _j\, v_j \log_e a_j = 0 \qquad [16]$$

Note that $_j\, v_j u_j^o$ is usually defined as the standard free energy change (G^o) of a reaction and $_j\, v_j \log_e a_j$ is $\log_e$ K, the equilibrium constant.

Since ions do not fit the definition of components or substances required for thermodynamic variables of state, the definition of ionic activities is a formal convention and not a strictly thermodynamic quantity. A single ion activity is conveniently defined by use of equation [15] with ions instead of components. If C is a cation, A an anion and m+ and n- are valences, then the activities of the ions of a solute C_nA_m are defined by:

$$u_C = u_C^o + nRT \log_e a_C \qquad [17a]$$

$$u_A = u_A^o + mRT \log_e a_A \qquad [17b]$$

The summation of the above equations shows that the individual ion activities are related to the activity of the solute by:

$$a_{CA} = a_C^n\, a_A^m. \qquad [18]$$

This is a convenient quantity: more useful than more consistent expressions for activity (i.e. mean ionic activity).

Application of Single Ion Activities to Phase Analysis of Pyrite Oxidation

The single ion concept may be extended to redefine the solutes in oxidation-reduction equation [13d] in terms of dissolved ions:

$$u(Fe(OH)_3, aq) = u(Fe^{3+}) + 3\ u(OH^-) \qquad [19a]$$

$$u(H_2SO_4, aq) = 2\ u(H^+) + u(SO_4^{2-}) \qquad [19b]$$

$$u(FeS_2, aq) = u(Fe^{2+}) + u(S_2^{2-}). \qquad [19c]$$

It is a logical extension of this formalism to consider the dissociation of H_2O into ions:

$$u(H_2O) = u(H^+) + u(OH^-). \qquad [20]$$

The chemical potential of H^+ is defined by:

$$u(H^+) = u^o(H^+) + RT\ \log_e a_{H^+} \qquad [21]$$

and the definition of pH is:

$$pH = -\log_{10} a_{H^+} \qquad [22]$$

so with only a change of a constant factor pH may be redefined as a function of chemical potentials:

$$pH = \frac{u^o(H^+) - u(H^+)}{RT\ \log e\ 10} \qquad [23]$$

Largely because of the ease of measurement of the potential difference in equation [23] using a glass membrane electrode, pH is a very popular measured variable. As an ionic species, however, it is not a strict thermodynamic property.

Comparing equation [23] with equation [20] it is clear

that pH is dependent on $u(H_2O)$ which is a thermodynamic state variable. Likewise equations [19a] and [19b] also contain variables which influence pH. Since the pH of a system is a useful variable for analytical and mathematical reasons, it should be recognized as a non-thermodynamic state variable related to thermodynamic state variables.

The remaining thermodynamic variable in the aqueous phase is $O_2(aq)$. Oxygen consumes two electrons per atom to achieve the oxidation state found in H_2SO_4 and $Fe(OH)_3$. The redox reactions for oxygen and the iron and sulfur compounds analogous to the ionic equilibria in equations [19a-c] are:

$$u(O_2) + 4\ u(e^-) = 2\ u(O^{2-}) \qquad [24a]$$

$$u(Fe^{2+}) = u(e^-) + u(Fe^{3+}) \qquad [24b]$$

$$u(S_2^{2-}) = 14\ u(e^-) + 2\ u(S^{6+}). \qquad [24c]$$

The free electron is also an extrathermodynamic concept and cannot be treated as thermodynamic state variable. Using the same approach as for H^+, it becomes a useful variable.

The chemical potential of the free electron is defined in a manner similar to aqueous ions:

$$u(e^-) = u^o(e^-) + RT \log_e a_{e^-}. \qquad [25]$$

The pe or redox potential of a solution is defined as:

$$pe = -\log_{10} a_{e^-}. \qquad [26]$$

The pe may be redefined in terms of chemical potentials:

$$pe = \frac{u^o(e^-) - u(e^-)}{RT \log_e 10}, \qquad [27]$$

which is completely analogous to pH.

The redox potential of a solution is not as conveniently measured as pH. The platinum electrode (a source or sink for electrons) is coupled with the standard hydrogen electrode to measure redox or oxidation potentials. The redox potential as measured by the platinum electrode (relative to the calomel electrode) has been used in soils (Ponnamperuma et al. 1966, 1967, Ponnamperuma, 1972, Turner and Patrick, 1968, Lindsay, 1979), but the results have been questioned (Lindberg and Runnells, 1984, Whitfield, 1974, Bohn, 1969). Another way of determining redox potential or the chemical potential of the electron is by measurement of the concentration (chemical potential) of the redox-active species in solution as suggested by equation [24b] for Fe(II) and Fe(III). Comparing this equation with equations [19a] and [19c] it is clear that pe is dependent on $u(Fe(OH)_3, aq)$ and $u(FeS_2, aq)$, which are thermodynamic variables of state for the pyrite system. This is a situation completely analogous to pH. Since pe is a useful mathematical, conceptual and possibly analytical tool it should, as was pH, be considered as a non-thermodynamic state variable related to thermodynamic state variables.

Application of State Variables pe and pH to Phase Dynamics in Oxidation of Pyrite

The utility of the variables pe and pH is demonstrated by substitution of these variables into the original description of pyrite redox equilibrium equation [13d]. When

equations [19a-c], [20] and [24a] are used to redefine the aqueous phase reaction, equation [28] results:

$$0 = u(Fe^{3+}) - u(Fe^{2+}) + 2\ u(SO_4^{2-}) - u(S_2^{2-}) + \\ + 1/2\ u(H^+) - 1/2\ u(OH^-) \\ + 15\ u(e^-) - 15/2\ u(O_2). \qquad [28]$$

This equation has eight variables where the original had only five. Note, however, that these variables are all dependent on the reactions [20] and [24a-c], so no independent variables have been added to the equation. Therefore, pe and pH are dependent variables and are mathematically related.

The use of the following basic relationships (with equilibrium constants for the dissociation of water, K_w, and the reduction of oxygen, K_o, included) allows expression of the variables $u(e^-)$, $u(H^+)$, $u(OH^-)$ and $u(O^{2-})$ in terms of pe or pH and constants:

$$u(e^-) = u^o(e^-) - (\log_e 10)\ RT\ pe \qquad [29a]$$

$$u(H^+) = u^o(H^+) - (\log_e 10)\ RT\ pH \qquad [29b]$$

$$u(OH^-) = u^o(OH^-) - (\log_e 10)\ RT\ (pK_w + pH) \qquad [29c]$$

$$u(O^{2-}) = u^o(O^{2-}) - (\log_e 10)\ RT\ (pK_o + 2\ pe) \qquad [29d]$$

Upon substitution in equation [28] for the redox reaction, reduction of terms, inclusion of standard chemical potentials in a single, pooled constant (u_p), the redox term containing pe and pH drops out of equation [28], leaving a constant function of the equilibrium constants:

$$0 = u(Fe^{3+}) - u(Fe^{2+}) + 2\ u(SO_4^{2-}) - u(S_2^{2-}) + \\ - 1/2\ (\log_e 10)\ RT\ (\ pK_w + 15\ pK_o) + u_p^o. \qquad [30]$$

This suggests that the pe and pH terms of the oxidation equation are related in a way which is mutually dependent. It may be argued that this makes them a natural choice for a pooled variable of state in thermodynamic systems containing redox reactions.

This relation between pe and pH is related to the designation of standard state conditions for e^- and H^+ in solution. The standard state conditions for H^+ are a 1 mol kg^{-1} solution (HCl) at standard temperature (298.15 K) and pressure. The conditions for e^- are a standard hydrogen electrode consisting of an inert, platinum electrode in a 1 mol kg^{-1} solution of H^+ at a standard 1 atm pressure of H_2 (g) at 298.15 K. The reaction defining the standard state electrochemical potential for e^- is:

$$H^+ + e^- = 1/2\ H_2\ (g), \qquad [31]$$

where H^+ and H_2 (g) are also in their standard states. Using equation [17] for chemical potentials of all species and elimination of standard state (zero) terms results in the relation:

$$pe + pH = -1/2\ \log_e\ (H_2). \qquad [32]$$

In aqueous solutions under aerobic conditions this reaction may be extended to:

$$H^+ + e^- + 1/4\ O_2\ (g) = 1/2\ H_2O \qquad [33]$$

resulting in the relation:

$$pe + pH - 1/4 \log_e (O_2) = - 1/2 \log_e (H_2O). \quad [34]$$

The reactions [31] and [33] describe the limits of reducing and oxidizing conditions in water. These relations are plotted in terms of pe and pH in Figure 1a. Above and below the region of stability defined by these equations water will tend to decompose to H_2 and O_2. Aqueous reactions should be limited to this region as well.

Using the pooled variable of state a different method of plotting the stability field of water is proposed. This method utilizes the standard state relationship between pe and pH to redefine the limits of the common predominance or phase diagram. The resulting plot will then reflect the deviations of the solid phase or solid/aqueous phase equilibria from the standard relation between pe and pH. The pe + pH term is properly called a redox state variable and reflects the choice of standard state for e^- as the hydrogen electrode. The use of pe + pH versus pH for the limits of oxidation and reduction in aqueous systems is shown in Figure 1b.

Comparison of Figures 1a and 1b shows that pe + pH is simply a transformation of the pe axis of the ordinary pe versus pH predominance diagram described by Delahay et al. (1950) and refined by Sillen (1952). The parallelogram which defines the region of water stability in Figure 1a is transformed into a rectangular area in Figure 1b.

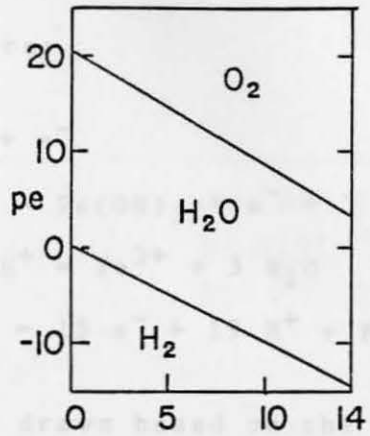

Figure 1a. Redox (pe) stability diagram for water as a function of pH.

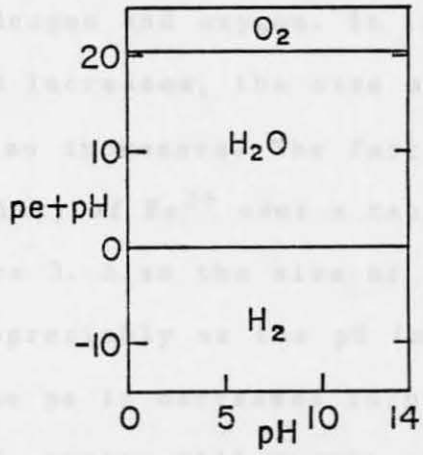

Figure 1b. Transformed redox (pe+pH) stability digram for water as a function of pH.

The use of this transformation with compounds found in the oxidation of pyrite is shown in Figures 2 and 3. The reactions used were:

$$Fe^{2+} = Fe^{3+} + e^- \quad [35a]$$

$$Fe^{2+} + 3\ H_2O = Fe(OH)_3 + e^- + 3\ H^+ \quad [35b]$$

$$Fe(OH)_3 + 3\ H^+ = Fe^{3+} + 3\ H_2O \quad [35c]$$

$$FeS_2 + 7\ H_2O = 15\ e^- + 19\ H^+ + Fe(OH)_3 + 2\ SO_4^{2-}. \quad [35d]$$

The diagrams were drawn based on the thermodynamic data of Lindsay (1979) assuming a total iron concentration of 0.1 mol m^{-3} and a sulfate concentration of 1 mol m^{-3}, similar to experimental conditions in this study.

Six fields of stability are shown in Figure 2, including upper and lower boundaries for the stability of water (H_2 and O_2), pyrite, iron (III) hydroxide and aqueous iron (II) and iron (III). Figure 3 omits the stability fields for hydrogen and oxygen. It is seen in both diagrams that as the pH increases, the size of the stability field for $Fe(OH)_3$ also increases. The fact that there is a pH of maximum stability of Fe^{2+} over a range of pe is more clearly shown in Figure 3. Also the size of the stability field is not reduced appreciably as the pH increases to 8.5 or 9. Clearly, if the pe is decreased in proportion to the increase in pH, pyrite will remain stable.

An obvious advantage of the pe + pH parameter in the redox diagram is the clarity with which the stability fields

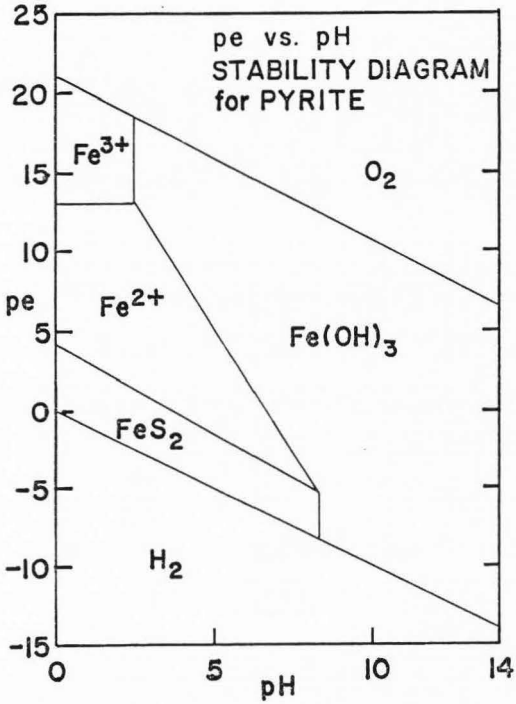

Figure 2. Redox (pe) stability diagram for aqueous oxidation of pyrite as a function of pH. Assumed activities of $Fe^{2+} = 10^{-4}$ M, $SO_4^{2-} = 10^{-3}$ M; sulfur oxidation is ignored.

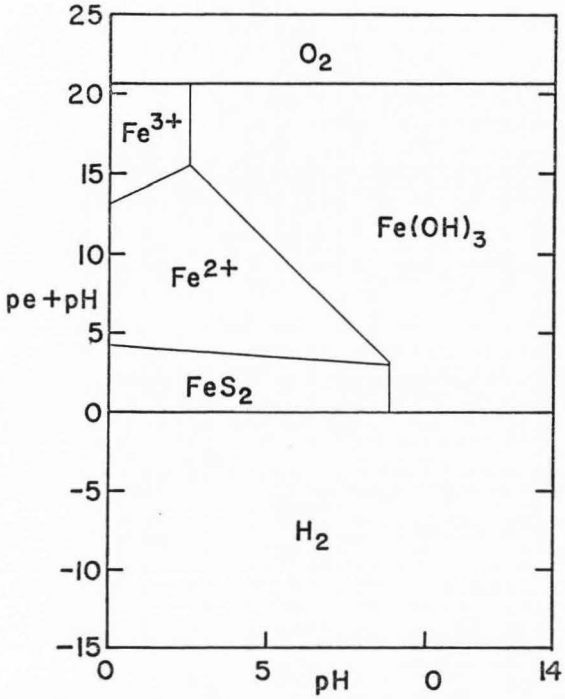

Figure 3. Transformed redox (pe+pH) stability diagram for aqueous oxidation of pyrite as a function of pH. Assumed activities of $Fe^{2+} = 10^{-4}$ M, $SO_4^{2-} = 10^{-3}$ M; sulfur oxidation is ignored.

are portrayed within the limits of stability of water. There is no space to fill in with relations thermodynamically meaningless for aqueous systems. The participation of water and oxygen in aqueous redox reactions is emphasised in the pe + pH parameter where the pe alone does not reflect this fact.

The pe + pH diagram is not unlike the combination diagram of Garrells and Christ (1965) which used ion ratios as axes. Those ratios were only used when there was a 1:1 stoichiometry of ions in the reactions in the system. There is a 1:1 stoichiometry of H^+ and e^- for the hydrogen electrode and for some solid phase equilibria, but not all. When plotting the combined parameter against an ion activity or partial pressure, the relative sizes of the stability fields might vary with pH or pe. This is observed on examination of Lindsay's (1979) two dimensional plots or Garrells and Christ's (1965) three dimensional plots.

The use of the term pe + pH has extended beyond equilibrium systems. The use of thermodynamics in the analysis of flooded soil and acid sulfate soil solution chemistry has required some minimal assumptions of equilibrium or near equilibrium. This has not hindered the analyses of Ponnamperuma et al. (1967), Goto and Patrick (1972) or Schwab and Lindsay (1983) and many others for iron in soils. Sadiq (1977) and Lindsay and Sadiq (1984) have demonstrated that redox poise (constant pe + pH) is maintained by the presence of equilibria among oxidizable

and reducible soil minerals and the soil solution. Such mineral equilibria determine the path of the redox reaction as reflected in the magnitude of the state variables pe and pH as well as the relative solution concentrations.

The reciprocal relationship between pe and pH is clear in the experiments reported by Huber and Garrells (1953) and Ponnamperuma et al. (1966) for laboratory and soil mixtures containing iron minerals. Although pe and pH were forced to change constantly in both cases, a linear combination of pe + pH remained constant, reflecting the redox properties of one or more iron oxide minerals. These systems were definitely not at equilibrium, however they were sufficiently close to afford reasonable analysis using thermodynamics. These observations may be employed usefully in the analysis of pyrite oxidation.

Thermodynamics of Electrochemical Reactions

A major application of redox stability diagrams is in the interpretation of the electrochemical reactions of metallic electrodes. Electrode potentials (E and pe) versus the standard hydrogen electrode are related to the change in Gibbs free energy (G) of the solid-solution, oxidation-reduction reaction by:

$$G = {}_{j} \; v_j u_j = - nFE \qquad [36]$$

where u_j is the chemical potential of the jth component, v_j is the stoichiometric coefficient for the jth component, n

is the number of electrons transferred per mole of reactants or products, F is the Faraday constant and E is the standard electrochemical potential (in volts). Rearrangement and substitution in equation [27] yields the relation between E and pe:

$$E = \frac{RT}{nF} (\log_e 10) \text{ pe} \qquad [37]$$

Evaluation of the constants at 298 K and n=1 yields the simple equation E = 0.059 pe, where E is in volts.

Two electrode reactions are represented in Figures 2 and 3 as the solid-solution phase boundaries between pyrite and Fe^{2+} and $Fe(OH)_3$ and Fe^{2+}. By measuring the electrochemical potential of the electrode and the pH it should be possible to determine the nature of the redox active solid phase. This has been done with some success for copper sulfide minerals, but Sato (1960b) was unable to deduce a satisfactory electrode reaction to explain the behavior of the pyrite electrode. Measured potentials at various pH plotted on a diagram similar to Figure 2 were fitted to the thermodynamic data for the reaction:

$$FeS_2 + 3\ H_2O = Fe(OH)_3 + S_2 + 3\ H^+ + 3\ e^-. \qquad [38]$$

The partial pressure of S_2 was assumed to be 1 atm for escape from pyrite to occur. When the same electrodes were exposed to reducing conditions (Na_2S and $FeCl_2$), the measured potential shifted in the reducing direction, but no suitable reaction could be found to correlate these potentials with thermodynamic data.

Peters and Majima (1968) investigated the electrochemical properties of pyrite in concentrated perchloric acid solutions and found that the rest potential of a pyrite electrode (0.62 V vs. SHE, or pe 10.5) was much higher than the thermodynamically calculated potential (0.35 V or pe 5.9). After the electrode had been exposed to a cathode current, generating H_2S and Fe^{2+}, the rest potential dropped to between 0.2 and 0.3 V (pe 3.4 and 5.1). This suggests the presence of an oxidized layer at the surface of natural pyrite which can be stripped by a cathode current. It has been shown by electrochemical and spectroscopic means that this is a thin layer of iron oxide.

Frost et al. (1977) used x-ray photoelectron spectroscopy (XPS) to measure the rate of oxidation of pyrite sulfur. By comparing XPS analysis of ground and unground samples it was clear that the oxidized sulfur was mainly on the surface of the pyrite. Mitchell and Woods (1978) used a similar method to demonstrate the presence of an oxygen-containing layer on polished pyrite crystals. The weight of the iron oxide film was also estimated by cyclic voltammetry and found to be a monolayer. The voltammetry also indicated that the oxidation/reduction reaction occurring at the pyrite surface was probably due to the $Fe(OH)_3/Fe(OH)_2$ couple rather than a reaction involving pyrite itself.

These studies of pyrite corrosion chemistry show that the aqueous oxidation of pyrite involves the formation of an oxide or hydroxide at the solid/solution interface. Solution and oxidation processes observed via solution chemistry must reflect the nature of the iron oxide surface of the pyrite. This iron oxide layer has the properties of a passive layer, a phenomenon which can be explained in two ways (Uhlig, 1971). The oxide film theory describes a diffusion barrier of oxidation products which separates the metal from the solution, limiting the corrosion rate. The adsorption theory describes a chemisorbed layer (of oxygen, for example) which prevents hydration and reaction of metal ions with the solution. Even less than a monolayer has been observed to have a passivating effect in some cases.

The effects of pH, ionic strength and solution composition on pyrite oxidation must depend on the properties of the passive layer. The effect of pH on oxide surface chemistry is to regulate the amount of adsorbed H^+ present. At low pH the surface sites can be represented by $Fe/(OH)_2^+$, resulting in a net positive surface charge. At high pH the surface sites are Fe/O^-, which results in a net negative surface charge. Iron oxide is very soluble at low pH and the tendency would be that the iron oxide layer on pyrite would dissolve, exposing FeS_2 directly to the solution.

The destruction of the passive layer on metallic iron at low pH leads to a dramatic increase in corrosion rates

(Uhlig, 1971). As long as an oxide layer is present, diffusion of oxygen to the metallic iron surface is rate-limiting, hence there is a constant rate of oxidation over a wide range of intermediate pH. The surface of iron in soft water is in contact with an alkaline layer of ferrous hydroxide. At very high pH the corrosion of iron is further limited, apparently by the adsorption of excess oxygen or a more stable oxide at the solid/solution interface.

Some dissolved, non-redox active salts (eg. NaCl) increase corrosion rates by the disruption of the stable passive layer (Uhlig, 1971). Hydrogen sulfide disrupts the passive layer through the introduction of H^+ ions. Other substances, such as KI and "pickling inhibitors" containing N, amine, S and OH functional groups are effective in preventing iron corrosion. At lower concentrations readily reduced ions such as NO_2^- can form effective passive layers, while ions such as SO_4^{2-}, ClO_4^- and Cl^- generally do not. These passivating substances must be present at certain minimum concentrations for passivation to occur. Below these concentrations they may actually enhance corrosion. Alkaline compounds such as NaOH, Na_3PO_4 and $Na_2B_4O_7$ also encourage passivation of steel by interacting with H^+ and allowing oxygen adsorption at the metal surface.

The electrochemical behavior of pyrite in a soil solution should be expected include passivation. The electrochemical potential of an electrode composed of pyrite

should be related to solution equilibrium chemistry.

Kinetics of Oxidation

The kinetics of pyrite oxidation are complicated by the presence of many components and phases just as the thermodynamics of the process are complicated by the relatively slow rates of reaction. The important chemical reactions that can be defined are the dissolution of pyrite, the electrochemical oxidation and subsequaent dissolution (equations [3a] and [3b]), the oxidation of aqueous iron(II) and the oxidation of aqueous sulfur compounds. Pyrite has a very low solubility, hence the oxidation reactions are expected to be most important in determining solution concentrations of iron and sulfur species. Since homogeneous (solution) oxidation processes have been most thoroughly studied and are most completely characterized, the oxidation of aqueous iron(II) is considered first.

Kinetics and Mechanisms of Homogeneous Oxidation of Aqueous Iron(II)

The oxidation of iron has been studied most extensively in solution reactions. The mechanism of iron oxidation and reduction is straightforward. Aqueous iron(III) can accept an electron from iron(II) through a slow outer sphere electron transfer (Taube, 1968). The slowness of this reaction has been attributed to the stabilizing effect of spin-pairing which can occur among the six 3d electrons of iron(II). Silverman and Dodson (1952) studied the kinetics

of this transfer in acidic sodium perchlorate solution and found both pH dependent and independent rate terms. The rate law determined corresponding to the acidic conditions of their experiment has the form:

$$\frac{d(Fe^{3+})}{dt} = k_1(Fe^{2+})(Fe^{3+}) + \frac{k_2K_1(Fe^{2+})(Fe^{3+})}{(H^+)} \qquad [39]$$

where k_1 and k_2 are empirically derived rate constants and K_1 is the equilibrium constant for the hydrolysis of aqueous iron(III):

$$Fe^{3+} + H_2O = Fe(OH)^{2+} + H^+. \qquad [40]$$

They suggested that the hydroxide complex of iron(III) was responsible for the pH-dependent reaction.

The oxidation of iron(II) by oxygen is more complicated. Stumm and Lee (1961) reported that the rate of oxidation had a first order dependence on iron(II) and oxygen pressure and second order dependence on OH^- for pH values greater than 6. The rate law determined was:

$$-\frac{d(Fe^{2+})}{dt} = k(Fe^{2+})(OH^-)^2PO_2 \qquad [41]$$

where $k = 5.7 \times 10^{13}$ mol^{-3} L^{-3} sec^{-1}, the rate constant and PO_2 the partial pressure of oxygen.

Goto et al. (1970) have proposed that the rate-determining step is the reaction between hydrolyzed iron(II) and oxygen:

$$FeOH^+ + O_2OH^- = Fe(OH)_2^+ + O_2^- \qquad [42]$$

where O_2OH^- is the dissociated form of hydrated oxygen. The electron-transfer process is controlled by the rate of

diffusion of the iron and oxygen species. This would involve the rearrangement of atoms and could be called an inner-sphere reaction.

Singer and Stumm (E.P.A., 1970) extended the study of Fe(II) oxygenation to show that the reaction was independent of pH below pH 3. Variation of PO_2 had little effect on oxidation rates except at low pressures. The rate equation found for constant PO_2 was approximately first order in iron(II) and may be represented by:

$$\frac{-d(Fe^{2+})}{dt} = k' \, (Fe^{2+}) \qquad [43]$$

where k' includes PO_2 and other rate constants. The similarities between this relation and the rate law of Silverman and Dodson (1952) in equation [39] are evident if (Fe^{3+}) is presumed to be nearly constant under Singer and Stumm's experimental conditions. Based on this it was inferred that the iron(II)-iron(III) electron transfer was a much more rapid reaction than the transfer of electrons to oxygen (Singer and Stumm, 1970).

Tamura et al. (1976a) studied the effects of various anions on the acceleration of iron(II) oxidation. It is clear that reactive and non-reactive complexes form between iron(II) and different anions. Silicate, sulfate, chloride and bromide anions supressed oxygenation relative to perchlorate while fluoride and phosphate anions had an accelerating effect. This effect is in competition with the effect of hydroxide anions. If the anion complex is more

plentiful or more active than the hydroxide complex, then two possibilities emerge: either the anion complex is more reactive toward hydrated oxygen or it is less reactive. These cases are represented in rate equations [44a] and [44b] respectively:

$$\frac{-d(Fe^{2+})}{dt} = \frac{k_1}{1 + k_2(X^-)} (Fe^{2+})(O_2)(OH^-)(X^-) \qquad [44a]$$

$$\frac{-d(Fe^{2+})}{dt} = \frac{k_3(OH^-) + k_4(X^-)}{1 + k_5(OH^-) + k_6(X^-)} (Fe^{2+})(O_2) \qquad [44b]$$

where k_1 through k_6 are arbitrary names for combined rate and equilibrium constants and X^- is one of the anions mentioned.

The data of Tamura et al. (1976a) were confirmed by Sung and Morgan (1980) who found the rate constant for equation [41] to be $1.2 \pm 0.2 \times 10^{13}$ mol^{-2} l^2 atm^{-1} min^{-1} at an ionic strength of 0.11 mol($NaClO_4$) l^{-1}, PO_2 = 0.2 atm, pH = 6.84.

The Kinetic Salt Effect

The effects of ionic strength on the kinetics of ionic reactions are well known but not well understood. One interpretation of the effect of ionic strength is that it affects the activities of the reactants in the formation of an intermediate state, the activated complex. According to this theory, the rate limiting step in a reaction is the formation of products from the activated complex. The

complex is assumed to be in equilibrium with the reactant species, hence an equilibrium constant for the reaction can be defined:

$$K^* = \frac{a^*}{a_A a_B} \qquad [45]$$

where a^* is the activity of the activated complex and a_A and a_B are the activities of the reactants. By substituting the expression for activity $a = rc$, where r is the activity coefficient (r=1 in dilute solutions) and c the concentration, an expression for the concentration of activated complex can be derived:

$$c^* = c_A \; c_B \; K^* \; \frac{r_A \; r_B}{r^*}. \qquad [46]$$

Transition state theory has been used to derive an expression for the rate of reaction in terms of the bimolecular rate constant k_2, Planck's constant h, Boltzmann's constant k and temperature T:

$$-\frac{dc_A}{dt} = k_2 \; c_A \; c_B = \frac{kT}{h} \; c^*. \qquad [47]$$

The activity coefficient r can be estimated for ionic species up to ionic strengths between 100 and 500 mol m^{-3} by use of the Davies equation:

$$\log r = - A \; Z^2 \; (\frac{I^{0.5}}{(1 + I^{0.5})} - 0.3 \; I). \qquad [48]$$

By substituting the Davies equation in the logarithm of equation [47] and rearrangement an expression relating the rate constant k_2 to ionic strength is obtained:

$$\log k_2 = \log (K^* \frac{kT}{h}) + 2 \; A \; Z_A Z_B \; (\frac{I^{0.5}}{(1 + I^{0.5})} - 0.3I). \qquad [49]$$

The first term on the right side of the equation is constant at a constant temperature. The coefficent A = 0.512 at 25 C (Sposito, 1981), hence, 2A = 1.024, approximately 1. Thus, this is a linear expression with a slope equal to the magnitude and sign of the product of the charges of a pair of reactants. Assuming activated complex theory is an accurate description of the reaction, the overall rate constant is a sufficient estimate of the rate constant for decomposition of the activated complex, k_2.

Based on this analysis the $Z_A Z_B$ predicted by the Goto et al. (1970) mechanism (equation 42) for homogeneous oxidation of Fe^{2+} is (+1) (-1) for a product of -1. This implies that the rate of reaction will decrease as ionic strength increases. Background anions or cations which affect the charges of the reactant species will also change the product $Z_A Z_B$ and the response of reaction rate to ionic strength.

Kinetics of Heterogeneous Oxidation of Aqueous Iron(II)

As iron(II) is oxidized to iron(III) in neutral solution, the solubility product of iron(III) hydroxide is very quickly exceeded. Sung and Morgan (1980) found, for example, that o-FeOOH was formed in less than an hour. Solid phase iron(III) hydroxide can adsorb aqueous iron(II) and oxygen and catalyze the oxidation reaction. This is an autocatalytic reaction, since one of the products promotes

the reaction. Tamura et al. (1976b) found the rate of oxidation for the heterogeneous reaction to have a homogeneous part (as in equation [41]) and a heterogeneous part. The latter is determined by the fraction of adsorbed Fe^{2+}, the mass of iron(III) hydroxide, pH and oxygen pressure. At constant pH (6-7) and oxygen pressure, the rate expression was found to be:

$$\frac{-d(Fe^{2+})}{dt} = (k_1 + k_2(Fe^{2+}))(Fe^{2+}) \qquad [50]$$

where k_1 and k_2 are mixed rate constants for the homogeneous and heterogeneous reactions, respectively. Values for k_2 were measured for various iron(III) oxides at pH 6.5 and an oxygen pressure of 1 atm (Tamura et al., 1980). Amorphous iron(III) hydroxide (of two different preparations) gave the largest k_2 values, probably a function of surface area. The k_2 values for o-FeOOH, o-FeOOH and B-FeOOH were lower than $Fe(OH)_3$ and decreased in that order.

Using infrared spectroscopy and x-ray diffraction, Sung and Morgan (1980) identified o-FeOOH as the hydrated iron(III) oxide formed from Fe^{2+} oxidation around pH 7. The values they reported for k_1 and k_2 in equation [45] were 0.056 min^{-1} and 360 mol^{-1} l min^{-1} for 0.5 mol($NaClO_4$) l^{-1}, pH 7.2, oxygen pressure 0.2 atm and 25°C.. An inhibitory effect of Cl^- and SO_4^{2-} was noted for the heterogeneous reaction. Based on the theory of Tamura, et al. (1976a), this may be due to the formation of neutral Fe^{2+} ion pairs which are less reactive with the iron oxide solid phase.

Kinetics of Pyrite Oxidation-Dissolution

Most studies of pyrite oxidation have been conducted under conditions of extreme acidity found either in industrial processes or acid mine drainage. McKay and Halpern (1958) studied pyrite oxidation at high temperatures (100-130° C) and pressures (0-4 atm O_2) used in a uranium acid-pressure-leach process. They found a rate law for 0.0 to 0.15 M H_2SO_4 or $HClO_4$ first order in O_2 and dependent on pyrite surface area (Equation [46]):

$$\frac{-d(FeS_2)}{dt} = k\ A_{FeS_2}\ P_{O_2} \qquad [50]$$

The rate constant was defined as a function of temperature (Equation [51]):

$$k = 0.125\ \exp(-13300/RT)\ (M\ cm^{-2}\ atm^{-1}\ min^{-1}) \qquad [51]$$

Sulfate and Fe^{3+} were measured while elemental sulfur was observed and calculated by difference. This rate law has been used recently to describe chemical oxidation at low temperatures (30° C) (Hoffmann et al. 1981). Under conditions of constant temperature, oxygen pressure and surface area this equation reduces to a pseudo-zero order expression (i.e. constant rate of oxidation). This has been observed by Hoffmann et al. (1981), Goldhaber (1980), and Vlek and Lindsay (1978).

Garrels and Thompson (1960) conducted oxidation experiments at 33° C and atmospheric pressure. Oxygen was excluded and iron(III) (as $Fe_2(SO_4)_3$) was used as the

oxidant in sulfuric acid solutions between pH 0 and 2. Only the disappearance of Fe^{3+} was measured. The acidity had no effect on the reaction rate and it was concluded that the iron(II)/iron(III) ratio controlled oxidation rates. Singer and Stumm (1970, EPA, 1970) extended these findings to conclude that the rate-determining step in the formation of acid-mine drainage was the reoxidation of Fe^{2+} formed in the Fe^{3+}-mediated oxidation of pyrite. The rate law for the homogeneous oxidation of iron(II) of Stumm and Lee (1961) was applied for the pH-dependent rate between 4.5 and 6 (Equation [41]) and a pH-independent rate equation proposed for pH below 3.5 (Equation [42]).

While Fe(III) mediated oxidation of pyrite may be a reasonable mechanism in acidic media, the solubility of iron(III) compounds at neutral pH limits the rate of homogeneous oxidation of Fe(II). If this were the only mechanism, oxidation rates would be tremendously reduced at higher pH. Smith and Shumate (1970) studied the oxidation of pyrite at various oxygen pressures, temperatures, Fe^{3+} concentrations and pH, measuring consumption of oxygen and sulfate production. Two "dual site" adsorption-desorption reaction rate equations were proposed, one for Fe(III) and one for dissolved oxygen. The oxygen adsorption equation is:

$$\frac{-d(FeS_2)}{dt} = \frac{k_0\ C_0}{(1+(K_0\ C_0\ )^{1/2} + K_N\ C_N\ )^2} \qquad [52]$$

where C_0 is oxygen concentration, C_N is the concentration of an inert gas competing for the reaction site and K_0 and K_N are adsorption equilibrium constants for oxygen and the inert gas, respectively. The Fe^{3+} adsorption equation is:

$$\frac{-d(FeS_2)}{dt} = \frac{k_{Fe^{3+}}}{(Fe^{3+})^{-1/2} + (K_1)^{1/2}} \qquad [53]$$

under the conditions that Fe(II)/Fe(III) is extremely small (oxidizing conditions) and K_1 is the adsorption constant for Fe^{3+}.

Smith and Shumate (1970) reported an increase in the rate of pyrite oxidation with pH. This is what would be expected if the mechanism of oxidation involved Fe^{3+} as described by Singer and Stumm (1970).

The rate of oxidation of pyritic sulfur is usually ignored (assumed very rapid). In recent years the fate of pyrite sulfur has been studied in increasing detail. Goldhaber and Reynolds (1977) and Goldhaber (1980) observed the rate of production of reduced sulfur intermediates in pyrite oxidation, including thiosulfate, mono-, di- and trisulfane disulfonate and sulfite. In highly controlled, short term experiments at 30°C they observed zero order rates of production for all species. The distribution of sulfur species varied over the pH range 6-9, which they were unable to explain. Steger and Desjardins (1978) also

observed thiosulfate as a major reaction product of pyrite under humid conditions.

A novel mechanism for metal sulfide oxidation (FeS) was proposed by Thom et. al. (1978). It was suggested that sulfite might be able to effectively oxidize iron sulfide through an adsorption mechanism. Thiosulfate was the major product observed, however, it was supposed that sulfane disulfonates and elemental sulfur were also being formed from the thiosulfate intermediate. Habashi (1981) argued that these observations were only of the secondary oxidation of elemental sulfur formed initially from electrochemical FeS oxidation.

Considerable evidence exists that pyrite sulfur does not oxidize instantaneously to sulfate. The electrochemical mechanism (equations [3a] and [3b]) presumes the formation of elemental sulfur, which is itself relatively inert, and also forms other reduced sulfur compounds. Sato (1960b) predicted that a series of sulfur oxidation reactions would be found involving diatomic sulfur which would parallel the iron(II)-iron(III) reaction. In addition to the electrochemical evidence already discussed, steric arguments concerning the structure of pyrite were invoked. Essentially, pyritic sulfur is diatomic within the crystal structure and would logically exit the structure in this conformation.

Structural Chemistry of Pyrite

The unit cell of pyrite is cubic with a cell length of 0.5404 nm (Elliott, 1960). This structure is characteristic of a group of metal sulfides and arsenides common enough to be called the "pyrite" structure.

The iron atoms of FeS_2 are octahedrally coordinated with paired sulfur atoms (Figure 4). The interatomic distances for sulfur to sulfur and iron to sulfur are 0.2171 and 0.2259 nm, respectively (Elliott, 1960). Based on the paramagnetic susceptibility of pyrite, which is nearly zero, the iron(II) atoms of pyrite are in the low-spin state with six electrons paired in the three bonding 3d orbitals and the two 3d antibonding orbitals empty (Kostov and Minceva-Stefanova, 1982, Elliott, 1960). These empty orbitals allow pyrite to exhibit semiconductor properties (both n and p type). This also permits transfer of electrons from anodic regions of the pyrite crystal to cathodic regions where they are consumed in the reduction of oxygen or iron(III).

The sulfur atoms of pyrite form hybrid orbitals with a closed-shell configuration. The filled antibonding 3p-II orbitals of the sulfur result in a sulfur to sulfur interatomic distance which is somewhat greater than that of elemental sulfur. The degree of sharing of the II^*-3p electrons with the iron(II) also influences the sulfur to sulfur bond length (Elliott, 1960). Oxygenation of the

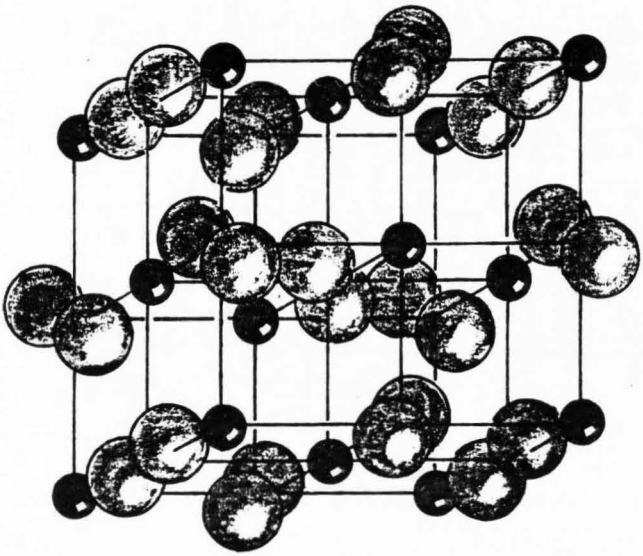

Figure 4. Pyrite crystal structure (redrawn from Wyckoff, 1948). Small spheres represent iron. Large spheres represent sulfur.

disulfide to thiosulfate would result in minimal disruption of the orbital structure while decreasing the total formal oxidation state of the sulfur.

Structural Chemistry of Soluble Reduced Sulfur Compounds

Sulfur has oxidation states ranging from -2 (as in H_2S, hydrogen sulfide) to +6 (as in H_2SO_4). Pyrite sulfur has an oxidation state of -1. Oxidation products observed, in order of oxidation states, are elemental sulfur (S through S_8), thiosulfate ($S_2O_3^{2-}$), sulfane disulfonates ($S_nO_6^{2-}$), sulfite (SO_3^{2-}) and sulfate. The structures of these compounds suggest their chemical interactions.

Elemental sulfur is most stable as a ring of eight sulfur atoms. Shorter chains of sulfur atoms are likely to occur, but do not form stable rings. Thiosulfate (Figure 5) consists of a single sulfur bound to a tetrahedral sulfonate group ($-SO_3$) and has simple C_{3V} symmetry. The sulfane disulfonates have only recently been accurately characterized (Ferrari, et al., 1977, Foss and Hordvick, 1964, Marøy, 1971). These consist of chains of sulfur atoms (sulfanes) with sulfonate groups at both ends of the chain (Figures 6, 7, 8 and 9). Both sulfite and sulfate have simple tetrahedral conformation. Sulfate has T_d and sulfite C_{3V} symmetry (Banister et al., 1968).

The bond lengths between sulfur atoms vary within the chain (Figures 5-9). The two sulfurs of thiosulfate have a

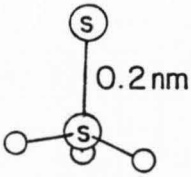

Figure 5. Thiosulfate.

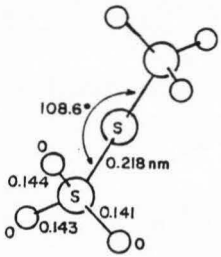

Figure 6. Monosulfane disulfonate (redrawn from Ferrari et al., 1977).

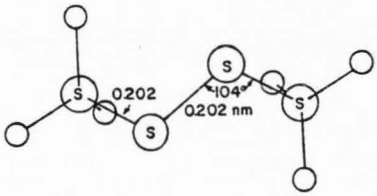

Figure 7. Disulfane disulfonate (Foss and Hordvik, 1964).

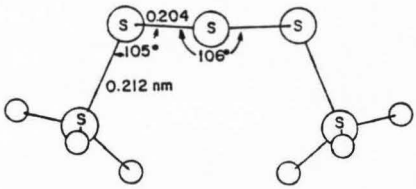

Figure 8. Trisulfane disulfonate (Marøy, 1971).

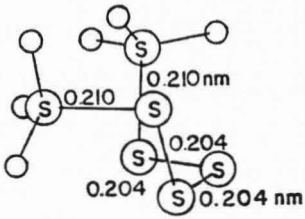

Figure 9. Tetrasulfane disulfonate (Marøy, 1973).

bond length of 0.200 nm. This is similar to the bond lengths of the internal sulfurs of the sulfane disulfonates (0.202 to 0.204 nm), the sulfanes and elemental sulfur (Cotton and Wilkinson, 1980). The shortness of the sulfur-oxygen bond is attributed to dll-pll multiple bonding (Cotton and Wilkinson, 1980). The sulfur-sulfur bond between the last sulfane sulfur and the sulfonate sulfur of the sulfane disulfonates is lengthened (0.212 nm) compared with the sulfane sulfur-sulfur bonds. This is due to delocalization of electrons in the pll orbital of the sulfane sulfurs (multiple bonding) while the electrophilic nature of the oxygen atoms of the sulfonate weakens the sulfonate sulfur to sulfane sulfur bond (Kwart and King, 1977, Schmidt and Siebert, 1973). This makes the terminal sulfur of the sulfane the best point of attack by a nucleophile such as sulfite or thiosulfate. It is the concantenation properties of sulfur which makes the chemistry of sulfur oxidation so complex.

Mechanisms of Aqueous Sulfur Oxidation

The homogeneous oxidation of sulfur is much less understood than iron(II). The problem is the numerous different products which result from the oxidation of $H_2S(aq)$ and the complexity of the reaction pathways necessary to explain their dependence on pH and concentrations. The mixture formed is often referred to as "Wackenroder's liquid" after a 19th century pharmaceutical

chemist who studied the reaction of $H_2S(aq)$ with $SO_2(aq)$ in a solution of hydrochloric acid (Wackenroder, 1847). The mixture of sulfur compounds formed includes thiosulfate, elemental sulfur, sulfane disulfonates, sulfite and sulfate, (Lyons and Nickless, 1968).

There has been considerable progress in recent years in the clarification of the mechanisms of sulfur oxidation. The breakthrough in research was due to the development of tracer experiments using ^{35}S. The experiments of Christiansen and Drost-Hansen (1949) confirmed the importance of neucleophilic displacement reactions in the sulfane disulfonates. Their experiment showed that labelled sulfite displaced thiosulfate from disulfane disulfonate in a relatively neutral solution (pH 6.1) as shown in equation [54].

$$S_4O_6^{2-} + {}^{35}SO_3^{2-} = {}^{35}S_3O_6^{2-} + S_2O_3^{2-} \qquad [54]$$

Fava and Divo (1953a, 1953b) conducted decomposition experiments with labelled disulfane and monosulfane disulfonates. In strong alkali (pH 14) hydroxide displaces thiosulfate from both compounds, leaving either sulfite or sulfate from disulfane and monosulfane disulfonates, respectively (equations [55] and [56]).

$$2\ S_4O_6^{2-} + 6\ OH^- = 3\ S_2O_3^{2-} + SO_3^{2-} + 3\ H_2O \qquad [55]$$

$$2\ S_3O_6^{2-} + 6\ OH^- = S_2O_3^{2-} + 4\ SO_4^{2-} + 3\ H_2O \qquad [56]$$

In neutral solutions, water would react in a similar manner

with monosulfane disulfonate (equation [57]).

$$S_3O_6^{2-} + H_2O = S_2O_3^{2-} + SO_4^{2-} + 2\ H^+ \qquad [57]$$

Several acid reactions with thiosulfate, monosulfane and disulfane disulfonate were also indicated. Thiosulfate displaces sulfite in the reverse of equation [54], resulting in higher order sulfane disulfonates (equations [58] and [59]).

$$S_2O_3^{2-} + S_3O_6^{2-} + H^+ = S_4O_6^{2-} + HSO_3^{2-} \qquad [58]$$

$$S_2O_3^{2-} + S_4O_6^{2-} + H^+ = S_5O_6^{2-} + HSO_3^{2-} \qquad [59]$$

The acid decomposition of thiosulfate to form sulfite and elemental sulfur was also evident.

Foss (1958) summarized the properties of the nucleophilic displacement reaction for sulfane disulfonates (equation [60]).

$$S_nO_6^{2-} + S_2O_3^{2-} = S_{n+1}O_6^{2-} + SO_3^{2-} \qquad [60]$$

The displacement reaction occurs at the second sulfur of the sulfur chain. The sulfonate sulfur and the terminal sulfane sulfur are displaced in the reverse reaction and the sulfonate sulfur in the forward reaction. The site of sulfite insertion is shown in Figure 10 for a representative sulfane disulfonate. This mechanism was only recently confirmed by Wagner and Schreier (1978a, 1978b).

The use of chromatographic separations has permitted

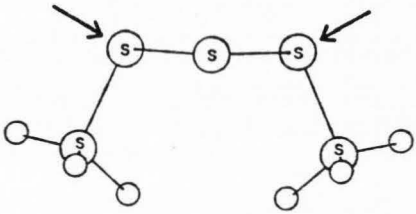

Figure 10. Sites (at arrows) for nucleophilic displacement of thiosulfate from trisulfane disulfonate.

the sorting of reaction products of thiosulfate and sulfane disulfonate decomposition. Blasius and Kremer (1962) showed that the acid decomposition of thiosulfate to sulfite, sulfur and sulfane disulfonates was more complex in concentrated acid than weak acid. In neutral to alkaline solution Blasius and Wermbeter (1962) demonstrated that disulfane disulfonate was quite inert, persisting for at least 30 days without extensive oxidation or decomposition. At higher pH there is some redistribution of sulfur to mono, tri and tetrasulfane disulfonate (equation [61]).

$$4\ S_4O_6^{2-} + 6\ OH^- = 2\ S_3O_6^{2-} + 5\ S_2O_3^{2-} + 3\ H_2O \qquad [61]$$

Trisulfane disulfonate tends to decompose more rapidly, forming mostly disulfane disulfonate, which is more persistent. Pollard, et al. (1964a, 1964b) confirmed the results of Blasius and coworkers, also showing that mono and disulfane disulfonates are relatively inert (at least 12 hours) in neutral to acidic solutions, even in the presence of thiosulfate. The removal of sulfite from the reaction by formalin had little effect on product distribution except at high acidities, where it promoted the formation of higher order sulfane disulfonates (equation [60]).

Sulfane disulfonates are relatively inert in aqueous solution. The length of the most inert sulfane disulfonate species decreases as acidity decreases from concentrated acids (Wackenroeder's liquid) to neutral or mildly alkaline solutions. Decomposition to thiosulfate, sulfite and sulfate occurs most rapidly at high pH. Sulfur from thiosulfate

decomposition was reported mainly in acidic solutions (Blasius and Kremer, 1962, Fava and Divo, 1953a, 1953b).

Thermodynamics of Reduced Sulfur Compounds

The distribution of reduced sulfur compounds in simple solutions appears to follow a regular pattern as pH increases. Goldhaber (1980) reported that product distribution in short-term pyrite oxidation experiments changed dramatically between pH 7 and 8. Below pH 7, the sulfur produced was found as disulfane disulfonate and sulfate. Above pH 8, thiosulfate became the predominant sulfur form followed by sulfate, disulfane disulfonate and sulfite (Figure 11). This phenomenon can be explained in terms of thermodynamic stabilities.

When a stability diagram is constructed for sulfur utilizing all thermodynamic data for all known redox reactions and species, a very simple picture results. Sulfate is more stable than any other oxygen-containing sulfur compounds and dominates the diagram. Elemental sulfur may occur as a stable species at higher acidities and hydrogen sulfide is the stable reduced species. Unfortunately, such a diagram provides no information concerning the relatively inert species thiosulfate and disulfane disulfonate or the more probable initial sulfur product of pyrite dissolution, disulfane (S_2^{2-}).

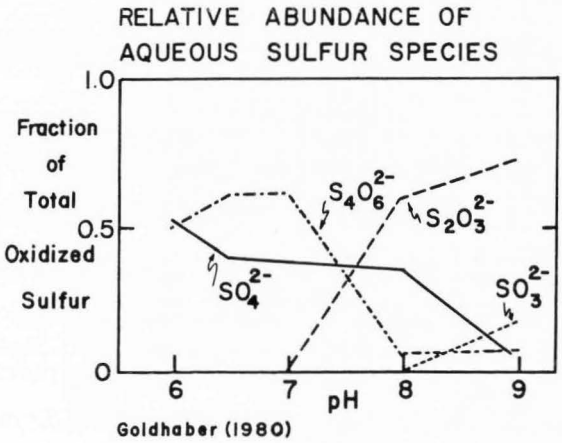

Figure 11. Relative abundance of aqueous sulfur species (as S) produced during short-term oxidation experiments as a function of pH. Partial pressure of oxygen 0.2 (Goldhaber, 1980).

A more useful approach to the thermodynamics of reduced sulfur species is to ignore sulfate and its reactions, replacing it with sulfite, a less oxidized, more reactive species. Sulfate is a relatively inert species. Sulfite and other reduced sulfur compounds are more reactive and, thus, more likely to reach equilibrium. The only attempt at such an approach was by Valensi (1973). Figure 12 is similar to those of Valensi (1973), but utilized the thermodynamic data of Garrels and Christ (1965), Lindsay (1979) and Schwartzenbach and Fischer (1960). Most significant is the pH independent boundary between disulfane disulfonate and thiosulfate at pe -0.5 and pH 5 to 7. Thus, as pH increases, thiosulfate becomes thermodynamically stable with respect to disulfane disulfonate, something not expected in terms of sulfur oxidation states.

When the stability of reduced sulfur compounds is plotted using the transformed redox parameter pe+pH it becomes evident that as pH increases, the stability field for sulfite also increases as that for thiosulfate decreases (Figure 13). Clearly there is a thermodynamic basis for the distribution of sulfur compounds formed during pyrite oxidation.

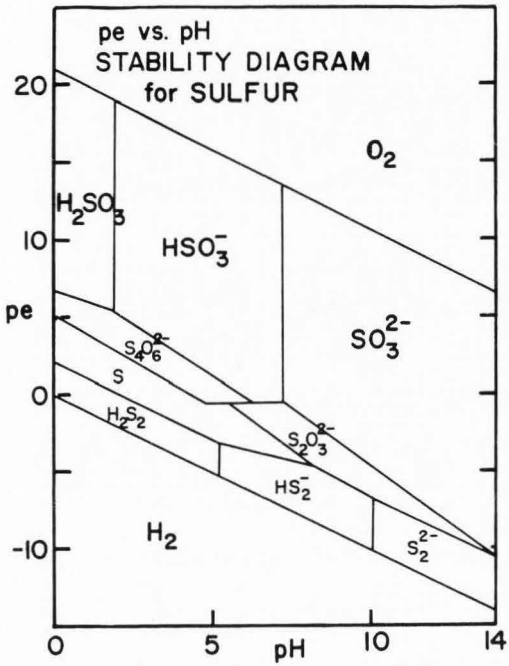

Figure 12. Redox (pe) stability diagram for reduced sulfur compounds as a function of pH. Assumed total sulfur concentration 10^{-3} M.

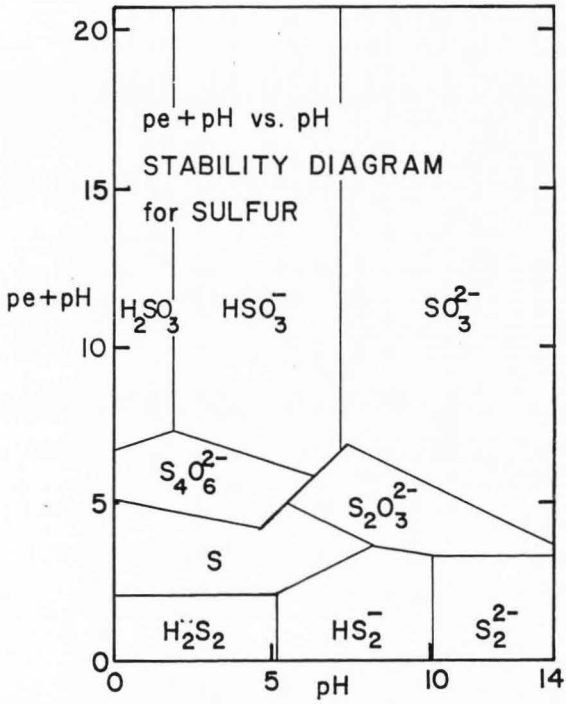

Figure 13. Transformed redox (pe+pH) stability diagram for reduced sulfur as a function of pH. Assumed total sulfur concentration 10^{-3} M.

Kinetics of Aqueous Sulfur Oxidation

The application of nucleophilic displacement reaction mechanisms to sulfur oxidation kinetics has been limited. Foss and Kringlebotn (1961) found that the rate constants for the addition of thiosulfate to sulfane disulfonates (equation [56]) were apparenly similar no matter what the length of the sulfane. At pH 6.8 there is no change in ionic strength during the reaction and a positive salt effect, which is consistent with a reaction between similarly charged ions. The rate law derived for the disappearance of thiosulfate in the complex reaction was:

$$\frac{-d(S_2O_3^{2-})}{dt} = k_2\ C_d\ (S_2O_3^{2-}) \qquad [62]$$

where $k_2 = 1.3 \times 10^{-3}\ mol^{-1}\ L\ s^{-1}$ is the rate constant for the addition of thiosulfate to disulfane disulfonate and C_d is the initial concentration of disulfane disulfonate.

An earlier study of the kinetics of thiosulfate decomposition in acidic solutions (Davis, 1958) included terms for H^+ concentration (equations [63a] and [63b]).

$$\frac{d(S_8)}{dt} = k_a\ (S_2O_3^{2-})^{3/2}(H^+)1/2 \qquad [63a]$$

$$\frac{d(SO_3^{2-})}{dt} = k_b\ (H)\ (S_2O_3^{2-})^2 \qquad [63b]$$

The mechanism identified as consistent with these rate laws was based on the proposals of Schmidt and Heinrich (1958) that long chain sulfane monosulfonates were important reaction intermediates. Sulfane monosulfonates other than

thiosulfate have not been found (Nickless, 1968).

The kinetics of sulfide oxygenation in dilute solutions has been studied extensively in recent years. Cline and Richards (1969) measured the disappearance of S^{2-} (aq) and O_2 (aq) from natural seawater at a neutral pH of 7.5 to 7.8. The rate of oxidation was found to be approximately first order for both oxygen and sulfide. They noted a catalytic effect of Fe^{2+} (aq) which favored the formation of thiosulfate. They measured the amount of thiosulfate and sulfite formed, but did not measure sulfate. Chen and Morris (1972) found initial sulfide oxidation rates in various buffers 1.34 order in sulfide and 0.56 order in oxygen. Peak rates of oxidation were measured at pH 7.5 and 11 and a minimum rate occurred below pH 6, all apparently independent of the pH buffers used (no allowance was made for specific salt effects). They supposed that sulfanes were the major products in the pH 9 region.

O'Brien and Birkner (1977) found a rate expression for the disappearance of sulfide and oxygen at pH 7.55 (equation [64]).

$$\frac{-d(S^{2-})}{dt} = k\ (S^{2-})^{1.02}\ (O_2)^{0.8} \qquad [64]$$

Sulfite and thiosulfate were also measured and the latter was a "stable" product with a rate of appearance zero order in oxygen concentration. Like the other studies, sulfate was estimated by difference, which was as much as 50% of the oxidized sulfur.

In none of these studies was the amount and distribution of products measured during the course of the reaction. This is unfortunate since the sulfite and thiosulfate detected and the excess of sulfide constitute the reactants of a Wackenroeder-type solution. Thus, it is possible that extensive interactions between reactants and products would confound empirically derived kinetic relations.

The reaction mechanism which has been assumed for aqueous sulfide oxygenation explains only the formation of sulfur, sulfite and thiosulfate (Abel, 1956). Clearly a more complex mechanism needs to be considered to include the sulfane disulfonates and sulfate in neutral solutions.

Microbial Catalysis of Pyrite Oxidation

The role of bacteria in promoting pyrite oxidation is well documented. The ecology of mixed populations of iron and sulfur oxidizing bacteria over the pH continuum has not been clearly defined, however.

Thiobacillus ferrooxidans is an acidophilic, chemoautotrophic bacterium which oxidizes iron(II) to iron(III) and also some sulfur compounds. It prefers a pH of 2.0 to 4.5; growth is optimum at pH 2.5 to 3.5 (Alexander, 1977). It is capable of surviving at higher pH (LeRoux et al.,1980, Kleinman and Crerar, 1979) but its influence on pyrite oxidation at alkaline pH should be questioned (Arkesteyn, 1980). Other, heterotrophic bacteria are also

capable of iron oxidation, including Metallogenium, which has an optimum pH range of 3.5 to 5.0 (Alexander, 1977). These organisms apparently do not oxidize sulfur.

Several other species of the genus Thiobacillus are capable of oxidizing various forms of sulfur. These include T. thiooxidans, T. thioparus, T. novellus, and T. denitrificans. All except for T. novellus are obligate chemoautotrophs and all are strict aerobes except T. denitrificans, which is a facultative anaerobe. Like T. ferrooxidans, T. thiooxidans is acidophilic, preferring a pH of 2.0 to 3.5. The other Thiobacilli prefer neutral to alkaline pH (Alexander, 1977).

Heterotrophic bacteria, yeasts and fungi are also apparently capable of oxidation of sulfur non-metabolic purposes. Members of the genuses Artrobacter, Bacillus, Flavobacterium, and Pseudomonas are able to oxidize elemental sulfur and thiosulfate to sulfate and Streptomyces are able to oxidize sulfur to thiosulfate (Alexander, 1977).

A mechanism of bacterial catalysis of pyrite oxidation was proposed by Temple and Delchamps (1953). The first step is a non-biological oxidation/dissolution of pyrite to form an acidic iron(II) sulfate solution:

$$FeS_2 + H_2O + 7/2\ O_2 = FeSO_4 + H_2SO_4. \qquad [65]$$

The iron(II) in solution is then oxidized by T. ferrooxidans to form an acid iron(III) sulfate solution:

$$2\ FeSO_4 + 1/2\ O_2 + H_2SO_4 = Fe_2(SO_4)_3 + H_2O \qquad [66]$$

Iron(III) is reduced at the surface of pyrite, regenerating iron(II) and oxidizing more pyrite:

$$Fe_2(SO_4)_3 + FeS_2 = 3\ FeSO_4 + 2\ S \qquad [67]$$

The elemental sulfur produced may be oxidized chemically by iron(III) or "biologically" by T. thiooxidans by equations [68] or [69], respectively:

$$2\ S + 6\ Fe_2(SO_4)_3 + 8\ H_2O = 12\ FeSO_4 + 8\ H_2SO_4 \qquad [68]$$

$$S + 3/2\ O_2 + H_2O = H_2SO_4 \qquad [69]$$

This sequence of reactions is widely accepted as the primary mechanism for acid production from pyrite oxidation in acid mine wastes (Singer and Stumm, 1970, Smith and Shumate, 1970, 1971, Stumm-Zollinger, 1972).

The kinetics of pyrite oxidation in the presence of microbial catalysts have been studied extensively. Stumm-Zollinger (1972) found zero order kinetics which were dependent on Ferrobacillus ferrooxidans biomass. Others, including Hoffman, et al. (1981), have related microbial growth rates to pyrite oxidation rates. Microbial growth is described by the Michaelis-Menten equation:

$$\frac{dB}{dt} = \frac{u_m\ A}{K + A}\ B \qquad [70]$$

where B is the "concentration" of active organisms, u_m is the maximum specific growth rate constant (t^{-1}), A is the surface area of the pyrite and K is the concentration of FeS_2 supporting maximum growth. The oxidation of pyrite is expressed as:

$$\frac{-d[FeS_2]}{dt} = \frac{u_m\ A}{(K + A)}\ \frac{B}{Y} \qquad [71]$$

where Y is the cell yield coefficient determined by:

$$\frac{dB}{dt} = -Y \frac{d[FeS_2]}{dt}. \qquad [72]$$

Bacterial catalysis of pyrite oxidation at pH 2.0 to 3.5 was modelled by Hoffman et al. (1981) using these equations. Unfortunately, rate constants had to be determined separately for each strain of bacteria tested.

While the role of microorganisms in pyrite oxidation below pH 3.5 is well established, their importance at neutral to alkaline conditions has not been resolved. T. ferrooxidans does not grow very well at pH greater than 4.0 when the pH is monitored and adjusted daily (Bloomfield, 1972). It can survive at least short periods of lowered acidity, but activity is suppressed until the pH returns to normal (Kleinman and Crerar, 1979, LeRoux, et al. 1980).

Arkesteyn (1980) systematically studied the relationship between microbial catalysis of pyrite oxidation and pH. This work confirms that T. ferrooxidans is the only Thiobacillus which effectively catalyzes the rate of oxidation of pyrite. Sulfur oxidizers T. thiooxidans, T. thioparus, T. perometabolis and T. intermedius had no effect on the overall rate of oxidation in the presence or absence of T. ferroxidans. The sulfur oxidizers apparently utilize S as it is released from pyrite by an independent mechanism, biological or physical. Innocculated and sterile pyrite preparations exhibited nearly identical oxidation rates (as iron and sulfur) in chemostats maintained at pH 7-8. These

rates were approximately half the microbially catalyzed rates at pH 2-3 as measured by iron alone. Calcium carbonate, while preventing a pH drop, did not affect non-biological oxidation of pyrite. Microbial catalysis of pyrite oxidation does not occur at neutral to alkaline pH even in the presence of Thiobacilli.

Pyrite Oxidation in Soils and Overburden

The acidification of soils resulting from pyrite oxidation is a complex process. In addition to the effects of surface area, pH and microbial catalysis, many other factors are important in determining the rate of oxidation in soils. These include the physical form of the pyrite (ie. reactive surface), the presence of lime, nutrients, moisture content and aeration.

Smith and Shumate (1970) showed that the morphology of the pyritic material had a large effect on the rate of oxidation. "Sulfur ball" pyrite separated from coal had a surface area of 1.12 m^2 g^{-1} (for the 60 to 150 mesh portion) while the same size fraction of ground, museum grade pyrite (massive crystals) had a surface area of only 0.12 m^2 g^{-1}. The rates of oxidation for the "sulfur ball" were an order of magnitude higher under the same conditions (12 pmol s^{-1} g^{-1} and 300 pmol s^{-1} g^{-1}, respectively). Pugh et al. (1981) found similar disparities in surface area between crushed massive pyrite and microcrystalline

"framboidal" pyrite from lignite. Surface areas of crushed massive pyrite were around 0.5 m^2 g^{-1} while framboidal pyrite had a surface area between 2 and 4 m^2 g^{-1}. This resulted in a much higher rate of oxidation of framboidal pyrite in weathering studies (Pugh et al., 1984). Vlek and Lindsay (1978) showed that for pyrite to be a useful soil amendment for sodic soils it must be very finely disintigrated to increase its reactive surface.

The effect of pH and lime (which raises the pH) on pyrite is not clearly understood. While Singer and Stumm (Harvard, 1970) would predict and Smith and Shumate (1970) showed in the laboratory that pyrite does oxidize several times faster under alkaline conditions, some research indicates the opposite (Ainsworth and Blanchar, 1984, Carrucio et al., 1981, MacIntyre et al., 1930). This is probably due to establishment of Thiobacillus ferrooxidans at low pH, although Bloomfield (1972) and Arkesteyn (1980) did not find this effect as dramatic as predicted by Singer and Stumm (1970).

In the presence of lime, oxidation rates are usually measured as a function of appearance of sulfate or acid production (Ainsworth and Blanchar, 1984, Carrucio et al., 1981, Arkesteyn, 1980, Bloomfield, 1972, MacIntyre et al., 1930). Reduced sulfur forms are rarely measured. Nor and Tabatabai (1977) measured sulfur oxidation in incubated soil samples and found that disulfane disulfonate was produced and persistent at pH 6.0 and 5.4 over two months.

The addition of phosphate fertilizers to soils containing pyrite apparently supresses oxidation rates (Weir, 1975). This contrasts with the stimulatory effect of phosphate on sulfur oxidation, particularly in neutral soils in the presence of lime (Bloomfield, 1967). Quispel et al. (1952) showed the oxidation rate of pyrite was less in phosphate buffers at pH 5.8 and 7.8 than phthalate and borate buffers at similar pH values. Apparently, iron(III) phosphate precipitated, removing it as an oxidant.

Chemoautotrophic microbial catalysts require inorganic nutrients for the oxidation of sulfur. Hoffman et al. (1981) adjusted N/P ratios to achieve optimum microbially catalyzed leaching rates in a coal slurry with minimum inhibition by phosphate complexes and precipitates. Ammonium salts were a better nitrogen source than urea.

Although excessive concentrations of metals found in acidic mine tailings may be toxic to plants, in spite of liming (Peterson and Nielson, 1973), they apparently do not affect microbial catalysis of pyrite oxidation (Bloomfield, 1972).

Moisture probably has a critical effect on pyrite oxidation in soils. Smith and Shumate (1970, 1971) found that as the ratio of pyrite to water was increased in their respirometers, the oxidation rate in the presence of microbial catalysts reached a plateau, while chemical oxidation rates continued to increase. At low water

contents, high salt concentrations probably inhibit microbial activity and chemical oxidation rates probably exceed biological rates. Kleinman and Crerar (1979) showed that periodic flushing of oxidation products allows bacterial activity to continue to contribute to oxidation. They also found that the bacterial contribution to oxidation was negligible under stagnant, saturated conditions.

Geidel (1980) found that the amount of acidity released by a coal sample was largely independent of the frequency of flushing. At higher frequencies, acid concentration was lower, hence acid products must accumulate at a constant rate under drying conditions. This contrasts with the production of alkalinity from shale, which was proportional to the frequency of flushing. The columns used in this experiment did not include a mixed shale-pyritic coal treatment. The presence of acid-producing material should cause the shale to weather more rapidly, and the higher pH should also affect the rate of oxidation of the pyrite.

The most important factor in oxidation of pyrite in soils appears to be aeration or oxygen concentration. Smith and Shumate (1971) calculated that the diffusion rate of oxygen through water was slow enough to restrict the rate of of oxidation of pyrite in flooded mines. This has been applied in reclamation of acid minesoils where by burying acid producing materials under a thin layer of soil it is hoped that acidification will be reduced and and revegetation occur (Sorenson et al., 1980).

Pyrite Oxidation and Soil Development

Acid sulfate soils are formed generally in poorly drained or recently drained areas where pyrite has been deposited under anaerobic conditions. Van Breemen (1982) has identified a sequence of development in which the nearly neutral (pH 6), unweathered pyritic material first oxidizes to form a highly acidic (pH 3-4) jarosite-rich horizon. This is followed by further oxidation and leaching to form an iron(III) oxide rich horizon which is less acidic (pH 5-6). Oxidation rates are limited by the slow diffusion of oxygen into the soil. Overall soil development is slowed by the poor growth of vegetation and low evapotranspiration. The jarositic horizon is well buffered at pH 3-4 by the presence of the minerals jarosite and amorphous $Fe(OH)_3$ (Miller, 1980).

Under well drained conditions, pyritic parent material can develop into neutral soils. Singh et al. (1982) found that pyritic sandstone weathered to form slightly acidic (pH 5) soils that were low in sulfate and high in exchangeable aluminum and oxidized iron. As the sandstone weathered, mica within it was apparently converted to vermiculite by the acid conditions. The weathered sandstone was fairly acidic in the top six meters, but low in total sulfur, which had already been leached to a deeper stratum. Below six meters, sulfur concentrations were higher but the rock was otherwise

relatively unweathered with a nearly neutral pH.

The revegetation of pyritic mine spoils is severely limited by physical and chemical characteristics of spoils which distinguish them from acid sulfate soils. Drainage tends to be relatively good due to the recent disturbance of the material. This makes them prone to drying, which harms plant establishment (Barnhisel et al., 1982) and might also allow greater ease of entry of oxygen and deeper oxidation.

Because of the relatively unweathered nature of spoils, they are generally poor in macronutrients, particularly potassium and phosphorus (Peterson and Nielson, 1973, Barnhisel et al., 1982). Liming has been observed to have an adverse effect on plant yields, in spite of concurrent fertilization. This is usually attributed to the presence of unusually high concentrations of metals which might further inhibit growth. This may also be a result of stabilization of more toxic reduced sulfur species thiosulfate ant sulfite as suggested by the data of Goldhaber (1980) in Figure 11.

Liming may also cause unusually high salt concentrations in spoils, particularly when magnesium contents are high in the liming material (Grove and Evangelou, 1982). This can cause dispersion of soil colloids and dramatic reduction in hydraulic conductivities, further exacerbating the problem of water availability (Evangelou et al., 1982).

Effect of Reduced Sulfur Compounds on Plant Growth

The effect of reduced sulfur componds on plant growth has been studied extensively for atmospheric pollutants (Taylor and Selvidge, 1984, Addison et al., 1984), but the role of the soil atmosphere appears to be relatively unexplored. Sulfur dioxide, is known to be quite toxic to plants, causing visible chlorosis and leaf burn. This gas dissolves in water to form sulfite in a manner similar to the way carbon dioxide forms carbonate. The distribution of protonated sulfite species is shown in Figure 14. Above a pH of approximately 7 the fully dissociated sulfite anion is the predominant species. This may be related to the persistence of sulfite at higher pH shown by Goldhaber (1980).

Addison et al. (1984) noted a predisposition of conifers grown on oil sands to more rapid decline in photosynthetic activity on fumigation with low levels of SO_2 (15.2 umol m^{-3}). Sodium and heavy metal toxicity were suggested as possible synergists. It may be that sulfite or other reduced sulfur compound from pyrite or organic sources in the tailings might contribute to the problem.

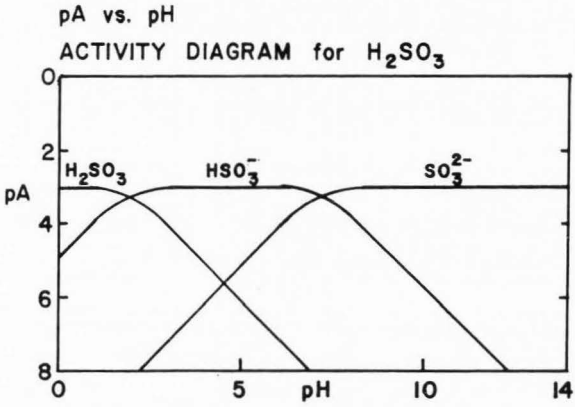

Figure 14. The distribution of sulfite species in water as a function of pH. Assumed total sulfite activity of 10^{-3} M.

Summary

The oxidation of pyrite involves a complex reaction. Analysis of the components and phases of the reaction shows that their number is not limited by the phase rule. For each additional component, an additional reaction maintains the validity of the phase rule. While thermodynamics can describe the overall oxidation of pyrite, it cannot predict the existence of unknown components and reactions. This has made it possible for thermodynamic analysis of pyrite oxidation oxidation to ignore sulfur oxidation reactions while treating the simpler iron oxidation reaction quite thoroughly.

The interdependence of redox potential (pe) and pH is related to the constraints of the phase rule and the standard state defined for pe. The combined term pe+pH can be used to separate the water redox reaction from the redox reaction of the component of interest in the aqueous phase.

The kinetics of pyrite oxidation can be treated as an overall reaction, or the reaction may be divided into its parts. The overall reaction order is related to experimental conditions, but depends on oxygen pressure, surface area and the concentration of other oxidants such as Fe^{3+}. At low pH (4-5) the reaction rate depends on the rate at which Fe^{2+} can be reoxidized to Fe^{3+}. At high pH (6-9) the rate is dependent on the rate at which oxygen can be reduced at the pyrite surface.

In order for a mechanistic description of any reaction to be make, all reactants and products must be known. This interest in mechanism distinguishes the kinetic analysis of a reaction from the thermodynamic analysis. Accordingly, it is necessary to sulfur oxidation reactions in addition to iron oxidation in order to allow a complete description of pyrite oxidation. This would account for the inability of electrochemical analysis based in thermodynamic theory to satisfactorily describe reactions at the pyrite electrode.

Oxidation of pyritic sulfur involves a loss of seven electrons per atom compared with a one electron loss for iron. Accordingly, there are many intermediate steps in the sulfur oxidation reaction. The components include the sulfanes, "elemental" sulfur, thiosulfate, the sulfane disulfonates and sulfite. The distribution of these products is pH dependent, with longer sulfane disulfonates and "elemental" sulfur predominant at lower pH and thiosulfate and sulfite at higher pH. This product distribution can be predicted by the nucleophilic displacement reaction, which produces longer or shorter sulfane disulfonates, and the alkaline decomposition of thiosulfate, which produces sulfite. The interconversion of thiosulfate and sulfane disulfonate is also an important reaction. Thermodynamic data is limited, but can be used to describe this system.

While microbiological processes are known to mediate to pyrite oxidation reaction, the acidophilic nature of the

organisms involved limit their influence at neutral to high pH. Other organisms may be important in sulfur oxidation under these conditions.

The interactions of reduced sulfur (non-sulfate) compounds with each other and other soil components such as metal oxides or lime may be useful in the study of soil development and reclamation. Reduced sulfur componds may be implicated in the reduction and transport of toxic metals. These sulfur compounds may be toxic themselves. Liming as a management practice may exacerbate any problems with sulfur by stabilizing sulfite and thiosulfate.

METHODS

Characterization of the Minerals Used

The pyrite used for this study was a ground, relatively pure mineral obtained from Kennecot Mining Corporation, Salt Lake City, Utah. Its density was measured by the displacement of water. Mineral purity was measured by fractionation: rinsing with concentrated HF to remove silicate minerals followed by digestion at 95°C in concentrated HNO_3 (Begheijin et al., 1978). Analysis of total iron and other metals was by standard atomic absorption methods.

The pyrite was prepared for the weathering experiments by washing with concentrated HF to remove iron oxides, silicate minerals and salt contaminants. This was followed by an ethanol rinse and drying at room temperature in a vacuum dessicator at approximately 1.3 Pa (10 um Hg). The sample was sieved and the less than 250 um (60 mesh) material used in experiments. A size analysis was performed and an estimate of surface area for each size fraction calculated geometrically, based on cubic forms.

The total surface area of untreated pyrite in the less than 250 um sieved fraction was determined using the standard ethylene glycol method (Bower and Gschwend, 1952). Samples of approximately 1 g placed in tared aluminum

moisture cans were dried in the presence of anhydrous P_2O_5 in a vacuum dessicator at about 1.3 Pa. After a constant weight was attained (24 hours), reagent grade ethylene glycol was added dropwise until the entire sample was wetted. The samples were evacuated and dried over anhydrous, ethylene glycol-free $CaCl_2$ until the weight of the standard surface area sample (Jury silty clay loam, 104 m^2 g^{-1}) was within 5% of the calculated area. The weight of ethylene glycol was assumed to be 0.31 mg m^{-2}. The surface area of precipitated calcium carbonate (Purecal O, lot P6D4E) was also measured.

Batch Experiments I:
Long Term Studies

The first set of experiments was conducted over a period of approximately 200 days to evaluate the feasibility of the method for determination of relative reaction rates and product distribution. The effect of calcium carbonate and bentonite as catalysts for pyrite oxidation was also studied.

Polyethylene 500 ml bottles containing 250 ml of distilled water and various pyrite treatments were kept at 25 $\pm$ 1 ^{o}C in a water bath. The pyrite was prepared by washing with concentrated HF, rinsing with distilled water and drying in a vacuum. The less than 250 um size fraction was used. The calcium carbonate used was Purecal O (lot P6D4E). The Wyoming bentonite (Baroid) used was Ca-saturated by washing with a solution of $CaCl_2 \cdot 2H_2O$ followed by washing

with distilled water and then vacuum dried.

The treatments used in the long-term studies are summarized in Table 1. The experiments were started on the addition of pyrite to the pre-conditioned mixtures of bentonite and/or calcium carbonate.

Table 1. Experimental treatments used in longterm studies.

	g per kg distilled water		
Code	Pyrite	$CaCO_3$	Ca-Bentonite
7	10	0	0
8	100	0	0
9	10	0	10
10	10	0	5
11	10	20	0
15	10	20	10

The pH, pe and EC of the solutions were monitored daily for three weeks, then at irregular intervals. The pH was measured with a glass electrode which was standardized daily. The pe was monitored with a pair of platinum electrodes connected in parallel against an Orion double junction Ag/AgCl reference electrode. The platinum electrodes were constructed and standardized with an iron(II)/iron(III) cyanide solution as described by Ponnamperuma (1972). An Orion Digital Ionanalyzer Model 801A with Model 605 electrode switch was used for the pH and pe (mV) measurements.

At the end of the experiment the solutions were filtered and analyzed for calcium, aluminum and total iron by atomic absorption using a Varian AA-375 Spectrophotometer. Reduced solution iron (Fe^{2+}) was measured with o-phenanthroline using the method of Tamura et al. (1974). A 3.0 M ammonium acetate solution was substituted for the hexamethyenetetramine buffer as suggested. This method was chosen because it was designed to give accurate results in the presence of high concentrations of oxidized iron (Fe^{3+}). Sulfate was measured by $BaCl_2$ titration (Rasnick and Nakayama, 1973).

The residual solid phase materials were analyzed for the extent of oxidation of iron. The alkaline sodium citrate extraction method of Jackson (1956) was used to determine oxidized iron. Total iron was determined from an HNO_3 digest. The extent of oxidation was determined algebraically as described in Appendix A.

Controlled pH Experiments

These experiments were conducted in aerated, stirred batch reactors in which the pH of the 1% by weight pyrite-solution slurry was maintained constant for a period of three to five days. The pH was controlled by an automatic titration unit consisting of a glass electrode, meter and relay connected to a Masterflex peristaltic pump configured to deliver 0.5 ml per minute. Sodium hydroxide was used to adjust the pH of the slurry. A constant ionic strength of 10

mol m^{-3} as $NaClO_4$ was used in all experiments. The batch size was increased to 2 L and aliquots were removed periodically to monitor solution iron and sulfur concentrations.

Sulfate was determined by the method of Rasnick and Nakayama (1973). Thiosulfate and sulfane disulfonate (tetrathionate) were measured promptly by the method of Nor and Tabatabai (1977). Total iron, Fe^{2+} and pH were also monitored.

The pyrite was retained at the end of the experiment for analysis of extent of oxidation in terms of iron (Appendix A).

Batch Experiments II:
Comprehensive Studies

A second series of experiments was conducted using the batch method described for long term studies. These experiments were of a shorter duration, designed to elucidate the kinetics and mechanism of chemical oxidation of pyrite. Reaction kinetics were studied relative to the surface area of the mineral and the order of the reaction in terms of iron oxidation products. The influence of ionic strength, specific inert salts and salts of reduced sulfur compounds was studied in an effort to characterize the reactant species.

Polyethylene 500 ml bottles containing 250 ml of inert salt solutions of various ionic strengths and pyrite were kept at 25 $\pm$ 1 ^{o}C in a water bath. The pyrite mineral was

washed with HF as described before. In all but the variable surface area experiments, 2.5 g of pyrite were used per 250 ml of solution. Disulfane disulfonate (tetrathionate) was prepared from a reagent grade sodium thiosulfate solution by oxidation with iodine followed by repeated precipitation in ethanol and washing with KCl and HCl. All other salts used were of reagent grade or better. The calcium carbonate used was Purecal O (Lot P6D4E). For the salt effect experiments, five ionic strengths each of $NaClO_4$, $NaHCO_3$, NaCl, Na_2SO_4 and K_2SO_4 were used. Replicates were run under similar conditions.

The pH, pe and EC of the solutions were measured as previously described daily or every two days until the end of each experiment, which lasted from one to three weeks. The platinum electrode was standardized using a saturated hydroquinone suspension at pH 4 described by Ponnamperuma (1972). Details of the preparation and use of this standard are found in Appendix B.

At the end of the experiments the solutions were filtered and analyzed for calcium, total iron, Fe^{2+}, thiosulfate, and disulfane disulfonate by the methods previously described. Sulfate was measured indirectly by a $BaSO_4$ precipitation method involving $BaClO_4$ (Nemeth, 1963). Results were corrected for thiosulfate and disulfane disulfonate interferences. This method is described in detail in Appendix C. Sulfite was measured by the method of

West and Gaeke (1956).

Residual solid phase materials were analyzed to determine the extent of oxidation of iron as described in Appendix A. To determine the order of the iron oxidation reaction, a series of experiments were conducted in which pyrite was allowed to oxidize for varying lengths of time up to ten days. Analysis of the solid phase then followed.

Pyrite Electrodes

Several pyrite electrodes were constructed for the purpose of determining the potential of the pyrite surface when allowed to equilibrate with various experimental solutions. Tharsis (Spanish) pyrite was crushed into angular, approximately 1 cm pieces, mounted on the end of 1 cm diameter glass tubes with silicone cement and sealed with heat shrink tape. Contact with a copper wire was made using a drop of mercury in the glass tube. Each electrode was mounted with a platinum electrode as a reference. HF was used to clean the pyrite surface for each experiment.

Measurements of potential were made using an Orion double junction reference electrode. They were corrected relative to the hydrogen electrode using the platinum electrode as a reference, based on the behavior of the platinum electrode in a saturated quinhydrone standard (Appendix B).

Column Study

A final experiment was conducted to demonstrate the influence of calcium carbonate on pyrite weathering products. The pyrite was not pretreated for this experiment to remove iron oxides and soluble salts, otherwise materials were the same as previous experiments. Acid-washed Ottowa sand was used to separate pyrite layers from $CaCO_3$ layers.

Three 20 mm diameter chromatography columns were filled with pyrite and calcium carbonate in different configurations simulating different reclamation or burial techniques. Column 1 contained 40 g of calcium carbonate overlain by 20 g of sand, which was in turn overlain by 80 g of pyrite. The packing density of the wet $CaCO_3$ was estimated at 1.10 Mg m^{-3} and the pyrite at 3.31 Mg m^{-3}. Column 2 contained the same materials in reverse order, with pyrite on the bottom of the column (closest to the outflow). The packing density of the $CaCO_3$ was 1.14 Mg m^{-3} and of the pyrite, 3.07 Mg m^{-3}. Column 3 contained the same quantities of materials, but the $CaCO_3$ and pyrite were thoroughly mixed before filling the column. The sand was placed at the bottom of the column. The packing density of the mixture was 1.51 Mg m^{-3}.

The ionic strength of the water flowing through the columns was kept at a constant head and flow was controlled to some extent with a variable speed, multiple channel Masterflex pump attached to the outlets of the three

columns. Flow rates averaged about 6.7 X 10^{-10} m^3 s^{-1} (2.5 ml h^{-1}). The flux was 2.1 X 10^{-10} m s^{-1} (7.6 cm h^{-1}). Column effluent was collected in three automatic samplers in the constant-volume mode. Samples were analyzed daily for pH, sulfate, disulfane disulfonate, thiosulfate, iron, copper and calcium. The experiment was continued for approximately one month.

RESULTS AND DISCUSSION

Characterization of the Minerals Used

The density of pyrite is 5.0 Mg m^{-3} (Weast, 1980). The measured density of the untreated pyrite sample was 4.76 Mg m^{-3}, approximately 95% of the pure mineral. After washing with concentrated HF, the measured density was 5.0 Mg m^{-3}. This confirms the identity of the mineral as pyrite as opposed to marcasite, which would have a density of around 4.8 Mg m^{-3} (Weast, 1980).

Chemical analysis by sequential fractionation of the untreated sample is shown in Table 2. The gram-molecular weight of FeS_2 is 119.98 g mol^{-1} (Weast, 1980), hence, the analysis of a pure sample should yield 8.3347 mmol(Fe) g^{-1}. On this basis, the study mineral was 85.3% pyrite. Extensive analysis of a sample of washed pyrite is shown in Table 3. This sample was 115% pyrite if based on the mole weight of iron. Titanium was shown to be a major contaminant, approximately 1% on a molar basis. Copper is a secondary contaminant, however, its catalytic effect could be out of proportion to its absolute concentration.

Table 2. Selective dissolution of standard pyrite.

	HF Soluble		HNO_3 Soluble	
	mg g^{-1}	umol g^{-1}	mg g^{-1}	umol g^{-1}
Fe	0.485	8.68	397	7108
Zn	0.105	1.61	0.0485	0.742
Cu	0.0183	0.288	0.0455	0.716

Table 3. Analysis of HF washed pyrite.

	mmol g^{-1}		mol mol$(Fe)^{-1}$
Fe	9.55	$\pm$ .113*	
Cu	0.0343	$\pm$ .00128	0.00359
Mn	0.000836	$\pm$ .0000403	0.0000875
Zn	0.000753	$\pm$ .000282	0.0000788
Ti	0.118	$\pm$ .0105	0.0124

* Confidence limits at the 0.05 level.

The results of the size analysis given in Table 4 show that the dominant size fraction is in the 106 to 50 um range. Assuming the ideal density of 5.0 Mg m^{-3} and cubic geometry, an approximate area for each size fraction was calculated. By summing each size fraction an estimate for the totalsurface area of 0.015 to 0.022 m^2 g^{-1} is obtained. This is probably a low estimate since the smallest size fraction, less than 50 um, is underestimated. Smith and Shumate (1970) measured a surface area of museum grade pyrite (massive) ground to less than 150 um (100 mesh), as 0.70 m^2 g^{-1} by nitrogen absorption. Their material is considered similar to the pyrite used in this experiment.

Table 4. Particle size analysis for pyrite standard.

Size Fraction: (um)	%	m^2 g^{-1}
250-106	8.67	0.000416-0.00098
106-50	57.1	0.00645-0.0137
50-	34.2	0.00821-
Total	100	0.0151-0.0229

Measurement of surface area by ethylene glycol adsorption resulted in fairly large variability due to the low surface. The untreated sample had a specific surface area of 3.49 $\pm$ 2.53 m^2 g^{-1}, the HF rinsed sample, 1.53 $\pm$

0.971 m^2 g^{-1} (95% confidence intervals). In comparison a sample which had weathered for several months in a dilute acidic solution (pH approximately 3.5) exhibited a surface area of 0.928 $\pm$ 1.86 m^2 g^{-1}. Based on these measurements the surface area selected for the washed pyrite used in the experiments was 1.5 m^2 g^{-1}. This estimate is 100 times larger than the area estimated by size fraction. It is speculated that micromorphological examination would probably show a flaked rather than cubic form for the pyrite sample, the result of crushing the ore before processing and separation of the pyrite. However, the morphology of the pyrite is of no consequence to the objectives of this experiment; the total surface area is the important variable.

The surface area of the calcium carbonate used was 6.87 $\pm$ 4.70 m^2 g^{-1}.

Long Term Oxidation of Pyrite

The EC of the solution with 1% pyrite (15 m^2 L^{-1}) increased linearly with time as shown in Figure 15. The increase in EC is directly proportional to the ionic strength of the solution. Since distilled water or a solution at equilibrium with $CaCO_3$ and/or bentonite was used as the starting condition any increase in EC is directly proportional to the amount of acid produced by pyrite oxidation and its subsequent effect on the other minerals

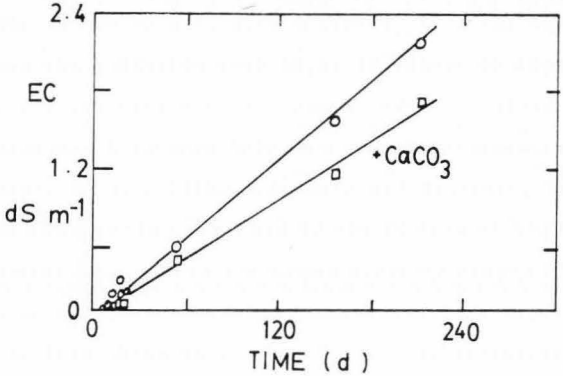

Figure 15. Effect of calcium carbonate on pyrite oxidation kinetics measured as conductivity.

present. The appearance of products in solution is, therefore, a linear function of time, which indicates oxidation followed zero-order kinetics. This is a consequence of the constant oxygen pressure and relatively constant surface area of the pyrite as predicted by McKay and Halpern (1958). Similar results were found for all treatments.

The use of 25 g of pyrite (150 m^2 L^{-1}) was expected to increase the oxidation rate up to 10 times. As shown in Figure 16, the rate was only approximately doubled. Calcium carbonate has long been believed to reduce oxidation rates (MacIntyre et al., 1930, Ainsworth and Blanchar, 1984). This is also apparently confirmed by the EC data of this experiment as shown in the lower curve of Figure 15. The slopes of the EC curves with time (rates) are reported in Table 5. From these data (code 9, 10, 15) bentonite appears to be a catalyst of pyrite oxidation. Lowson (1982) lists bentonite as having a significant effect on pyrite oxidation rates.

The pH and pe were found to vary inversely during the course of the experiment as shown in Figures 17 through 19. This is as expected for an oxidation reaction involving a solid phase. Similar data are found in the literature (Ponnamperuma et al., 1966, Huber and Garrels, 1953). The sum of pe and pH was nearly constant for the first 60 days of this experiment, then increased slightly. In the presence

Table 5. Rates of oxidation of pyrite in long term experiments (5040 h).

Code[a]	Ionic Strength	Oxidation Rates[b]			
	(mol m^{-3})	Fe pmol	SO_4^{2-} pmol	H^+ pmol	EC(25) dS m^{-1}
7	18.4	7.2	24.6	0.00127	8.01
8	48.6	3.8	5.2	0.00212	32.8
9	26.6	9.6	25.1	0.00359	49.8
10	26.2	13.6	25.8	0.00669	129.5
11	33.2	6.5	28.3	0.0	5.34
15	34.9	8.9	37.7	0.0	4.93

[a]See Table 1 for explanation of code.
[b]Rates expressed on a m^{-2} s^{-1} basis.

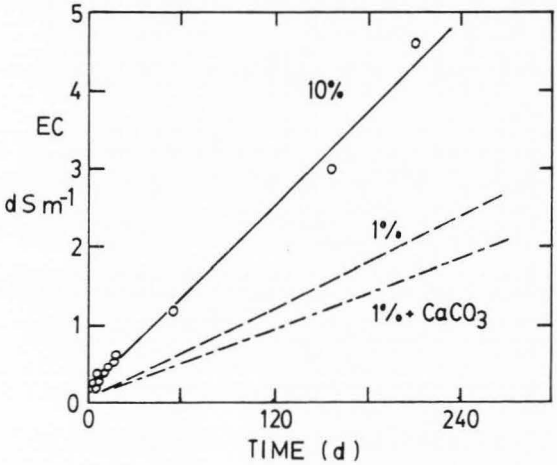

Figure 16. Effect of increased surface area on the rate of pyrite oxidation measured as solution conductivity.

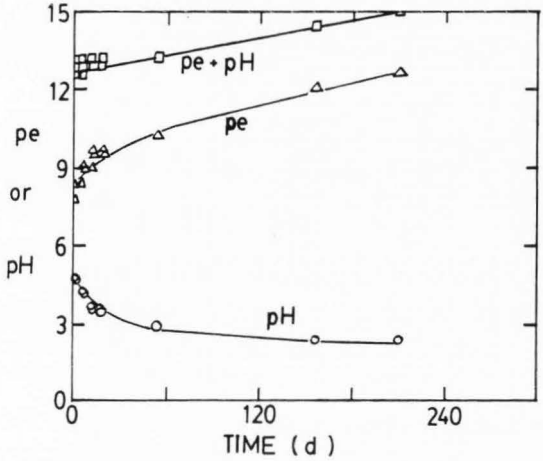

Figure 17. Long term pyrite oxidation: pH and redox changes with time.

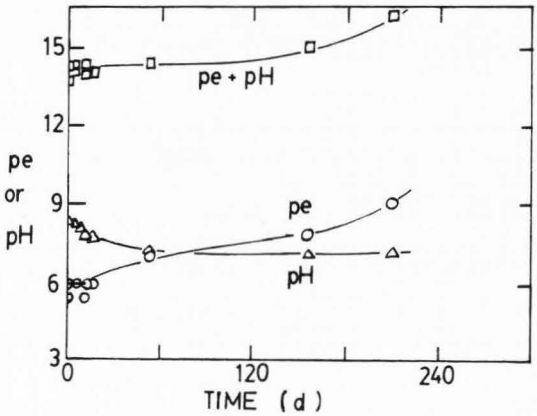

Figure 18. Long term pyrite oxidation in the presence of calcium carbonate: pH and redox changes with time.

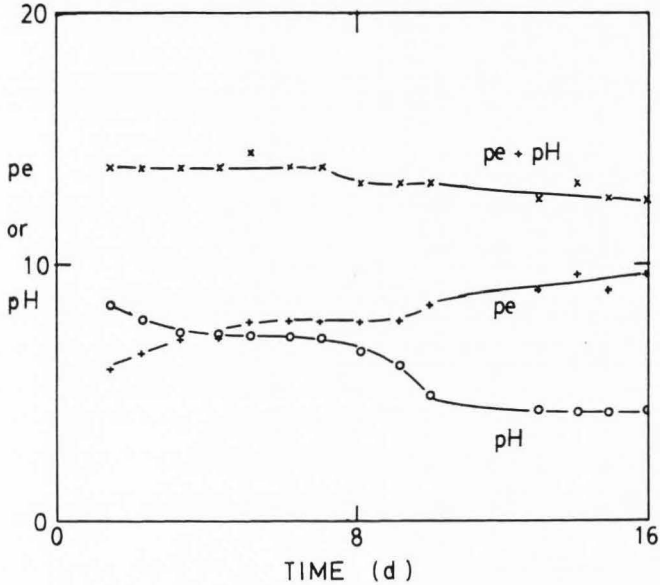

Figure 19. Pyrite oxidation in the presence of calcium saturated bentonite: changes in pH and redox.

of $CaCO_3$, pH was higher and pe proportionally lower (Figure 18).

The most dramatic effects of oxidation on pe+pH were observed in the presence of 1.25 g Ca-bentonite (code 9). Exchangeable calcium appeared to buffer pH for nearly 10 days, when the pH dropped precipitously and pe rose (Figure 19). The pe+pH of the system dropped slightly. This might be indicative of a shift in the solid-solution phase equilibrium.

The initial (first day) pH and the final pe, pH and pe+pH of the experiments are listed in Table 6. The initial high pH of the Ca-bentonite-containing suspensions (code 9, 10, 15) reflects the exchangeable-Ca effects on pH. It is also evident that the $CaCO_3$-containing suspensions had not yet reached equilibrium pH (8.2-8.4). By the end of the experiment the pH of the $CaCO_3$-containing slurries had dropped to near 7.0, while the buffering capacity of the bentonite suspensions had long been exceeded. The pH of the latter was close to that of the 1% pyrite suspension with no amendments.

Solution data reflect the extent of oxidation of the pyrite as well as the pH of the solution which was sampled. The dissolution of calcium carbonate and Ca-bentonite contributed the calcium and aluminum measured (Table 7). Comparison of the total iron and Fe^{2+} shows that a large

Table 6. Redox data for long term pyrite oxidation experiment.

Code[a]	Initial	Final			
	pH	Eh (mV)	pe	pH	pe+pH
7	4.65	423	12.5	2.46	14.9
8	3.58	413.5	12.3	2.22	14.5
9	8.32	432	12.6	3.01	15.6
10	8.13	416	12.3	2.74	15.1
11	8.90	224	9.10	7.16	16.3
15	8.94	240	9.38	7.26	16.6

[a]See Table 1 for explanation of code.

proportion of the solution iron is Fe^{3+}. The total iron concentration in solution did not correspond to the amount of sulfate formed. This is due to the reprecipitation of iron as oxides or other insoluble compounds such as the mineral hydronium jarosite ($H_3OFe_3(SO_4)_2(OH)_6$).

Table 7. Solution composition after 5040 h pyrite oxidation.

Code[a]	Concentrations (mol m^{-3})					
	Ca^{2+}	Al^{3+}	Fe_T	Fe^{2+}	Fe^{3+}	SO_4^{2-}
7	0.0802	0.0158	1.69	1.145	0.545	6.72
8	0.0891	0.0319	8.1	6.669	1.431	14.3
9	4.47	0.408	0.699	0.396	0.303	6.84
10	2.54	0.489	1.99	1.613	0.377	7.02
11	8.9	0	0	0.0243	0	7.7
15	7.19	0	0	0.00657	0	10.3

[a]See Table 1 for explanation of code.

The Fe^{2+} data, pe and pH can be used to provide circumstantial evidence of the presence of specific solid phases. Thermodynamic data for $Fe(OH)_3$, $Fe_3(OH)_8$, FeOOH and Fe_2O_3 obtained from Lindsay (1979) and data for hydronium jarosite obtained from Bladh (1982) were used to predict pe and Fe^{2+} concentrations based on the measured pH, Fe^{2+} and

pe. Corrections were made for ionic strength.

The data collected are in reasonable agreement with both amorphous iron hydroxide ($Fe(OH)_3$) and jarosite thermodynamic data. As shown in Table 8 this agreement is

Table 8. Thermodynamic phase analysis of long term pyrite oxidation experiment.

Code[a]	Measured			Calculated		
				$Fe(OH)_3$	Hydronium jarosite	
	pe	pH	Fe^{2+} (mol m^{-3})	pe	pe	Fe^{2+} (mol m^{-3})
7	12.5	2.46	1.15	12.9	12.6	0.822
8	12.3	2.22	6.67	12.8	12.0	1.25
9	12.6	3.01	0.396	11.7	12.2	0.0985
10	12.3	2.74	1.61	11.9	12.0	0.273
11	9.10	7.16	0.0243	0.434	6.42	0.0
15	9.38	7.26	0.00657	0.702	6.74	0.0

[a]See Table 1 for explanation of code.

best at higher acidities. Miller (1980) suggested the interconversion of iron(III) hydroxide and jarosite to be an important buffering mechanism for the pH of acid minespoils. At the higher pH, agreement between observed and calculated

pe was poor. This is probably due to the extremely low solubility of the redox-active species, iron, at pH 7. At this pH, the platinum electrode responds to the hydrogen ion (pH) rather than to solution iron. This phenomenon is described by Whitfield (1974).

Since the kinetics of pyrite oxidation are zero order, the extent of oxidation reflected in solution concentrations and solid phase analysis can be used as a measure of the rate of oxidation simply by considering pyrite surface area and time. The rates of oxidation of iron and sulfate sulfur are represented in picomoles per meter squared per second (pmol m^{-2} s^{-1}) in Table 5. Corrections were made for solution iron in the solid phase analysis.

In terms of iron the rates (extent) of oxidation in the presence of Ca-bentonite and calcium carbonate appear to be quite similar. They are also measurably higher than the rates in the absence of these amendments. This is in contradiction to the previous conclusions based on EC alone. Thus, consideration of the solid phase appears essential in evaluation of pyrite oxidation rates.

The agreement between the rates estimated by iron(III) and sulfate is poor in this set of experiments. Two moles of sulfate should be present for each mole of iron. The concentrations of reduced sulfur compounds were not measured in this experiment.

Oxidation of Pyrite at Constant pH and Ionic Strength

As with the long term batch studies of pyrite oxidation, the short term oxidation of pyrite also appeared to follow a pattern of zero order kinetics. This is demonstrated in Figure 20, which shows that at pH 6, sulfate, sulfane disulfonate and thiosulfate concentrations increase linearly with time. The importance of sulfane disulfonate and thiosulfate as relatively inert products of pyrite oxidation is also apparent from this figure. On a molar basis, the concentrations of reduced sulfur species appear small, but on the basis of moles of sulfur per molecule, the reduced sulfur species account for an amount at least equivalent to the fully oxidized sulfate.

The results of the controlled pH experiments are summarized in Table 9. Oxidation rates are expressed on a surface area basis and are calculated as the slope of the linear plot of the mmol m^{-2} of product versus time (s). Iron oxidation was estimated in the manner described from an analysis of the pyrite at the end of the experiment. Stoichiometric agreement is not ideal: sulfur is present in molar quantities slightly greater than twice the amount of iron. The trend to higher rates of oxidation at higher pH is evident.

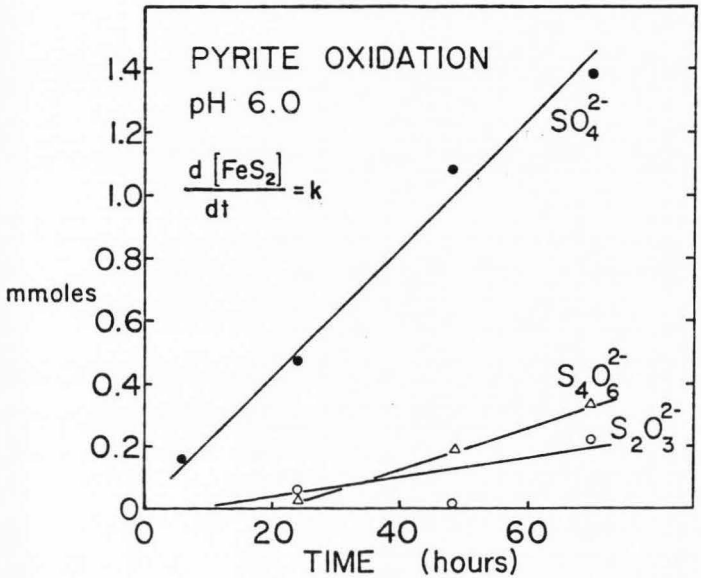

Figure 20. Sulfur products of pyrite oxidation at pH 6.

Table 9. Oxidation of pyrite at controlled pH.

pH	Time (h)	Rates: pmol m^{-2} s^{-1} Fe	SO_4^{2-}	$S_4O_6^{2-}$	$S_2O_3^{2-}$	H^+
5.04	72	10	10.4	M	M	33.5
6.03	73.5	14	29.4	M	M	109
6.97	48	16	32	M	M	M
7.93	74	83	105	22.6	1.58	495
8.16	96	30	62.1	3.65	7.38	226

M denotes data not collected.

Thermodynamic calculations failed to identify solution equilibrium with known solid phases. It is likely that these experiments were too short for substantial amounts of solid phase products to form and solid-solution quasi-equilibrium to be obtained.

The Effect of Surface Area on Pyrite Oxidation Rates

As predicted by the equation of McKay and Halpern (1958), the rate of pyrite oxidation increases linearly with surface area. Thus, the rate constant is the slope of the product vs. time curve. Table 10 shows the experimental conditions and rates of oxidation found as iron and as sulfate. The same data are plotted in Figure 21. The non-linearity in the sulfate data can be explained as an effect

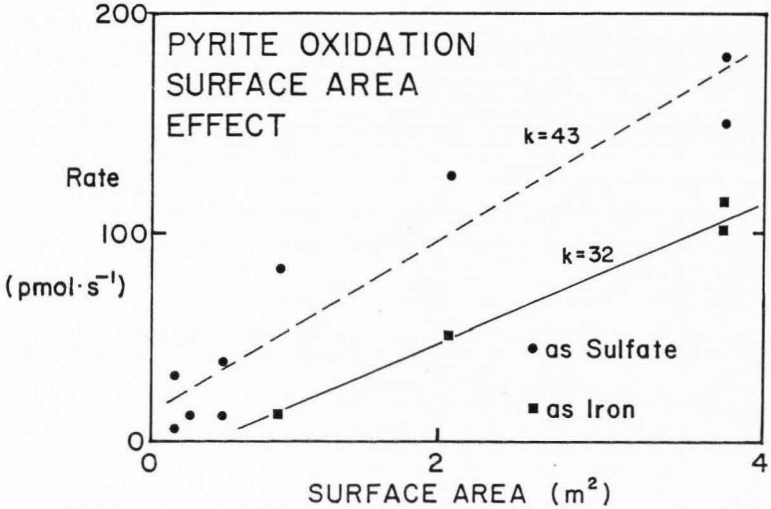

Figure 21. Effect of surface area on pyrite oxidation rate measured as production of sulfate and iron(III).

of pH on the distribution of sulfur oxidation products. The rate of oxidation expressed as iron is 32 pmol m^{-2} s^{-1} for a pH range between 3.4 and 3.6. Expressed as sulfate the rate is 43 pmol m^{-2} s^{-1}. If the pyrite disulfide was oxidizing stoichiometrically to sulfate, a rate of 64 pmol m^{-2} s^{-1} would be expected.

Table 10. Effect of surface area on pyrite oxidation rate at constant ionic strength (I = 10 mol m^{-3}).

Pyrite Slurry % w/w	Surface Area m^2	pH	Time h	SO_4^{2-} pmol s^{-1}	Fe pmol s^{-1}
0.01	0.04	4.73	308	27	M
0.02	0.08	4.40	308	0	M
0.05	0.19	4.21	263	4.5	M
0.10	0.38	4.02	262	8.6	M
0.10	0.38	3.90	308	31	M
0.20	0.75	3.62	308	80	18
0.50	1.88	3.47	262	120	71
1.00	3.75	3.50	262	150	68
1.00	3.75	3.35	307	180	65

M insufficient sample

Reaction Order for Pyrite Oxidation Expressed as Iron Oxidation Products

Pyrite was allowed to oxidize in 10 mol($NaClO_4$) m^{-3} solution which had a pH of about 3.5 during the course of the experiment. As can be seen in Table 11, a large portion of the iron oxidized remained in solution in the reduced form. This is a result of the reduction of solution Fe^{3+} by

pyrite. All iron in solution is considered to be produced by pyrite oxidation, not dissolution. The oxidation data of Table 11 are plotted in Figure 22 which clearly shows that the reaction is zero order with a rate of 27 pmol m^{-2} s^{-1}. This compares very favorably with the rate calculated for this pH by varying surface area: 32 pmol m^{-2} s^{-1}.

In a second phase of this study, 0.625 g of $CaCO_3$ was

Table 11. Kinetic data for pyrite oxidation at pH 3.5 expressed as iron oxidized.

Time	Conc. Iron in Sol'n.	Iron oxidized on an areal basis			
		Oxide	Sol'n + Oxide	Oxide + Pyritic	Iron Oxidized[a]
h	mmol m^{-3}	mmol m^{-2}	mmol m^{-2}	mol m^{-2}	mmol m^{-2}
0.0	18.4	8.4	9.6	6.08	8.8
1.0	27.0	9.2	11.0	6.00	10.2
2.0	38.2	10.5	13.1	6.11	11.9
3.5	36.0	10.2	12.6	6.21	11.2
8.0	53.7	9.8	13.3	6.15	12.0
22.0	71.8	11.0	15.8	6.18	14.2
33.0	76.6	8.7	13.8	6.28	12.2
46.0	99.1	11.4	18.0	6.19	16.2
66.5	129.5	10.7	19.3	6.25	17.2
125.0	205.4	13.4	27.1	5.93	25.4
147.0	228.4	11.2	26.5	6.14	24.0
166.0	240.7	13.8	29.8	6.04	27.4
166.0	233.7	12.3	27.8	6.70	23.1
166.0	241.2	12.7	28.8	6.06	26.4
166.0	248.1	12.4	28.9	6.08	26.4
166.0	255.1	16.5	33.5	6.15	30.2
166.0	250.8	14.9	31.6	6.02	29.2

[a]Details of this calculation are explained in Appendix A.

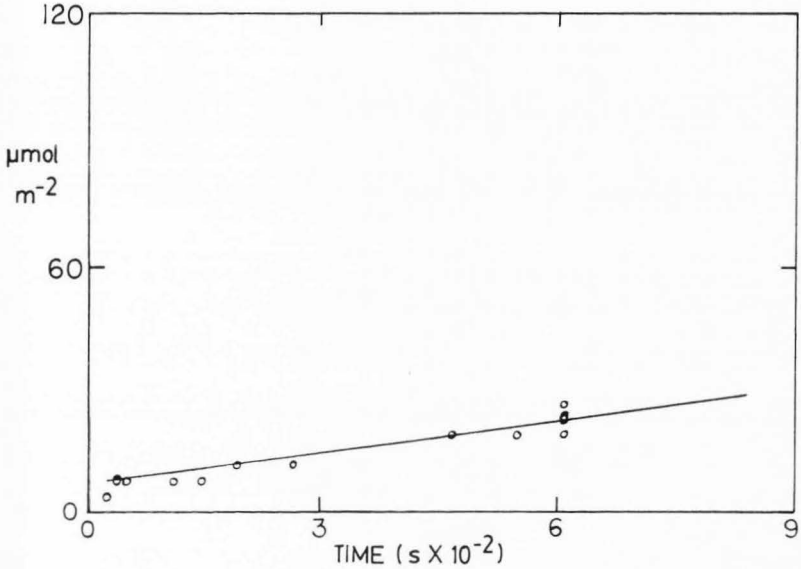

Figure 22. Pyrite oxidation kinetics at pH 3.5. Background electrolyte 10 mol($NaClO_4$) m^{-3}. Zero order rate constant 27 pmol(Fe) m^{-2} s^{-1}.

added to the 10 mol($NaClO_4$) m^{-3} and allowed to reach an equilibrium pH of approximately 8.2. Very little of the $CaCO_3$ was expected to dissolve so that about 16 m^2 L^{-1} would be left to buffer pH. The amount of oxidized iron in solution was below the limit of detection of the AA (1 mmol m^{-3}) and as is seen in Table 12, the oxidized iron was in the solid phase. Figure 23 shows the reaction to be zero order with a rate of 45 pmol m^{-2} s^{-1}.

Table 12. Kinetic data for pyrite oxidation at pH 8.2 expressed as iron oxidized.

Time	Iron oxidized on an areal basis		
h	Oxide mmol m^{-2}	Oxide + Pyritic mol m^{-2}	Iron Oxidized[a] mmol m^{-2}
0.0	16	5.35	17.0
1.0	13	4.91	15.2
2.0	13	5.14	14.2
4.0	15	4.86	17.1
6.0	17	5.08	18.6
8.0	17	4.55	20.4
12.5	18	4.97	20.3
25.0	17	4.94	19.0
31.0	18	5.15	19.3
49.0	20	5.11	22.0
62.5	24	5.03	26.7
74.5	30	4.97	33.0
83.0	26	4.86	29.7
95.0	26	4.76	30.9
126.0	32	4.76	37.5

[a]Details of this calculation are explained in Appendix A.

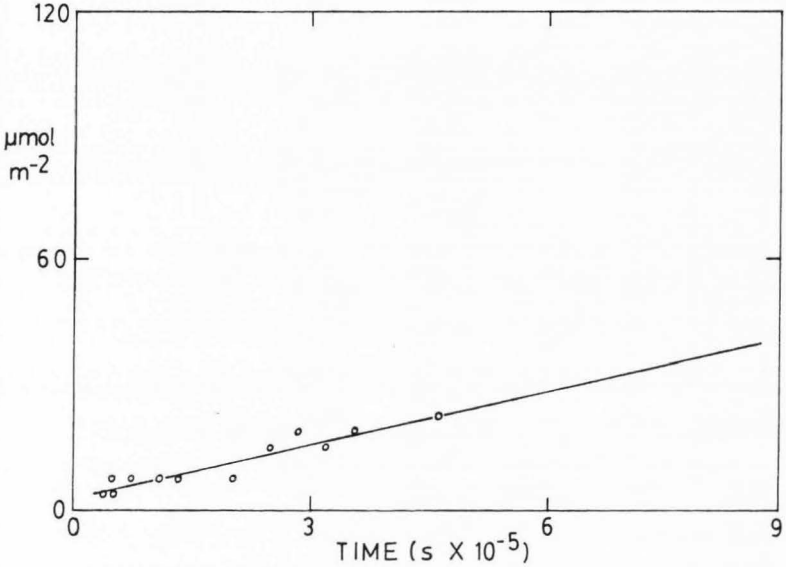

Figure 23. Pyrite oxidation kinetics at pH 8.2 in the presence of calcium carbonate. Background electrolyte 10 mol($NaClO_4$) m^{-3}. Zero order rate constant 45 pmol(Fe) $m^{-2}s^{-1}$.

The final phase of this study was conducted in 10 mol ($NaHCO_3$) m^{-3} solution which maintained a pH of about 9.0. As is seen in the data of Table 13, the amount of oxidized iron in the solid phase is greater than at lower pH. A zero order reaction is indicated in Figure 24 with a rate of 119 pmol m^{-2} s^{-1}.

Table 13. Kinetic data for pyrite oxidation at pH 9 expressed as iron.

Time	Iron oxidized on an areal basis		
	Oxide	Oxide + Pyritic	Iron Oxidized[a]
h	mmol m^{-2}	mol m^{-2}	mmol m^{-2}
0.0	5.9	5.40	6.1
21.5	6.7	5.71	6.5
52.0	10.8	5.63	10.7
71.8	20.4	5.77	19.7
96.9	38.2	5.79	36.6
124.9	45.4	5.59	45.1
147.1	54.1	5.92	50.8
176.8	94.0	5.77	90.5
191.5	69.3	5.87	65.6
219.7	90.5	5.78	87.0
243.2	104.5	5.64	103.0
243.3	117.5	5.80	112.6
243.4	97.7	5.90	92.0

[a]Details of this calculation are explained in Appendix A.

This series of experiments demonstrates clearly that the chemical oxidation of pyrite is a zero order reaction which is in agreement with the qualitative results of McKay

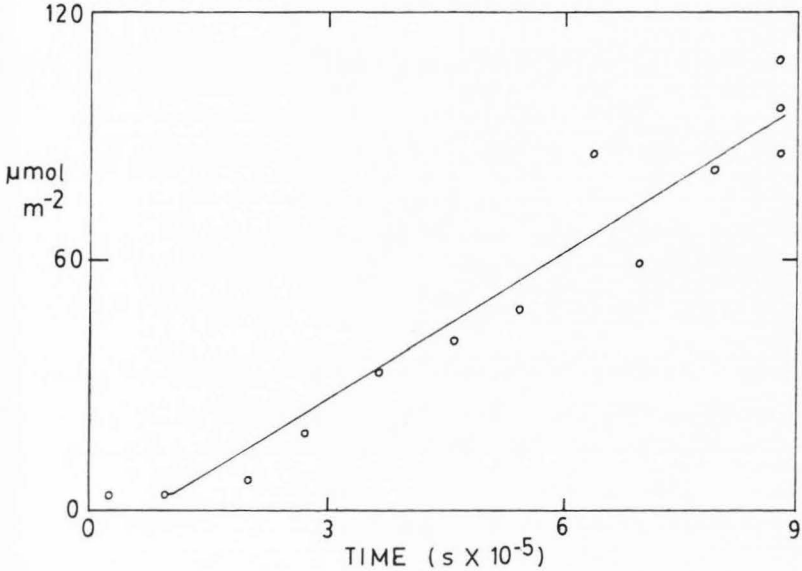

Figure 24. Pyrite oxidation kinetics at pH 9. Background electrolyte 10 mol($NaHCO_3$) m^{-3}. Zero order rate constant 119 pmol(Fe) m^{-2} s^{-1}.

and Halpern (1958) obtained at higher temperatures and oxygen pressures. The rate of oxidation increases with pH, however, which was not considered in the McKay and Halpern experiments. Singer and Stumm (1970) predicted an increase in pyrite oxidation rates with pH based on the chemistry of solution phase iron oxidation. Smith and Shumate (1970) reported an increase in pyrite oxidation rates with pH expressed as sulfate. Quantitative comparison of their data with the present experiments is difficult because of the difference in pretreatment and surface areas of the pyrites and the analytical methods used. The rates reported here are about two orders of magnitude lower than those of Smith and Shumate (1970).

It is not clear that the only effect of the $NaClO_4$, $CaCO_3$ and $NaHCO_3$ electrolytes on pyrite oxidation is a pH effect. Ionic strength effects should have been minimized by the use of 10 mol m^{-3} solutions of sodium salts. It is apparent that specific salt effects cannot be ruled out on the basis of these data alone.

The Effect of Ionic Strength on Pyrite Oxidation

Five different electrolytes were used to define the salt effect on pyrite oxidation. Sodium perchlorate was used as the background electrolyte in the controlled pH and variable surface area experiments because of its tendency to have the least complexing capacity and the least inhibitory

effect on iron oxidation. The logarithm of the pyrite oxidation rate as both iron and sulfate was plotted against the modified Brønsted function of the ionic strength to yield the logarithm of the oxidation rate at zero ionic strength and $Z_A Z_B$, the product of the charges of the reactant species. The final pH at zero ionic strength was derived similarly. These data are shown in Table 14.

Table 14. Effect of specific salts and ionic strength on kinetics of pyrite oxidation using the modified Brønsted equation.

Salt	-log(Rate[a]) at I=0		Brønsted Slope[b]		pH at I=0
	as Fe	as SO_4^{2-}	as Fe	as SO_4^{2-}	
$NaHCO_3$	-7.57	-6.84	2.00	-9.40?	7.31
$NaClO_4$	-7.60	-7.34	0.075	-1.71	3.42
NaCl	-7.67	-7.3	-1.18	-1.14	3.5
K_2SO_4	-7.676	M	-0.791	M	3.38
Na_2SO_4	-7.8	M	-0.438	M	3.12

[a]Rates as mmol m^{-2} s^{-1}.
[b]Brønsted slope as mmol m^{-2} s^{-1} $(mol\ L^{-1})^{-0.5}$.
M denotes data not collected.
? questionable data.

Pyrite oxidation is most rapid in sodium bicarbonate, but this effect is most likely due to pH rather than specific ionic interactions. This was demonstrated in the

controlled pH experiments. Of the salts tested at similar pH, sodium perchlorate has the least inhibitory effect on pyrite oxidation. Sodium chloride, potassium sulfate and sodium sulfate have increasingly greater inhibitory effects on oxidation rates. This is consistent with the data of Tamura et al. (1976a) and Sung and Morgan (1980) for the homogeneous oxidation of aqueous iron(II) in the presence of sodium salts of perchlorate, chloride and sulfate. These data support the hypothesis that at low pH, at least, it is the rate of oxidation of Fe^{2+} which determines the rate of pyrite oxidation.

The Brønsted slope, $Z_A Z_B$, is derived with the assumption that it is a bimolecular reaction which is responsible for the formation of the activated complex. This is the type of mechanism proposed by Goto et al. (1970):

$$FeOH^+ + O_2OH^- = Fe(OH)_2^+ + O_2^-, \qquad [73]$$

where the charges of the reactant species are +1 and -1. Hydrated oxygen and iron(II) presumably dissociate, each losing one H^+ before they react with each other. The Brønsted slopes for NaCl and K_2SO_4 are negative and nearly unity, consistent with this proposed mechanism. For the perchlorate salt the slope is essentially zero (as iron), suggesting that one of the reactants has no charge in this electrolyte. When the rate of oxidation is expressed as sulfate, however, a slope more consistent with the other salts appears.

The fractional Brønsted slopes exhibited in the presence of the sulfate salts should not be construed to indicate the presence of complex reactants with fractional charges. Other ionic interactions in the background electrolyte make the simple assumptions of the Brønsted equation inaccurate at high ionic strengths (Moore, 1972). The strong tendency of sulfate to form ion pairs should be suspected as influencing the Brønsted slope in this case.

The mechanism proposed by Tamura et al. (1976a) for aqueous iron(II) oxidation in the presence of various anions affords an additional interpretation of the fractional Brønsted slopes. In this mechanism anions such as Cl^- and SO_4^{2-} compete with OH^- to form ion pairs which can then react more or less vigorously with dissociated hydrated oxygen. This is represented by:

$$FeX^+ + O_2OH^- = Fe^{3+} + O_2^-, \qquad [74]$$

where X^- is an anion such as Cl^- or SO_4^{2-}. Fractional slopes would reflect the reduced reactivity of the FeX^+ ion pair.

The Brønsted slope exhibited in the presence of $NaHCO_3$ is dramatically different from that in the other electrolytes. A mechanism involving reactants with charges of +1 and +2 or -1 and -2 is implied, which is not consistent with the mechanism of Goto et al. (1970). Tamura et al. (1976b) proposed a mechanism of Fe^{2+} oxidation in the presence of solid phase iron oxides in which adsorbed Fe^{2+} undergoes electrochemical oxidation. This mechanism does not provide a satisfactory analogy given the insolubility of

both pyrite and $Fe(OH)_3$ at high pH. The activated complex under these conditions is most likely at the solution-iron oxide coating interface. This might involve the adsorption of dissociated hydrated oxygen on a negatively charged iron oxide surface followed by electrochemical oxidation of the pyrite:

$$FeS_2\text{-}FeO(OH)_3^{2-}\ (c) + O_2OH^- =$$

$$FeOH^{2+} + S_2^{2-} + FeO(OH)_3^{2-} + O_2^-. \qquad [75]$$

Although this mechanism is physically consistent with the electrochemical mechanism of oxidation and the product of the charges of the reactants satisfies the Brønsted equation, independent determination of reactant identities would be needed for confirmation.

Sulfur Oxidation

During the initial phase of this research it became clear that sulfate sulfur was not an accurate measure of pyrite oxidation. The data of the controlled pH experiments and the batch experiments are combined in Figures 25 and 26 to show the rate of appearance of the products, iron and sulfate respectively, versus pH. Expressed as iron, pyrite oxidation increases with pH as predicted by the kinetics of homogeneous and heterogeneous iron(II) oxidation. Sulfate data displayed more variability, partly due to the detection limit of the $BaSO_4$ precipitation method and partly due to the greater precision of the iron calculations. There was no

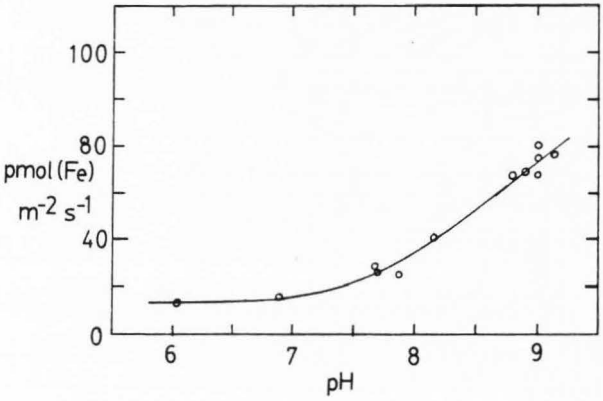

Figure 25. pH dependence of pyrite oxidation rate as pmol(Fe) m^{-2} s^{-1}.

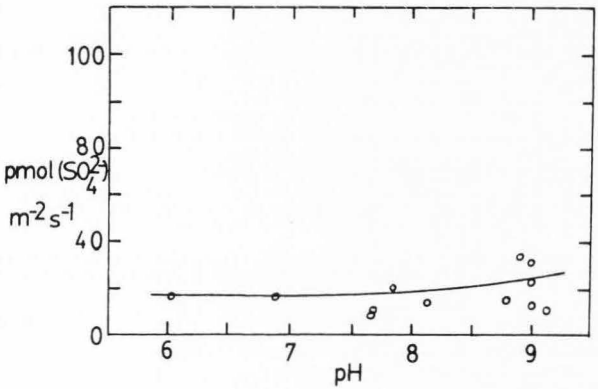

Figure 26. pH dependence of pyrite oxidation rate as pmol(SO_4^{2-}) m^{-2} s^{-1}.

increase in oxidation rates expressed as sulfate; at the highest pH encountered, rates actually decreased. Finally, while agreement is not bad at lower pH, sulfate rates at neutral and higher pH underestimate rates expressed as iron.

The reason for the discrepancies between sulfate and iron data becomes evident in Tables 15 and 16 which show the effect of pH (and electrolyte) on the distribution of sulfur products. At the lower pH in sodium perchlorate, sulfate and disulfane disulfonate are the principal sulfur oxidation products. At the higher pH in sodium bicarbonate,

Table 15. Effect of ionic strength on pyrite oxidation (as $NaClO_4$).

Ionic Strength		Time	Oxidation Rate	Sol'n. Concentration mol m^{-3}		
mol m^{-3}	pH	h	pmol m^{-2} s^{-1}	SO_4^{2-}	$S_4O_6^{2-}$	$S_2O_3^{2-}$
6.75	3.41	304	39	0.29	0.040	0.0
6.96	3.65	264	17	0.54	0.034	0.0
11.2	3.56	264	5.8	0.61	M	0.0
11.9	3.40	318	24	0.41	0.061	0.0
12.2	3.41	305	25	0.50	0.044	0.0
12.5	3.42	318	30	0.46	0.067	0.0
52.4	3.49	305	27	0.52	0.065	0.0
54.2	3.53	264	25	1.41	0.037	0.0
102	3.57	265	22	0.38	0.036	0.0
102	3.52	305	27	0.44	0.064	0.0
501	3.56	305	21	0.0	0.065	0.0
502	3.54	317	33	0.16	0.089	0.0
502	3.61	265	80	0.20	0.051	0.0
502	3.50	317	30	0.14	0.099	0.0

Table 16. Effect of ionic strength on pyrite oxidation (as NaCl).

Ionic Strength		Time	Oxidation Rate	Sol'n. Concentration mol m^{-3}		
mol m^{-3}	pH	h	pmol m^{-2} s^{-1}	SO_4^{2-}	$S_4O_6^{2-}$	$S_2O_3^{2-}$
7.24	3.53	264	18	0.32	0.044	0.0
8.89	3.58	265	14	1.33	0.028	0.0
12.4	3.53	264	21	0.33	0.043	0.0
14.5	3.60	264	14	1.69	0.029	0.0
51.6	3.61	264	15	0.06	0.045	0.0
52.1	3.61	265	13	0.42	0.039	0.0
52.2	3.62	265	17	0.31	0.053	0.0
54.5	3.62	265	10	1.68	0.035	0.0
102	3.63	265	11	0.44	0.043	0.0
102	3.63	264	15	0.35	0.053	0.0
502	3.69	264	12	0.33	0.072	0.0
503	3.67	265	8.2	0.68	0.058	0.0

thiosulfate replaces sulfate as a major reaction product. This shift in sulfur oxidation products is displayed graphically in Figure 27 and is qualitatively similar to the data of Figure 11 (Goldhaber, 1980).

The rates of oxidation of thiosulfate and disulfane disulfonate in the absence of pyrite are shown in Tables 17 and 18. It is clear that disulfane disulfonate is a relatively inert compound in the pH region 4.5 to 5 since no sulfate formed in over 260 hours. Thiosulfate is less inert, partially oxidizing in the same time period to disulfane

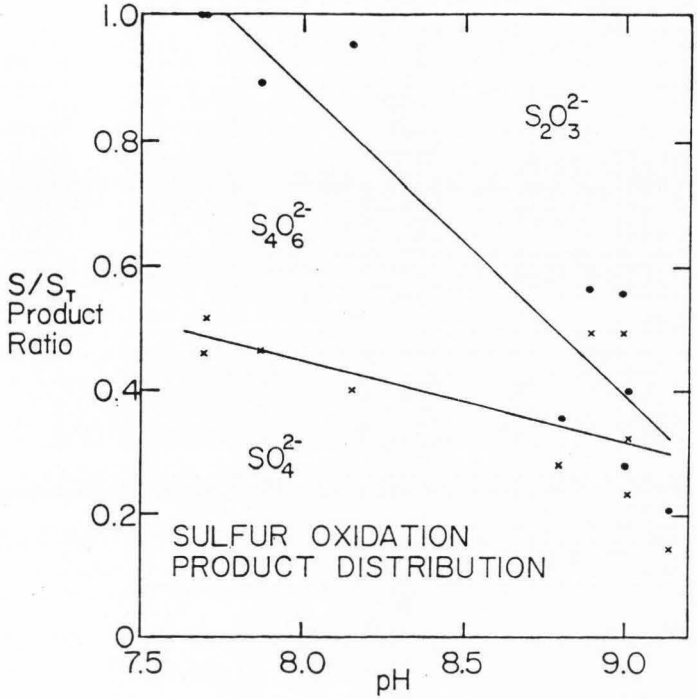

Figure 27. Distribution of pyritic sulfur oxidation products sulfate, sulfane disulfonate and thiosulfate between pH 7.5 and 9.

Table 17. Effect of ionic strength on disulfane disulfonate oxidation (Initial concentration 0.1 mol($K_2S_4O_6$) m^{-3} in $NaClO_4$).

Ionic Strength		Time	Sol'n. Concentration mol m^{-3}		
mol m^{-3}	pH	h	$S_2O_3^{2-}$	$S_4O_6^{2-}$	SO_4^{2-}
5.34	4.47	261	0.0	0.0944	0.0
10.4	4.61	262	0.0	0.0963	0.0
50.5	5.03	262	0.0	0.0973	0.0
100	5.13	262	0.0	0.0982	0.0
500	5.13	262	0.0	0.0973	0.0

Table 18. Effect of ionic strength on thiosulfate oxidation (Initial concentration 0.1 mol($Na_2S_2O_3$) m^{-3} in $NaClO_4$).

Ionic Strength		Time	Sol'n. Concentration mol m^{-3}		
mol m^{-3}	pH	h	$S_2O_3^{2-}$	$S_4O_6^{2-}$	SO_4^{2-}
5.39	4.58	261	0.0372	0.0060	0.0
10.4	4.66	262	0.0359	0.0050	0.0
50.4	5.58	262	0.0286	0.0022	0.04
100	5.30	262	0.0617	0.0013	0.0
501	4.59	262	0.0520	0.0050	0.02

disulfonate and sulfate. Sulfur recovery was not complete, suggesting the formation of insoluble elemental sulfur or polysulfane disulfonates other than the disulfane.

As indicated by the sulfur data in Table 18, there is a pronounced ionic strength effect on thiosulfate oxidation

(perhaps confounded by pH). The disulfane disulfonate concentrations are proportional to thiosulfate oxidation rate in the Brønsted plot of Figure 28. The negative slope indicates the charges of the reactant species are opposite in sign. One may speculate that a protonation reaction is the rate determining step in the oxidation of thiosulfate to disulfane disulfonate. One possible representation of this reaction would be:

$$S_2O_3^{2-} + H^+ = HS_2O_3^-, \qquad [76]$$

where the $HS_2O_3^-$ would then rapidly react with oxygen and thiosulfate to form sulfane disulfonate.

Oxidation of thiosulfate in the pH range 7.5 to 8 was studied in the presence and absence of pyrite. There is a profound catalytic effect of pyrite on thiosulfate oxidation as shown in Figure 29. In the absence of pyrite at this neutral pH, thiosulfate is more inert with sulfate as the principal oxidation product. When pyrite is present, thiosulfate is less inert, but the principal oxidation product appears to be disulfane disulfonate, rather than sulfur of a higher oxidation state.

The sulfur redox reaction which is consistent with these data is:

$$2\ S_2O_3^{2-} + 1/2\ O_2 + H_2O = S_4O_6^{2-} + 2\ OH^-, \qquad [77]$$

particularly since an increase in pH (OH^- production) was

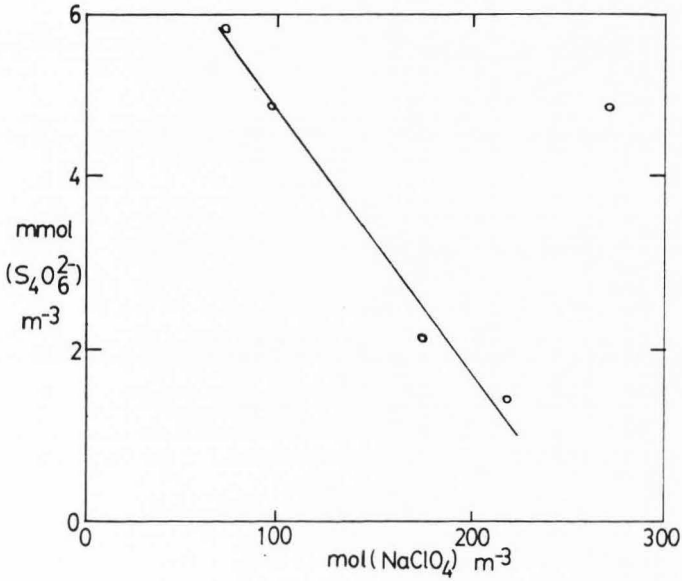

Figure 28. The effect of ionic strength on thiosulfate oxidation measured as disulfane disulfonate (background electrolyte, $NaClO_4$).

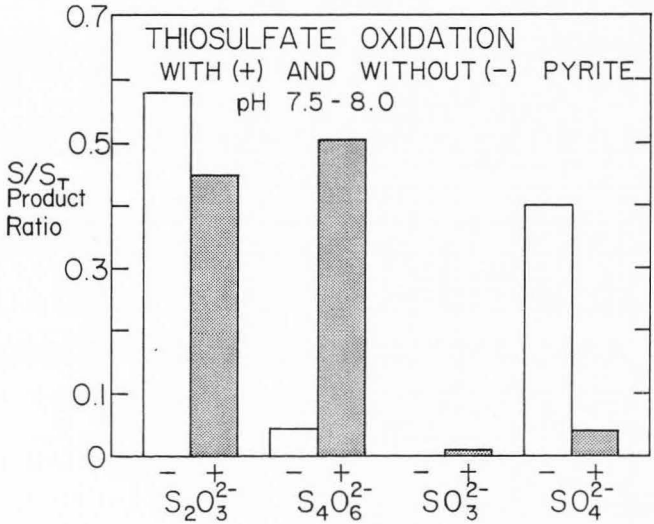

Figure 29. Distribution of thiosulfate oxidation products in the presence and absence of pyrite.

noticable. The alkaline decomposition of disulfane disulfonate characterized by Fava and Divo (1953b):

$$3\ S_2O_3^{2-} + SO_3^{2-} + 3\ H_2O = 2\ S_4O_6^{2-} + 6\ OH^-, \qquad [78]$$

is also consistent with this data. The nucleophilic displacement reaction:

$$S_3O_6^{2-} + S_2O_3^{2-} = S_4O_6^{2-} + SO_3^{2-} \qquad [79]$$

studied by Christiansen and Drost-Hansen (1949), generallized by Foss (1958) and proven by Wagner and Schreier (1978a, 1978b) would also describe sulfur oxidation in the presence of pyrite, however, monosulfane disulfonate could not be distinguished by the analytical methods used in this study.

Effect of Reduced Sulfur Compounds on Pyrite Oxidation Rate

A simple batch oxidation experiment was conducted to exaluate the interaction between pyrite and partially

Table 19. Effect of reduced sulfur compounds on pyrite oxidation rate ($I = 500$ mol m^{-3} as $NaClO_4$).

	Oxidation Rate as pmol m^{-2} s^{-1}		
Treatments	No Sulfur	5 mol m^{-3} Na_2SO_3	5 mol m^{-3} $Na_2S_2O_3$
No $CaCO_3$	21	21	33
$CaCO_3$	41	38	30

oxidized sulfur products. The rates of pyrite oxidation in the presence of sodium thiosulfate and sodium sulfite are shown in Table 19. Calcium carbonate was used to buffer the pH of the sodium perchlorate solutions near 8. The effect of adding $CaCO_3$ was to approximately double the oxidation rate from 21 to 41 mol m^{-3} s^{-1}.

Sodium sulfite appears to have very little effect on oxidation rates. This is probably due to the rapid oxidation of sulfite to sulfate. A separate experiment demonstrated almost complete oxidation of a calcium sulfite solution in less than 24 hours. Complete oxidation is confirmed by the sulfate data in Table 20, which shows that nearly all sulfite was recovered as sulfate. Thiosulfate did have an effect on pyrite oxidation rate although it was confounded by pH changes. Table 21 summarizes the average final pH measurements for duplicate batches. Sodium thiosulfate oxidation raised the pH to nearly the same level as the calcium carbonate batch. However, at the rate of 30 mol m^{-3} s^{-1} pyrite oxidation was significantly less at this higher pH in the presence of excess thiosulfate.

The pH effect of thiosulfate oxidation is explained most simply by reaction [77]. That disulfane disulfonate is the major sulfur oxidation product in this case is confirmed by the sulfur data in Table 20. A similar, competing reaction between thiosulfate and Fe^{3+} (aq) or $Fe(OH)_3$ (c) may account for the reduced rate of pyrite oxidation. While

Table 20. Effect of reduced sulfur compounds on pyrite oxidation in the presence and absence of $CaCO_3$.

Oxidation in the presence of $CaCO_3$

S added[a]	pH	$[Ca^{2+}]$[b]	Oxidation Rate[c]	$[SO_4^{2-}]$	$[S_4O_6^{2-}]$	$[S_2O_3^{2-}]$
None	7.69	1.34	41	0.06	0.149	0.023
None	7.76	1.00	40	0.00	0.148	0.034
Na_2SO_3	7.78	1.17	35	4.70	0.144	0.044
Na_2SO_3	7.77	1.21	40	4.50	0.149	0.041
$Na_2S_2O_3$	8.23	0.83	30	0.0	1.16	2.60
$Na_2S_2O_3$	8.25	0.80	29	0.0	1.06	3.03

Oxidation in the absence of $CaCO_3$

S added[a]	pH	$[Ca^{2+}]$[b]	Oxidation Rate[c]	$[SO_4^{2-}]$	$[S_4O_6^{2-}]$	$[S_2O_3^{2-}]$
None	3.52	0.0	23	4.38	0.093	0.0
None	3.53	0.0	19	4.43	0.094	0.0
Na_2SO_3	3.50	0.0	20	0.14	0.099	0.0
Na_2SO_3	3.54	0.0	22	0.16	0.089	0.0
$Na_2S_2O_3$	7.61	0.0	32	0.0	1.28	2.34
$Na_2S_2O_3$	7.53	0.0	34	0.0	1.34	2.18

[a]Sulfur compounds added at the rate of 5 mol m^{-3}.
[b]Concentrations expressed as mol m^{-3}.
[c]Rate of oxidation expressed as pmol(Fe) m^{-2} s^{-1}.

Table 21. Effect of oxidation of reduced sulfur compounds on pH in the presence of pyrite and $CaCO_3$ ($I = 500$ mol m^{-3} as $NaClO_4$).

	Oxidation Rate as pmol m^{-2} s^{-1}		
Treatments	No Sulfur	5 mol m^{-3} Na_2SO_3	5 mol m^{-3} $Na_2S_2O_3$
No $CaCO_3$	3.52	3.53	7.57
$CaCO_3$	7.73	7.78	8.24

the reaction with Fe^{3+} would not necessarily produce OH^-, the oxidation of thiosulfate to disulfane disulfonate at the surface of solid $Fe(OH)_3$ would produce results similar to the reaction:

$$2\ S_2O_3^{2-} + 2\ Fe(OH)_3 = S_4O_6^{2-} + 2\ Fe(OH)_2 + 2\ OH^-. \quad [80]$$

This implies that there is a redox buffering effect of reduced sulfur compounds at a neutral and higher pH which could interfere with known pyrite oxidation mechanisms. The reduction of Fe^{3+} may remove the most effective oxidizing agent, thus decrease pyrite oxidation rates.

That pyrite is oxidized by an electrochemical mechanism is quite apparent, however the identity of the oxidizing agent is not. Smith and Shumate (1970) acknowledged the fact that both O_2 and Fe^{3+} could directly oxidize pyrite. The emphasis of electrochemical studies has been on the direct discharge of O_2 at the pyrite surface as in the work of

Biegler (1976), Biegler et al. (1975) and Biegler and Swift (1979). Singer and Stumm (1970) argued that the solution oxidation of Fe^{2+} was the rate determining step, producing Fe^{3+} for oxidation of pyrite. During the course of the controlled pH pyrite oxidation experiments, where thiosulfate was added, oxygen concentrations were measured periodically and found to match values measured in control solutions containing no pyrite. Oxidation rates were lowered in spite of this; which tends to favor the iron(III) mediated mechanism. The passivation of the pyrite surface by the adsorption of thiosulfate is also a possible explanation, but would require more corroborating evidence.

The Effect of DTPA on Pyrite Oxidation

The thermodynamically well-characterized chelate, DTPA, was added to a set of batch experiments to assess the effect of this ligand on pyrite oxidation and solution equilibria. This ligand has a strong affinity for solution iron and has been used to experimentally determine the solubility products for relatively insoluble iron compounds (Vlek et al., 1974). The experiments were conducted in 10 mol($NaClO_4$) m^{-3} with a DTPA concentration of 0.1 mol m^{-3} in the presence and absence of $CaCO_3$.

The results in Table 22 show that DTPA had no apparent effect on pyrite oxidation rates as expressed as iron; control rates at pH 3.4 were 14 and 19 nmol m^{-2} s^{-1} and DTPA treatment rates were 1.9 and 2.0 at the same pH. The

significant point is that oxidation rates did not increase dramatically at pH 7.9 in the experiment to which both DTPA and $CaCO_3$ had been added. Thus, DTPA inhibits the rate of pyrite oxidation at high pH.

Table 22. Effect of DTPA on pyrite oxidation (I = 10 mol m^{-3}).

Treatment[a]	pH	Oxidation Rate[b]	$[Fe^{2+}]$[c]	$[Fe^{3+}]$	$[S_4O_6^{2-}]$	$[S_2O_3^{2-}]$
None	3.42	19	0.211	0.219	0.067	0.0
None	3.40	14	0.187	0.141	0.061	0.0
DTPA	3.37	20	0.115	0.297	0.062	0.0
DTPA	3.41	19	0.112	0.290	0.067	0.0
DTPA/CaCO3	7.85	21	0.008	0.081	0.055	0.009
DTPA/CaCO3	7.91	22	0.009	0.077	0.053	0.014

[a]DTPA 0.1 mol m^{-3}.
[b]Oxidation rate expressed as pmol(Fe) m^{-2} s^{-1}.
[c]Concentrations expressed as mol m^{-3}.

The concentrations of solution iron and reduced sulfur compounds are shown in Table 22. The DTPA appears to have only a modest influence on solution iron concentrations at pH 3.4. Iron concentrations exceed the concentration of DTPA, indicating that uncomplexed or "free" iron must be present in solution. Reduced sulfur species are similar in both the treatment and control. In the presence of $CaCO_3$ the pH is increased and solution iron concentrations are lower. Solution iron must all be associated with DTPA. Thiosulfate

also appears in solution at the higher pH, as expected.

The total solution concentrations of Na^+, Ca^{2+}, Fe^{2+}, Fe^{3+}, SO_4^{2-}, ClO_4^-, $S_2O_3^{2-}$ and DTPA were used along with pH, measured pe and an assumed partial pressure of CO_2 to calculate the distribution of solution species at equilibrium. The well-known computer program GEOCHEM was used to make the calculations, which are corrected for ionic strength and account for a large number of possible complexes and solid precipitates. In these calculations, the solid phase $Fe(OH)_3$ was considered, but jarosite compounds were not. Disulfane disulfonate data were not used because of the lack of thermodynamic data on this compound. The data used and results of the equilibrium calculations using GEOCHEM are listed in Tables 23 and 24.

As shown by the calculations in Table 23, at pH 3.4 the DTPA is essentially all complexed with iron and the excess iron exceeds the solubility of $Fe(OH)_3$, which is predicted to precipitate. The calculations indicate that both iron(II) and iron(III) may exist in equilibrium in non-DTPA, free or complexed forms in solution. Sulfate and hydroxyl are probable ligands for iron(III) complexation. This is contrasted with the calculations of Table 24, which indicate that all of the iron in solution is associated with DTPA. Some of the calcium from the $CaCO_3$ is also present as a DTPA complex. Calculated concentrations of free iron are very minute, probably beyond the precision of the computer used.

Table 23. Calculations of solution equilibria in the presence of DTPA and pyrite using GEOCHEM (at pH 3.4).

THESE COMPUTATIONS INVOLVE 4 METALS, 5 LIGANDS, 48 COMPLEXES AND 4 POSSIBLE SOLIDS.

THE CONDITIONS FOR THE DIFFERENT CASES ARE[a]

METAL	CASE 1	CASE 2	LIGAND	CASE 1	CASE 2
Na^+	2.000	2.000	SO_4^{2-}	2.860	2.896
Fe^{3+}	3.528	3.537	DTPA	4.000	4.000
Fe^{2+}	3.938	3.952	ClO_4^-	2.000	2.000

	CASE 1	CASE 2
F I X E D P H	3.370	3.410
$P(CO_2)$ (ATM)	3.500	3.500
REDOX POTENTIAL (pe)	11.730	11.720

THE REDOX REACTION Fe^{2+}/Fe^{3+} WAS CONSIDERED

Table 23. Continued.

CASE NUMBER 1

SOLID $Fe(OH)_3$ PRECIPITATES

CALCULATED IONIC STRENGTH= 0.012660303 mol L^{-1}.

SOLID	MOLES PER LITER OF SOLUTION
$Fe(OH)_3$	0.00030771995

	FREE MET	CO_3^{2-}	SO_4^{2-}	DTPA	ClO_4^-	OH^-
FREE LIG		14.70	2.90	31.32	2.00	10.56
Na^+	2.00	9.85	4.01	b	b	12.85
Fe^{3+}	6.85	9.23	6.35	4.13	b	5.71
Fe^{2+}	5.84	11.29	6.95	4.58	b	12.09
H^+	3.37	5.00	4.45	19.04	b	b

PRIMARY DISTRIBUTION OF METALS AND LIGANDS

Na^+	AS A FREE METAL/	99.0 PERCENT
	BOUND WITH SO_4^{2-}/	1.0 PERCENT
Fe^{3+}	BOUND WITH SO_4^{2-}/	0.1 PERCENT
	BOUND WITH DTPA/	17.9 PERCENT
	BOUND WITH OH^- /	0.5 PERCENT
	IN SOLID FORM WITH OH^- /	74.7 PERCENT
Fe^{2+}	AS A FREE METAL/	0.4 PERCENT
	BOUND WITH DTPA/	6.4 PERCENT
CO_3^{2-}	BOUND WITH H^+ /	10.0 PERCENT
	IN SOLID FORM WITH H^+ /	90.0 PERCENT[c]
SO_4^{2-}	AS A FREE LIGAND/	90.3 PERCENT
	BOUND WITH NA^+ /	7.1 PERCENT
	BOUND WITH H^+ /	2.5 PERCENT
DTPA	BOUND WITH Fe^{3+} /	73.8 PERCENT
	BOUND WITH Fe^{2+} /	26.2 PERCENT
ClO_4^-	AS A FREE LIGAND/	100.0 PERCENT

Table 23. Continued.

CASE NUMBER 2

CALCULATED IONIC STRENGTH= 0.012451466 mol L^{-1}.

SOLID	MOLES PER LITER OF SOLUTION
$Fe(OH)_3$	0.00029881339

	FREE MET	CO_3^{2-}	SO_4^{2-}	DTPA	ClO_4^-	OH^-
FREE LIG		14.63	2.94	31.25	2.00	10.52
Na^+	2.00	9.82	4.04	b	b	12.80
Fe^{3+}	6.98	9.29	6.52	4.15	b	5.77
Fe^{2+}	5.96	11.38	7.11	4.55	b	12.16
H^+	3.41	5.01	4.53	19.08	b	b

PRIMARY DISTRIBUTION OF METALS AND LIGANDS

Na^+	AS A FREE METAL/	99.1 PERCENT
	BOUND WITH SO_4^{2-}/	0.9 PERCENT
Fe^{3+}	BOUND WITH DTPA/	17.8 PERCENT
	BOUND WITH OH^- /	0.4 PERCENT
	IN SOLID FORM WITH OH^- /	74.3 PERCENT
Fe^{2+}	AS A FREE METAL/	0.3 PERCENT
	BOUND WITH DTPA/	7.1 PERCENT
CO_3^{2-}	BOUND WITH H^+ /	9.8 PERCENT
	IN SOLID FORM WITH H^+ /	90.2 PERCENT[c]
SO_4^{2-}	AS A FREE LIGAND/	90.5 PERCENT
	BOUND WITH Na^+ /	7.1 PERCENT
	BOUND WITH H^+ /	2.3 PERCENT
DTPA	BOUND WITH Fe^{3+} /	71.5 PERCENT
	BOUND WITH Fe^{2+} /	28.5 PERCENT
ClO_4^-	AS A FREE LIGAND/	100.0 PERCENT

Table 23. Continued.

---

[a]Concentrations are expressed as the pC, the -log(Concentration) of the ion. Concentrations are as mol L^{-1}.

[b]Extremely small number.

[c]The term "solid form" refers to H_2CO_3 which dehydrates to form CO_2, an artifact of the way equilibrium is calculated.

Table 24. Calculations of solution equilibria in the presence of DTPA, $CaCO_3$ and pyrite using GEOCHEM (pH 7.9).

THESE COMPUTATIONS INVOLVE 5 METALS, 6 LIGANDS, 59 COMPLEXES AND 7 POSSIBLE SOLIDS

THE CONDITIONS FOR THE DIFFERENT CASES ARE[a]

METAL	CASE 1	CASE 2	LIGAND	CASE 1	CASE 2
Ca^{2+}	2.920	2.970	SO_4^{2-}	3.098	3.061
Na^{+}	2.000	2.000	$S_2O_3^{2-}$	5.050	4.840
Fe^{3+}	4.094	4.112	DTPA	4.000	4.000
Fe^{2+}	5.120	5.040	ClO_4^{-}	2.000	2.000

	CASE 1	CASE 2
F I X E D P H	7.850	7.910
$P(CO_2)$ (ATM)	3.500	3.500

NO REDOX REACTIONS WERE CONSIDERED

Table 24. Continued.

CASE NUMBER 1

IONIC STRENGTH= 0.013794079 mol L^{-1}.

	FREE MET	CO_3^{2-}	SO_4^{2-}	$S_2O_3^{2-}$	DTPA	ClO_4^-	OH^-
FREE LIG		5.73	3.16	5.07	11.74	2.00	6.08
Ca^{2+}	2.95	5.37	4.24	6.55	4.93	b	7.82
Na^+	2.00	5.37	4.28	6.70	b	b	8.37
Fe^{3+}	30.82	18.14	30.61	32.62	4.09	b	19.63
Fe^{2+}	34.92	35.53	36.31	b	5.12	b	36.69
H^+	7.85	3.46	9.20	11.41	9.04	b	b

PRIMARY DISTRIBUTION OF METALS AND LIGANDS

Ca^{2+}	AS A FREE METAL/	93.8 PERCENT
	BOUND WITH CO_3^{2-}/	0.4 PERCENT
	BOUND WITH SO_4^{2-}/	4.8 PERCENT
	BOUND WITH DTPA/	1.0 PERCENT
Na^+	AS A FREE METAL/	99.4 PERCENT
	BOUND WITH SO_4^{2-}/	0.5 PERCENT
Fe^{3+}	BOUND WITH DTPA/	100.0 PERCENT
Fe^{2+}	BOUND WITH DTPA/	100.0 PERCENT
CO_3^{2-}	BOUND WITH H^+ /	3.5 PERCENT
	IN SOLID FORM WITH H^+ /	96.4 PERCENT[c]
SO_4^{2-}	AS A FREE LIGAND/	86.2 PERCENT
	BOUND WITH Ca^{2+} /	7.2 PERCENT
	BOUND WITH Na^+ /	6.6 PERCENT
$S_2O_3^{2-}$	AS A FREE LIGAND/	94.6 PERCENT
	BOUND WITH Ca^{2+} /	3.1 PERCENT
	BOUND WITH Na^+ /	2.3 PERCENT
DTPA	BOUND WITH Ca^{2+}/	11.9 PERCENT
	BOUND WITH Fe^{3+}/	80.5 PERCENT
	BOUND WITH Fe^{2+}/	7.6 PERCENT
ClO_4^-	AS A FREE LIGAND/	100.0 PERCENT

Table 24. Continued.

CASE NUMBER 2

CALCULATED IONIC STRENGTH= 0.013696394 mol L^{-1}.

	FREE MET	CO_3^{2-}	SO_4^{2-}	$S_2O_3^{2-}$	DTPA	ClO_4^-	OH^-
FREE LIG		5.62	3.12	4.86	11.63	2.00	6.01
Ca^{2+}	3.00	5.35	4.25	6.39	4.87	b	7.80
Na^+	2.00	5.32	4.24	6.49	b	b	8.30
Fe^{3+}	31.01	18.00	30.76	32.61	4.11	b	19.63
Fe^{2+}	35.07	35.60	36.42	b	5.04		36.77
H^+	7.91	3.41	9.22	11.26	9.03	b	b

PRIMARY DISTRIBUTION OF METALS AND LIGANDS

Ca^{2+}	AS A FREE METAL/	93.0 PERCENT
	BOUND WITH CO_3^{2-}/	0.4 PERCENT
	BOUND WITH SO_4^{2-}/	5.2 PERCENT
	BOUND WITH DTPA/	1.3 PERCENT
Na^+	AS A FREE METAL/	99.4 PERCENT
	BOUND WITH SO_4^{2-}/	0.6 PERCENT
Fe^{3+}	BOUND WITH DTPA/	100.0 PERCENT
Fe^{2+}	BOUND WITH DTPA/	100.0 PERCENT
CO_3^{2-}	BOUND WITH H^+ /	3.9 PERCENT
	IN SOLID FORM WITH H^+ /	96.0 PERCENT[c]
SO_4^{2-}	AS A FREE LIGAND/	86.9 PERCENT
	BOUND WITH Ca^{2+} /	6.4 PERCENT
	BOUND WITH Na^+ /	6.7 PERCENT
$S_2O_3^{2-}$	AS A FREE LIGAND/	94.9 PERCENT
	BOUND WITH Ca^{2+} /	2.8 PERCENT
	BOUND WITH Na^+ /	2.3 PERCENT
DTPA	BOUND WITH Ca^{2+}/	13.6 PERCENT
	BOUND WITH Fe^{3+}/	77.3 PERCENT
	BOUND WITH Fe^{2+}/	9.1 PERCENT
ClO_4^-	AS A FREE LIGAND/	100.0 PERCENT

Table 24. Continued.

==========

[a]Concentrations are expressed as the pC, the -log(Concentration) of the ion. Concentrations are as mol L^{-1}.

[b]Extremely small number.

[c]The term "solid form" refers to H_2CO_3 which dehydrates to form CO_2, an artifact of the way equilibrium is calculated.

Thiosulfate was calculated to form complexes with calcium and sodium.

The inhibition of pyrite oxidation by DTPA may provide further information on the mechanism of oxidation at high pH. If the mechanism of pyrite oxidation involved the adsorption and reduction of solution oxygen at the pyrite surface as assumed by Smith and Shumate (1970) and Bailey and Peters (1976), DTPA should have no effect on pyrite oxidation. Since it does appear to have an effect, and since iron is the most prominent solution species interacting with DTPA, the reduction of iron at the pyrite surface and subsequent reoxidation by oxygen is the likely mechanism, even at high pH. This agrees with the prediction of Singer and Stumm (1970).

There are at least two possible explanations for the effect of DTPA on pyrite oxidation at high pH. It may be that iron-DTPA complexes are not readily oxidized or reduced, preventing the regeneration of iron(III) oxidant and the discharge of oxidant at the pyrite surface. A second possibility is that the DTPA at high pH is specifically adsorbed to iron on the pyrite surface forming a barrier to approach or discharge of oxidants (either iron(III) or oxygen). This is a passivation mechanism, commonly utilized to prevent corrosion of metals (Uhlig, 1971). More information is needed to confirm either of these mechanisms.

The Effects of Other Specific Ions, Ion Exchange and Specific Minerals on Pyrite Oxidation

The batch experiment method was used to screen various amendments for their effect on the rate of pyrite oxidation. Thiosulfate, DTPA and possibly hematite were found to have some effect on oxidation rate, expressed as iron produced. The pH effect probably accounts for most other observed catalysis.

The concentration of calcium was adjusted in a constant ionic strength 500 mol($NaClO_4$) m^{-3} medium using $Ca(ClO_4)_2$. This is compared with a similar experiment using $CaCO_3$ to adjust calcium concentration in Table 25. The rates of pyrite oxidation expressed as iron are all similar in the

Table 25. Effect of solution calcium on pyrite oxidation.

Treatment	$[Ca^{2+}]$ mol m^{-3}	pH	Ionic Strength mol m^{-3}	Oxidation Rate[a] pmol m^{-2} s^{-1}
None	0.0	3.50	502	20
None	0.0	3.54	502	22
$CaClO_4$	0.90	3.52	506	32
$CaClO_4$	0.92	3.46	505	22
$CaClO_4$	2.57	3.48	513	22
$CaClO_4$	2.87	3.47	513	22
$CaClO_4$	5.58	3.51	523	22
$CaClO_4$	5.80	3.48	524	18
$CaCO_3$	1.34	7.69	503	41
$CaCO_3$	1.00	7.76	502	40

[a]Oxidation rate expressed as pmol(Fe) m^{-2} s^{-1}.

$Ca(ClO_4)_2$ solutions, which are similar to the control rates, between 18 and 22 pmol m^{-2} s^{-1}. The $CaCO_3$ amended experiment resulted in a rate of oxidation twice that of the control, about 40 pmol m^{-2} s^{-1}. Since the dissolution of $CaCO_3$ in the 500 mol($NaClO_4$) m^{-3} would result in a solution nearly indistinguishable from the $CaClO_4$ solutions, except for pH, it is concluded that only pH is responsible for the increased rate.

Calcium carbonate, calcium sulfate and a calcium saturated exchange resin are compared in Table 26 for the possible effects of calcium containing minerals on pyrite oxidation rate. The ionic strengths of the solutions

Table 26. Effect of calcium-containing minerals $CaCO_3$, $CaSO_4$ and exchange resin on pyrite oxidation.

Treatment	$[Ca^{2+}]$ mol m^{-3}	pH	Ionic Strength mol m^{-3}	Oxidation Rate[a] pmol m^{-2} s^{-1}
None	0.0	3.42	12.5	19
None	0.0	3.40	11.9	14
Ca-Resin	2.61	3.55	8.91	20
Ca-Resin	2.61	3.59	12.50	14
$CaCO_3$	1.48	7.70	3.87	26
$CaCO_3$	1.40	7.69	3.68	29
$CaSO_4$	14.15	3.62	59.24	16
$CaSO_4$	15.78	3.58	62.59	18

[a]Oxidation rate expressed as pmol(Fe) m^{-2} s^{-1}.

containing the calcium minerals were not adjusted, but

results are compared with controls of similar ionic strength (as $NaClO_4$). Only the $CaCO_3$ appeared to have any effect on oxidation rates, and this is due to the increased pH of the solution.

Cation exchange resins saturated with Ca^{2+} and Na^+ and an anion exchange resin saturated with ClO_4^- were added in separate experiments in amounts such that the exchange capacity of the system would be ten times the expected production of cations or anions. The ionic strengths of the experiments were not adjusted, but results are compared with controls of similar ionic strength in Table 27. None of these amendments appeared to have any effect on pyrite

Table 27. Effect of anion and cation exchange on pyrite oxidation.

Treatment	pH	Ionic Strength mol m^{-3}	$[Ca^{2+}]$ mol m^{-3}	Oxidation Rates pmol m^{-2} s^{-1} Fe	SO_4^{2-}
None	3.42	12.46	0.0	19	27
None	3.40	11.94	0.0	14	24
Na-Resin	3.82	11.29	0.0	13	33
Na-Resin	3.88	11.30	0.0	15	33
Ca-Resin	3.55	8.91	2.61	20	0.36
Ca-Resin	3.59	12.50	2.61	14	0.0
(-)-Resin	3.53	7.24	0.0	18	23
(-)-Resin	3.53	12.35	0.0	21	23

oxidation rates as expressed as iron. The appearance of sulfate did appear to be enhanced in the presence of the Na-resin and supressed in the presence of the Ca-resin. The enhancement may be associated with the fact that 1.27 mmol(SO_3^{2-}) m^{-3} was present in the Na-resin solution, 0.72 mmol m^{-3} in the Ca-resin solution and 0.1 mmol m^{-3} in the control. It is unclear what the interaction between the resin and the sulfur compounds may be in these experiments. The cation exchange resins contain sulfonate functional groups as exchange sites, which may induce polymerization or catalysis of sulfur oxidation.

Hematite which had been washed and allowed to become fully hydrated in 50 mol($NaClO_4$) m^{-3} appeared to have a strong effect on the rate of pyrite oxidation. Measured rates (as iron) were 185 and 188 pmol m^{-2} s^{-1}, compared with control rates of 14 and 19 mol m^{-2} s^{-1}. This is consistent with a mechanism of oxidation involving oxidized iron as the electron acceptor. The rate of oxidation measured as sulfate was less, 41 and 53 pmol m^{-2} s^{-1} compared with 40 pmol m^{-2} s^{-1} in the control. Disulfane disulfonate concentrations were higher in the control at the end of the 262 hour experiment with 0.063 mol m^{-3} in the control compared with 0.036 mol m^{-3} in the hematite experiment. Incomplete digestion of the hematite in the nitric acid digestion (see Appendix A) could cause overestimation of the oxidation rate as iron. The pH of the control and the hematite-amended experiments was approximately 3.4.

Thermodynamics of Pyrite Oxidation

The pe and pH of the solutions in each of the one to two week experiments were measured with a platinum and glass electrode, respectively. When these data are plotted on the pe+pH vs. pH diagram (Figure 30), a constant pe+pH is apparent with a value of 15.2. This may be interpreted in two ways. One is that there is a single solid phase which is controlling the solubility of a redox-active compound over the pH range of interest (Lindsay, 1979). Thermodynamic data for a wide variety of iron-containing compounds (jarosite, natrojarosite, hydrojarosite, iron(III) hydroxide) were compared with the measured pe and pH data. Hydrojarosite solid-solution equilibria best fit the data, although iron(III) hydroxide would also fit well at low pH. These data are compared in Figure 31. This is consistent with the theory of Miller (1980) in which jarosite-iron(III) hydroxide equilibria buffer the pH of acid mine drainage near 4.0. The second way of interpreting the pe+pH constancy is that the platinum electrode may simply be behaving as a platinum oxide pH electrode. A pe+pH of 15.2 would not be unreasonable when compared with the data compiled by Whitfield (1974) and a 1:1 stoichiometric ratio of e^- and H^+ would be expected for a pH electrode.

In an attempt to escape the problems with the platinum electrode, pyrite electrodes were constructed and allowed to

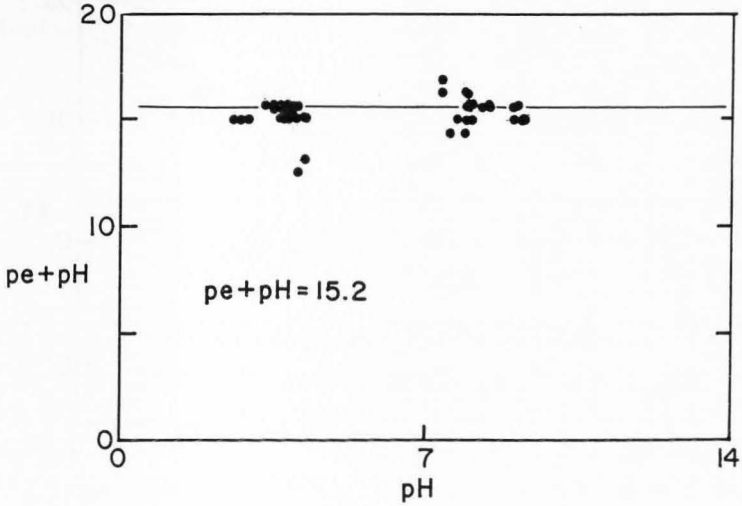

Figure 30. Redox equilibrium diagram: measured pe+pH and pH of all batch experiments.

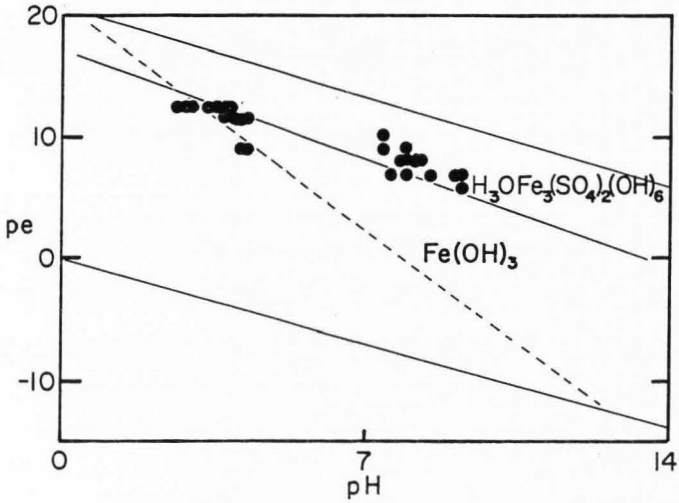

Figure 31. Comparison of measured pe and pH with calculated iron(III) hydroxide and hydronium jarosite redox equilibria.

equilibrate in solutions similar to the solutions used in the experiments with ground pyrite. Potential (pe) measurements vs. solution pH are shown in Figure 32. The platinum electrode behaved as before with a constant pe+pH, suggestive of a platinum oxide pH electrode. The pyrite electrode behaved differently. The e^- to H^+ ratio was 4:3 such that 4pe+3pH was a constant 13.2. None of the equilibrium data tried seem to fit this relation.

The most useful approach to the thermodynamic interpretation of the solution data is to consider the interaction between iron and reduced sulfur compounds. Figure 33 is a highly simplified version of Figure 13, considering only the reactions among disulfane disulfonate, thiosulfate and elemental sulfur. The reaction between iron(III) hydroxide and Fe^{2+} is also superimposed, crossing the disulfane disulfonate/thiosulfate stability boundary at about pH 7. Data for Fe^{2+}, disulfane disulfonate and thiosulfate were used to calculate the pe+pH of the solution. As can be seen in Figure 33, at a given pH the calculated pe+pH for these two redox couples is similar, consistent with the presence of iron(III) hydroxide solid phase, not a jarosite solid phase. This also implies that the system is approaching redox equilibrium. This is an exception to the reservations of Lindberg and Runnells (1984) who doubt the existence of overall redox equilibria in geologically significant systems.

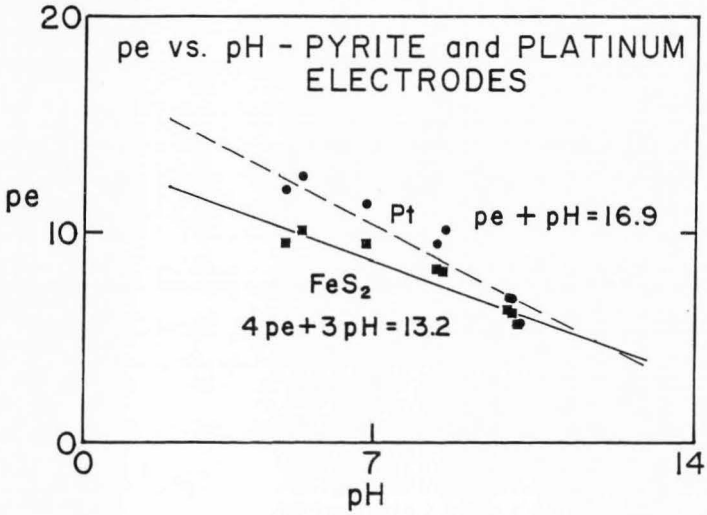

Figure 32. Pyrite and platinum electrode pe measurements versus glass electrode pH.

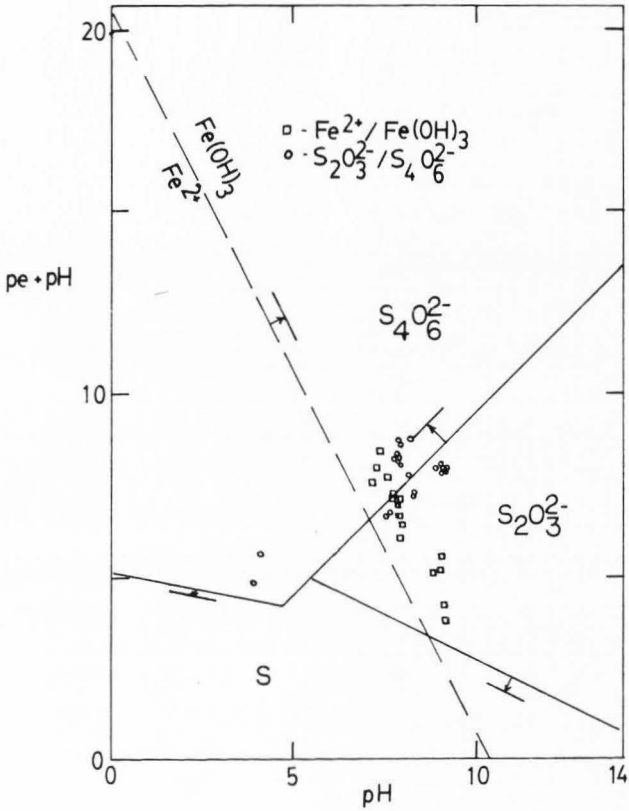

Figure 33. Comparison of measured thiosulfate, disulfane disulfonate, Fe^{2+} and pH with redox equilibria for reduced sulfur compounds and iron(III) hydroxide.

Combining the results of the direct pe measurements at low pH and the calculated pe at neutral and higher pH it is evident that $Fe(OH)_3$ is the iron-containing solid phase which is controlling iron solubility and redox. The reduced sulfur compounds sulfane disulfonate and thiosulfate are also probably contributing to the redox equilibrium of solution iron. It is possible that a redox buffering mechanism may be operating at neutral pH, similar to that proposed by Miller (1980) for iron(III) hydroxide and jarosite at low pH.

Column Studies: The Influence of Calcium Carbonate on Pyrite Oxidation Products

The composition of the effluents from the three columns reflected the sequence of packing of the pyrite and calcium carbonate. Sulfate accumulated in the effluent was scaled by the surface area of pyrite used and the rate shown to vary with time in Figure 34.

Column 2 exhibited very rapid accumulation of sulfate initially, followed by a relatively slow rate. In this column sulfate released from the pyrite was not retained by the $CaCO_3$ (as $CaSO_4$) as it was in the other two columns. Calcium concentrations reflected $CaCO_3$ saturation in the solution before it reached the pyrite. Copper concentrations were very high initially, apparently from soluble salts in the pyrite. Iron was also present in the effluent due to the low pH (4.2).

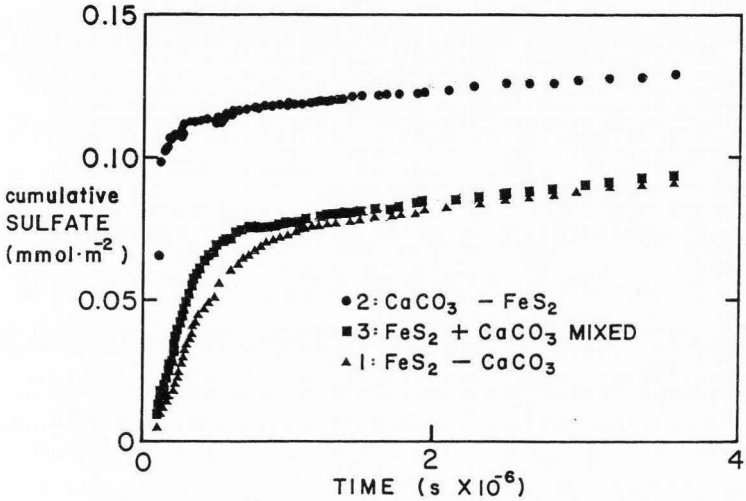

Figure 34. Accumulation of sulfate in the effluents of three columns containing pyrite and calcium carbonate in different sequences.

Column 1 had the lowest initial rate of release of sulfate. Concentrations were apparently influenced by precipitation or adsorption in the $CaCO_3$ layer below the pyrite, although pH and concentrations did not reach those predicted for gypsum saturation. Copper and iron concentrations were also low due to the formation of copper carbonates and iron hydroxides (which were visible). The effluent pH was maintained at 8.2 by the $CaCO_3$ layer.

Column 3 exhibited an intermediate initial rate of accumulation of sulfate, but had the highest rate of accumulation after the initial phase. Like column 1, sulfate, iron and copper were influenced by the $CaCO_3$. Calcium concentrations and the pH of 8.3 do not indicate gypsum saturation, however.

This experiment shows that two reactions are occurring during the leaching process. The first is a rapid dissolution of readily soluble salts which is dependent on pH and the vertical configuration of the pyrite and calcium carbonate layers. This may be a diffusion-controlled reaction, however sulfate data do not fit the first or second laws of diffusion. Rates of production of sulfate and other ions have no relation to the rate of pyrite oxidation.

After the initial release of soluble salts, the only source of additional sulfate is pyrite oxidation. In these experiments this appears as the approximately linear rate of accumulation of sulfate after about a week. This continued until the termination of the experiment after a month. As

predicted by the batch experiments, the highest rate of pyrite oxidation (as sulfate accumulation) during the second phase was found at the highest effluent pH, 8.3, in column 3. The lowest was at pH 4.2 in column 2. Linear rates of sulfate accumulation in the three columns for both the initial dissolution reaction and the second oxidation reaction are shown in Table 28.

The rates of pyrite oxidation based on sulfate are less than those found for the batch experiments. For example, 80 to 120 pmol(SO_4^{2-}) m^{-2} s^{-1} would be expected at pH 8.3 and 30 to 40 pmol(SO_4^{2-}) m^{-2} s^{-1} at pH 4.2. This could be due to interactions with calcium carbonate to reduce the concentration of sulfate in solution, the presence of reduced sulfur compounds in the effluent, or the physical limitations of a packed column compared with an occasionally agitated bottle (batch) experiment.

The rates of accumulation of disulfane disulfonate and thiosulfate were calculated in the same manner as sulfate and are shown in Table 28. As predicted by the pH dependence of the thiosulfate to disulfane disulfonate reaction, disulfane disulfonate accumulated at a much higher rate in the pH 4.2 effluent of column 2 than in the other two columns. The highest rate of accumulation of thiosulfate was in the mixed pyrite-calcium carbonate column 3 at pH 8.3.

Table 28. Rates of production of soluble sulfur compounds in column effluent (Ionic strength=500 mol($NaClO_4$) m^{-1}).

	Column 1	Column 2	Column 3
Sequence:	FeS_2->$CaCO_3$	$CaCO_3$->FeS_2	Mixed
Effluent pH	8.2	4.21	8.3
pmol(SO_4^{2-}) m^{-2} s^{-1}			
first reaction	119	174	183
second reaction	6.9	4.9	7.7
pmol($S_4O_6^{2-}$) m^{-2} s^{-1}			
first reaction	a	2.3	a
second reaction	0.0029	0.18	0.069
pmol($S_2O_3^{2-}$) m^{-2} s^{-1}			
first reaction	0.15	0.022	0.34
second reaction	0.0099	0.00014	0.062

[a] Two reactions could not be distinguished.

Implications for Reclamation of Mine Spoils and Tailings

The rate of pyrite oxidation cannot be calculated directly from the rate of sulfate accumulation from columns as has been suggested by Geidel (1980) and Carrucio, et al. (1981). The error in this analysis is demonstrated in Table 29, which shows the ratios of thiosulfate and disulfane disulfonate sulfur in the effluents from the three columns. When the effluent from pyrite oxidation passed through a $CaCO_3$ layer (column 1), the production of reduced sulfur compounds was least, less than 1%. In the mixed pyrite-$CaCO_3$ (column 3), 5% of the effluent sulfur was present as reduced compounds. In column 2, 12% of the sulfur was present in a reduced form, primarily disulfane disulfonate. This represents a considerable portion of the total reducing potential of the pyrite disulfane.

Table 29. Ratio of reduced sulfur compounds to total sulfur in column effluent.

	Column 1	Column 2	Column 3
Sequence:	FeS_2->$CaCO_3$	$CaCO_3$->FeS_2	Mixed
Effluent pH	8.2	4.21	8.3
S203-S/Total-S	0.00283	0.000051	0.0153
S406-S/Total-S	0.00167	0.125	0.0374
Reduced-S/Total-S	0.00450	0.125	0.0528

Sulfate sulfur is the 100% oxidized state, having released 7 moles of electrons for every mole of pyrite sulfur. Thiosulfate has only released 3 of the 7 moles of electrons and disulfane disulfonate 3.5 moles. Thus, these compounds are only half oxidized and are capable of reducing more oxygen as well as metal oxides in their path. This has been proposed as a mechanism for the formation of roll-type uranium deposits in Wyoming (Goldhaber, 1980). This could also affect the mobilization of toxic metals during the disposal of pyritic mine spoils and mill tailings.

These experiments demonstrated that liming of pyritic materials will increase the rate of oxidation. Soluble, reduced sulfur compounds such as thiosulfate, disulfane disulfonate and sulfite make the analysis of pyrite oxidation products and rates more complex than usually assumed. Analysis of iron oxidation products may be one method of circumventing the analytical problem.

Column studies do not accurately predict the acid potential of pyritic materials, but they may be useful for planning treatment strategies. Burial over a calcareous bed may help mitigate the transport of reduced sulfur compounds. Mixing of calcareous materials with pyritic materials may cause problems due to the increased rate of pyrite weathering at high pH and the production of reduced sulfur compounds.

CONCLUSIONS

Analytical Chemistry

The products of pyrite oxidation include solution phase Fe^{2+}, Fe^{3+}, $S_2O_3^{2-}$, $S_4O_6^{2-}$, SO_3^{2-} and SO_4^{2-}. Other sulfur compounds are certainly present but were not measured in this study. The solid phase product measured in this study was $Fe(OH)_3$. The presence of jarosite compounds at low pH would be consistent with solution equilibrium data.

An accurate description of the thermodynamics, kinetics or microbial catalysis of pyrite oxidation requires that all products and reactants be considered. Sulfate production is not a sufficient indicator of the rate or extent of decomposition of the mineral. The production of solution iron plus solid-phase iron oxide (citrate-bicarbonate extractable) is a more rigorous approach to the extent of reaction.

The importance of the reduced sulfur compounds in pyrite oxidation is out of proportion to their molar concentrations due to the greater reductive capacity of a mole of disulfane compared with a mole of iron(II). Each mole of the pyritic disulfane must lose 7 electrons in oxidation to sulfate, while iron(II) loses only one electron. Soluble reduced sulfur compounds may be important in the mobilization of many toxic metals.

Thermodynamics

The pyrite oxidation reaction never even approached real equilibrium in this study since pyritic residue was left over at the end of every experiment. Metastable equilibrium states were reached, however. These states cannot be eliminated on the basis of the restrictions of the phase rule; neither can they be predicted.

It was found that solution concentration data were consistent with the presence of $Fe(OH)_3$ at low pH and probably also at higher pH. Solution concentration data for the thiosulfate-sulfane disulfonate redox couple were found to be consistent with a redox equilibrium among solution iron and sulfur species at pH 6 to 9.

The distribution of sulfur oxidation products is pH dependent and can be interpreted in terms of a metastable equilibrium among the reduced forms thiosulfate, disulfane disulfonate and sulfite. Thiosulfate and sulfite predominate in the pH range greater than about pH 7 or 8. Sulfane disulfonates are more predominant at more acid pH.

Direct measurement of solution redox potential with the platinum electrode gave results consistent with the iron(II)/iron(III) redox couple in the pH 4 to 5 range. Potentials were in agreement with the equilibrium constants for hydronium jarosite over the entire pH range measured. The accuracy of the platinum electrode at higher pH is questionable, however, as it may respond more to pH changes

than to redox. The pe+pH of the system was observed to be constant, which is consistent with the behavior of a pH electrode.

Pyrite Electrochemistry

The pyrite electrode does not exhibit the potential predicted based on the equilibrium between pyrite and oxygenated water. The higher potentials measured are indicative of greater stability which may be a result of any one of several passivation mechanisms. Iron oxide forming on the surface of the pyrite electrode may become sufficiently thick to impede the diffusion of oxidant (oxygen or Fe^{3+}) to the pyrite surface. Alternatively, a mixed oxidation state iron oxide or reduced sulfur compounds such as thiosulfate may serve as a redox buffer, lowering the redox potential of the solution in the vicinity of the electrode surface. Pyrite oxidation rates were lower in the presence of thiosulfate. Oxidation rates were also reduced in the presence of DTPA, which presumably prevents solution iron from oxidizing, another method of passivation.

Reduced sulfur compounds may also influence the potential of the pyrite electrode. Potentials measured in this study were not consistent with any known iron or sulfur components or phases.

Kinetics

The extent of pyrite oxidation was measured in terms of

iron produced (solution and solid phase) and compared with the sulfur produced. The oxidation rates determined based on iron products were generally higher than those based on sulfur. Reduced sulfur compounds were found to be a significant portion of the sulfur oxidation products.

Linear or zero-order kinetics were found to be sufficient for description of pyrite oxidation in this study. Linear kinetics were observed as electrical conductivity, solution sulfur products and solution plus solid phase iron products.

The rate of pyrite oxidation is pH dependent, increasing from 10 - 20 pmol(Fe) m^{-2} s^{-1} to 40 - 60 pmol(Fe) m^{-2} s^{-1} between pH 5 and 9. This is consistent with an oxidation mechanism which has the reoxidation of solution phase Fe^{2+} via a reaction between an iron hydroxide complex and hydrated oxygen as the rate-determining step. The effect of background electrolytes on oxidation rates at low pH also supports this mechanistic interpretation.

The interactions between pyrite oxidation and various minerals and electrolytes can be related to the pH effect. The effect of calcium carbonate, sodium bicarbonate and calcium-saturated bentonite is to increase pH. Thiosulfate also increases pH as it oxidizes. However, specific interactions between thiosulfate and pyrite or pyrite oxidation products appeared to supress oxidation rates compared with controls at similar pH. The chelate DTPA appeared to have a specific inhibitory effect as well.

Implications

The view that pyrite oxidation is a microbially controlled process is an incomplete one and inaccurate at neutral to high pH. Both the biological and non-biological mechanisms advanced must account for the presence and interactions of the reduced sulfur compounds thiosulfate, the sulfane disulfonates and sulfite.

The reduced sulfur compounds may be important in the reduction and mobilization of toxic metals in soild and groundwater. They may also have a direct toxic effect on plant growth.

The disposal of pyritic mine spoils or tailings must take the production of reduced sulfur compounds into consideration. Mixing with calcareous material may produce the greatest amounts of thiosulfate, which is a good reducing agent for toxic metals. Placing lime below buried pyritic materials may protect groundwater quality more effectively than application of lime to the surface.

LITERATURE CITED

Abel, E. 1956. Uber autoxydation in der schwefelgruppe. Mh. Chem. 87:498-502.

Addison, P. A., S. S. Malhotra and A. A. Khan. 1984. Effect of sulfur dioxide on woody boreal forest species grown on native soils and tailings. J. Environ. Qual. 13:333-336.

Ainsworth, C. C. and R. W. Blanchar. 1984. Sulfate production rates in pyritic pennsylvanian-aged spoils. J. Environ. Qual. 13:193-196.

Alexander, M. 1977. Introduction to Soil Microbiology. John Wiley & Sons, New York.

Arkesteyn, G. J. M. W. 1980. Pyrite oxidation in acid sulfate soils: the role of microoganisms. Plant Soil. 54:119-134.

Baas Becking, L. G. M., I. R. Kaplan and D. Moore. 1960. Limits of the natural environment in terms of pH and oxidation-reduction potentials. J. Geol. 68:243-284.

Bailey, L. K. and E. Peters. 1976. Decomposition of pyrite in acids by pressure leaching and anodization: the case for an electrochemical mechanism. Can. Metall. Q. 15:333-344.

Banister, A. J., L. F. Moore and J. S. Padley. 1968. Structural studies on sulfur species. p. 137-200. In: G. Nickless (ed.) Inorganic sulphur chemistry. Elsevier, Amsterdam.

Barnhisel, R. I., J. L. Powell, G. W. Akin, and M. W. Ebelhar. 1982. Characteristics and reclamation of "acid sulfate" mine spoils. p. 225-234. In: J. A. Kittrick, D. S. Fanning and L. P. Hossner (eds.). Acid Sulfate Weathering. Soil Sci. Soc. Am., Madison, Wisconsin.

Begheijn, L. Th., N. Van Breemen and E. J. Velthorst. 1978. Analysis of sulfur compounds in acid sulfate soils and other recent marine soils. Commun. Soil Sci. Plant Anal. 9:873-882.

Biegler, T. 1976. Oxygen reduction on sulphide minerals part II. relation between activity and semiconducting properties of pyrite electrodes. J. Electroanal. Chem. 70:265-275.

Biegler, T. and D. A. Swift. 1979. Anodic behaviour of pyrite in acid solutions. Electrochim. Acta. 24:415-420.

Biegler, T., D. A. J. Rand and R. Woods. 1975. Oxygen reduction on sulphide minerals part I. kinetics and mechanism at rotated pyrite electrodes. Electroanal. Chem. Interf. Electrochem. 60:151-162.

Bladh, K. W. 1982. The formation of goethite, jarosite and alunite during the weathering of sulfide-bearing felsic rocks. Econ. Geol. 77:176-184.

Blasius, E. and R. Kremer. 1962. Untersuchung der Wackenroderschen reaktion mit hilfe der radiopapierchromatographischen methode. V. Z. Anorg. Allg. Chem. 318:113-121.

Blasius, E. and G. Wermbeter. 1962. Untersuchungen der Wackenroderschen reaktion mit hilfe der radiopapierchromatographischen methode. IV. Z. Anorg. Allg. Chim. 316:251-260.

Bloomfield, C. 1967. Effect of some phosphate fertilizers on the oxidation of elemental sulfur in soil. Soil Sci. 103:219-223.

Bloomfield, C. 1972. The oxidation of iron sulphide in soils in relation to the formation of acid sulphate soils and of ochre deposits in field drains. J. Soil Sci. 23:1-16.

Bohn, H. 1969. The emf of platinum electrodes in dilute solutions and its relation to soil pH. Soil Sci. Soc. Am. Proc. 33:639-640.

Bower, C.A. and F. B. Gschwend. 1952. Ethylene glycol retention by soils as a measure of surface area and interlayer swelling. Soil Sci. Soc. Proc. 16:342-345.

Caruccio, F.T., G. Geidel and M. Pelletier. 1981. Occurrence and prediction of acid drainages. Proc. Am. Soc. Civil Engr. EY1. 107:167-178.

Chen, K. Y. and J. C. Morris. 1972. Kinetics of oxidation of aqueous sulfide by O_2. Environ. Sci. Tech. 6:529-537.

Christiansen, J. A. and W. Drost-Hansen. 1949. Mechanism of decomposition of polythionates and formation of a sulphinic acid. Nature. 164:759.

Cline, J. D. and F. A. Richards. 1969. Oxygenation of hydrogen sulfide in seawater at constant salinity, temperature and pH. Environ. Sci. Tech. 3:838-843.

Cotton, F. A., and G. Wilkinson. 1980. Advanced inorganic chemistry. John Wiley & Sons, New York.

Davis, R. E. 1958. Displacement reactions at the sulfur atom. I. an interpretation of the decomposition of acidified thiosulfate. J. Am. Chem. Soc. 80:3565-3569.

Delahay, P., M. Pourbaix and P. Van Rysselberghe. 1950. Potential-pH diagrams. J. Chem. Educ. 27:683-688.

Elliott, N. 1960. Interatomic distances in FeS_2, CoS_2 and NiS_2. J. Chem. Phys. 33:903-905.

Evangelou, V. P., R. E. Phillips and J. S. Shepard. 1982. Salt generation in pyritic coal spoils and its effect on saturated hydraulic conductivity. Soil Sci. Soc. Am. J. 46:457-460.

Fava, A. and D. Divo. 1953a. Indagini sulla decomposizione delle soluzioni dei politionati mediante zolfo radioattivo.-nota I. decomposizione del tritionato in mezzo alcalino e neutro. Gazz. Chim. Ital. 82:558-563.

Fava, A. and D. Divo. 1953b. Indagini sulla decomposizione delle soluzioni dei politionati mediante zolfo radioattivo.-nota II. decomposizione del tetrationato in ambiente alcalino. Gazz. Chim. Ital. 82:564-566.

Ferrari, M. B., G. G. Fava and C. Pelizzi. 1977. Synthesis and x-ray crystal structure of a bis(2,2'-bipyridyl) trihionatocopper(II) complex. J. C. S. Chem. Comm. 1977:8-9.

Foss, O. 1958. Remarks on the reactivities of the penta- and hexathionate ions. Acta Chem. Scand. 12:959-966.

Foss, O and A. Hordvik. 1964. The crystal structure of sodium tetrathionate dihydrate. Acta Chem. Scand. 18:662-670.

Foss, O. and I. Kringlebotn. 1961. Displacement of sulphite groups of polythionates by thiosulphate. Acta Chem. Scand. 15:1608-1609.

Frost, D. C., W. R. Leeder, R. L. Tapping and B. Wallbank. 1977. An xps study of the oxidation of pyrites in coal. Fuel. 56:277-280.

Garrels, R. M. and C. L. Christ. 1965. Solutions, minerals and equilibria. Freeman, Cooper & Co., San Francisco, California.

Garrels, R. M. and M. E. Thompson. 1960. Oxidation of pyrite by iron sulfate solutions. Am. J. Sci. 258-A:57-67.

Geidel, G. 1980. Alkaline and acid production potentials of overburden material: the rate of release. Reclamation Rev.2:101-107.

Gibbs, J. W. 1961. On the equilibrium of heterogeneous substances. p. 55-371. In: The Scientific Papers of J. Willard Gibbs, Vol. I. Thermodynamics. Dover Publ., New York.

Ginzburg, I. I., Ya. I. Ol'shanskii and V. V. Belyatskii. 1961. Oxidation of sulfides, experimental studies. (In Russian). Trudy Inst. Geol. Rudnykh Mestorozhden., Petrog., Mineral. i Geokhim. 59:1-131. (Chem. Abs. 56:180-181).

Goldhaber, M. 1980. Experimental study of pyrite oxidation at pH 6-9 and 30 C. USGS Open File Report 80-1272.

Goldhaber, M. and R. L. Reynolds. 1977. Experimental study of pyrite oxidation at pH 5-9.5; implications for formation of roll-type uranium deposits. Am. Assoc. Pet. Geol. Bulletin. 61:1379.

Goto, K., H. Tamura and M. Nagayama. 1970. The mechanism of oxygenation of ferrous ion in neutral solution. Inorg. Chem. 9:963-964.

Goto, S. and W. H. Patrick. 1972. Transformation of manganese in a waterlogged soil as affected by redox potential and pH. Soil Sci. Soc. Am. Proc. 36:738-741.

Granger, F. S. and J. M. Nelson. 1921. Oxidation and reduction of hydroquinone and quinone from the standpoint of electromotive-force measurements. J. Am. Chem. Soc. 43:1401-1415.

Grove, J. H. and V. P. Evangelou. 1982. The role of lime in salty spoil genesis. p. 1-4. In: 1982 Symp. on Surface Mining Hydrology, Sedimentology, and Reclamation.

Habashi, F. 1981. Formation and decomposition of thiosulfate in the ferrous sulfide-sulfur dioxide reaction. Inorg. Chem. 20:4027-4028.

Hamilton, I. C. and R. Woods. 1981. An investigation of surface oxidation of pyrite and pyrrotite by linear potential sweep voltammetry. J. Electroanal. Chem. 118:327-343.

Harvard University. 1970. Oxygenation of ferrous iron. FWQA No. 14010-06/69. U. S. Government Printing Office, Washington, DC.

Hoffman, M. R., B. C. Faust, F. A. Panda, H. H. Koo, and H. M. Tsuchiya. 1981. Kinetics of the removal of iron pyrite from coal by microbial catalysis. Appl. Environ. Microbiol. 42:259-271.

Huber, N. K. and R. M. Garrels. 1953. Relation of pH and oxidation potential to sedimentary iron mineral formation. Econ. Geol. 48:337-357.

Ivarson, K. C., G. J. Ross and N. M. Miles. 1982. Microbiological transformations of iron and sulfur and their applications to acid sulfate soils and tidal marshes. p. 57-76. In: J. A. Kittrick, D. S. Fanning and L. P. Hossner (eds.). Acid Sulfate Weathering. Soil Sci. Soc. Am., Madison, Wisconsin.

Jackson, M. L. 1956. Soil Chemical Analysis--Advanced Course. Pub. by the author, Dept. of Soils, Univ. of Wis., Madison.

Kleinman, R. L. P. and D. A. Crerar. 1979. Thiobacillus thiooxidans and the formation of acidity in simulated coal mine environments. Geomicrobiol. J. 1:373-388.

Kostov, I. and J. Minceva-Stefanova. 1982. Sulphide minerals - crystal chemistry, paragenesis and systematics. E. Schweizerbart'sch Verlagsbuchandlung, Stuttgart.

Kwart, H. and K. King. 1977. d-Orbitals in the chemistry of silicon, phosphorus and sulfur. Springer-Verlag, Berlin.

LeRoux, N. W., P. W. Dacey and K. L. Temple. 1980. The microbial role in pyrite oxidation at alkaline pH in coal mine spoil. p. 515-520. In: P. A. Trudinger, M. R. Walter and B. J. Ralph (eds.) Biogeochemistry of ancient and modern environments. Springer-Verlag, Berlin.

Lindberg, R. D. and D. D. Runnells. 1984. Ground water redox reactions: an analysis of equilibrium state applied to Eh measurements and geochemical modelling. Science. 225:925-927.

Lindsay, W. L. 1979. Chemical equilibria in soils. John Wiley & Sons, New York.

Lindsay, W. L. and M. Sadiq. 1984. Use of pe + pH to predict and interpret metal solubility relationships in soils. (Accepted) Sci. Total Environ.

Lowson, R. T. 1982. Aqueous oxidation of pyrite by molecular oxygen. Chem. Rev. 82:461-497.

Lyons, D. and G. Nickless. 1968. The lower oxyacids of sulphur. p. 509-533. In: G. Nickless (ed.) Inorganic sulphur chemistry. Elsevier, Amsterdam.

MacIntyre, W. H., W. M. Shaw and J. B. Young. 1930. The oxidation of pyrite and sulfur as influenced by lime and magnesia-a 12-year lysimeter study. Soil Sci. 30:443-457.

Marøy, K. 1971. The crystal structure of potassium pentathionate hemihydrate. Acta Chem. Scand. 25:2580-2590.

Marøy, K. 1973. Refinement of the crystal structure of trans-dichlorobis(ethylenediamine)cobalt(III) hexathionate monohydrate. Acta Chem. Scand. 27:1705-1716.

McKay, D. R. and J. Halpern. 1958. A kinetic study of the oxidation of pyrite in aqueous suspension. AIME Trans. 212:301-309.

Meyer, R. E. 1979. Electrochemistry of FeS_2. J. Electroanal. Chem. 101:59-71.

Mishra, R. K. 1973. Low temperature surface reactions in leaching of chalcopyrite and pyrite. Ph. D. Thesis. Metallurgy. Univ. Utah.

Miller, S. D. 1980. Sulfur and hydrogen ion buffering in pyritic strip mine spoil. p. 537-543. In: P. A. Trudinger, M. R. Walter and B. J. Ralph (eds.). Biogeochemistry of Ancient and Modern Environments. Springer-Verlag, Berlin.

Mitchell, D. and R. Woods. 1978. Analysis of oxidized layers on pyrite surfaces by x-ray emission spectroscopy and cyclic voltammetry. Aust. J. Chem. 31:27-34.

Moore, W. J. 1972. Physical Chemistry. Prentice Hall. Englewood Cliffs, New Jersey.

Nemeth, K. 1963. Eine photometrische bestimmungsmethode fur sulfationen in bodenlosungen. Z. Pflanzenernahr. Dung. Bodenkunde. 103:193-196.

Nickless, G. 1968. Inorganic Sulphur Chemistry. Elsevier Pub. Co., Amsterdam.

Nor, Y. M. and M. A. Tabatabai. 1977. Oxidation of elemental sulfur in soils. Soil Sci. Soc. Am. J. 41:736-741.

Nordstrom, D. K. 1982. Aqueous pyrite oxidation and the consequent formation of secondary iron minerals. p. 37-56. In: J. A. Kittrick, D. S. Fanning, L. P. Hossner (eds.). Acid Sulfate Weathering. Soil Sci. Soc. Am., Madison, Wisconsin.

O'Brien, D. J. and F. B. Birkner. 1977. Kinetics of oxygenation of reduced sulfur species in aqueous solution. Environ. Sci. Tech. 11:1114-1120.

Peters, E. and H. Majima. 1968. Electrochemical reactions of pyrite in acid perchlorate solutions. Can. Metall. Q. 7:111-117.

Peterson, H. B. and R. F. Nielson. 1973. Toxicities and deficiencies in mine tailings. p. 15-25. In: R. J. Hutnik and G. Davis (eds.). Ecology and Reclamation of Devistated Land, Vol. 1.

Pollard, F. H., G. Nickless and R. B. Glover. 1964a. Chromatographic studies on sulfur compounds part IV. The decomposition of acidified thiosulphate and polythionate solutions. J. Chromatography. 15:518-532.

Pollard, F. H., G. Nickless and R. B. Glover. 1964b. Chromatographic studies on sulphur compounds part V. A study to separate thiosulphate, sulphite and the lower polythionates by anion-exchange chromatography. J. Chromatog. 15:533-537.

Ponnamperuma, F. N. 1972. The chemistry of submerged soils. Adv. Agron. 24:29-96.

Ponnamperuma, F. N., E. Martinez and T. Loy. 1966. Influence of redox potential and partial pressure of carbon dioxide on pH values and the suspension effect of flooded soils. Soil Sci. 101:421-431.

Ponnamperuma, F. N., E. M. Tianco and T. Loy. 1967. Redox equilibria in flooded soils: I. The iron hydroxide systems. Soil Sci. 103:374-382.

Pugh, C. E., L. R. Hossner and J. B. Dixon. 1981. Pyrite and marcasite surface area as influenced by morphology and particle diameter. Soil Sci. Soc. Am. J. 45:979-982.

Pugh, C. E., L. R. Hossner and J. B. Dixon. 1984. Oxidation rate of iron sulfides as affected by surface area, morphology, oxygen concentration and autotrophic bacteria. Soil Sci. 137:309-314

Quispel, A., G. W. Harmsen and D. Otzen. 1952. Contribution to the chemical and bacteriological oxidation of pyrite in soil. Plant Soil. 4:43-55.

Rasnick, A. and F. S. Nakayama. 1973. Nitrochromeazo titrimetric determination of sulfate in irrigation and other saline waters. Comm. in Soil Sci. Plant Anal. 4:171-174.

Sadiq, M. 1977. Use of electron titration to study Fe and Mn in soils. Ph. D. Thesis. Agronomy. Colorado State Univ.

Sato, M. 1960a. Oxidation of sulfide ore bodies, 1. Geochemical environments in terms of Eh and pH. Econ. Geol. 55:928-961.

Sato, M. 1960b. Oxidation of sulfide ore bodies, II. Oxidation mechanisms of sulfide minerals at 25 C. Econ. Geol. 55:1202-1231.

Schmidt, M. and H. Heinrich. 1958. Beitrag zur losung des problems der wackenroderschen flussigkeit. Angew. Chem. 70:572-573.

Schmidt, M. and W. Siebert. 1973. Sulphur. p. 795-933. In: J. C. Bailar, H. J. Emeleus, R. Nyholm, A. F. Trotman-Dickenson (eds.) Comprehensive Inorganic Chemistry. vol. 2. Permagon Press, Oxford.

Schwab, A. P. and W. L. Lindsay. 1983. Effect of redox on the solubility and availability of iron. Soil Sci. Soc. Am. J. 47:201-205.

Schwartzenbach, G. and A. Fischer. 1960. Die aciditat der sulfane und die zusammensetzung wasseriger polysulfidlosungen. Helv. Chim. Acta. 43:1365-1390.

Sillen, L. G. 1952. Redox diagrams. J. Chem. Educ. 29:600-608.

Silverman, J. and R. W. Dodson. 1952. The exchange reaction between the two oxidation states of iron in acid solution. J. Phys. Chem. 56:846-852.

Singer, P. C. and W. Stumm. 1970. Acidic mine drainage: the rate-determining step. Science. 167:1121-1123.

Singh, R. N., W. E. Grube, Jr., R. M. Smith and R. F. Keefer. 1982. Relation of pyritic sadstone weathering to soil and minesoil properties. p. 193-208. In: J. A. Kittrick, D. S. Fanning and L. P. Hossner (eds.). Acid Sulfate Weathering. Soil Sci. Soc. Am., Madison, Wisconsin.

Smith, E. E. and K. S. Shumate. 1970. Sulfide to sulfate reaction mechanism. FWPCA No. 14010 FPS.

Smith, E. E. and K. S. Shumate. 1971. Rate of pyrite oxidation and acid production rate in the field. p. 11-18. In: M. Ahmad (ed.). Proc. Acid Mine Drainage Workshop, Ohio Univ., Athens.

Sorensen, D. L., W. A. Kneib, D. B. Porcella and B. Z. Richardson. 1980. Determining the lime requirement for the blackbird mine spoil. J. Environ. Qual. 9:162-166.

Sposito, G. 1981. The thermodynamics of soil solutions. Oxford Univ. Press, New York.

Steger, H. F. 1977. Oxidation of sulfide minerals, I. determination of ferrous and ferric iron in samples of pyrrotite, pyrite and chalcocite. Talanta. 24:268-270.

Steger, H. F. and L. E. Desjardins. 1978. Oxidation of sulfide minerals, 4. Pyrite, chalcopyrite and pyrrhotite. Chem. Geol. 23:225-237.

Stokes, H. N. 1901. On pyrite and marcasite. USGS Bulletin No. 186. U. S. Government Printing Office, Washington.

Stumm, W. and G. F. Lee. 1961. Oxygenation of ferrous iron. Ind. Eng. Chem. 53:143-146.

Stumm, W. and J. J. Morgan. 1981. Aquatic chemistry. John Wiley & Sons, New York.

Stumm-Zollinger, E. 1972. Die bacterielle oxydation von pyrit. Arch. Mikrobiol. 83:110-119.

Sung, W. and J. J. Morgan. 1980. Kinetics and products of ferrous iron oxygenation in aqueous systems. Envi. Sci. Tech. 14:561-568.

Tamura, H., K. Goto and M. Nagayama. 1976a. Effect of anions on the oxygenation of ferrous ion in neutral solutions. J. Inorg. Nucl. Chem. 38:113-117.

Tamura, H., K. Goto and M. Nagayama. 1976b. The effect of ferric hydroxide on the oxygenation of ferrous ions in neutral solutions. Corrosion Sci. 16:197-207.

Tamura, H., K. Goto, T. Yotsuyanagi and M. Nagayama. 1974. Spectrophotometer determination of iron(II) with 1,10-phenanthroline in the presence of large amounts of iron(III). Talanta 21:314-318.

Tamura, H., S. Kawamura and M. Nagayama. 1980. Acceleration of the oxidation of Fe2+ ions by Fe(III)-oxyhydroxides. Corrosion Sci. 20:963-971.

Taube, H. 1968. Mechanisms of oxidation-reduction reactions. J. Chem. Educ. 45:452-461.

Taylor, G. E. and W. J. Selvidge. 1984. Phytotoxicity in bush bean of five sulfur-containing gasses released from advanced fossil fuel technologies. J. Environ. Qual. 13:224-230.

Temple, K. L. and E. W. Delchamps. 1953. Autotrophic bacteria and the formation of acid in bituminous coal mines. Appl. Microbiol. 1:255-258.

Thom, G. C., P. F. Waters and A. F. Hadermann. 1978. Formation and decomposition of thiosulfate in the ferrous sulfide-sulfur dioxide reaction. Inorg. Chem. 17:1693-1696.

Turner, F. T. and W. H. Patrick, Jr. 1968. Chemical changes in waterlogged soils as a result of oxygen depletion. Trans. Int. Congr. Soil Sci., 9th. 4:53-65.

Uhlig, H. H. 1971. Corrosion and corrosion control. John Wiley & Sons, New York.

Valensi, G. 1973. Electrochemical behavior of sulfur: potential-pH equilibrium diagrams of the sulfur-water system at 25 C, 1 atm. (In French) Centre Belge d'Etude de la Corrosion, Rapports Techniques. 121:207/1-207/22.

Van Breemen, N. 1982. Genesis, morphology and classification of acid sulfate soils in coastal plains. p. 95-108. In: J. A. Kittrick, D. S. Fanning and L. P. Hossner (eds.). Acid Sulfate Weathering. Soil Sci. Soc. Am., Madison, Wisconsin.

Vlek, P. L. G. and W. L. Lindsay. 1978. Potential use of finely disintegrated iron pyrite in sodic and iron-deficient soils. J. Environ. Qual. 7:111-114.

Vlek, P. L. G., T. J. M. Blom, J. Beek and W. L. Lindsay. 1974. Determination of the solubility product of various iron hydroxides and jarosite by the chelation method. Soil Sci Soc. Am. Proc. 38:429-432.

Wackenroder, M. H. 1847. Sur un nouvel acide du soufre. Ann. Chim. Phys. 20:144-162.

Wagner, H. and H. Schreier. 1978a. Investigations on the alkaline degredation of the pentathionate. Phosphorus and Sulfur. 4:281-284.

Wagner, H. and H. Schreier. 1978b. Investigations on the sulfite degredation of polythionates. Phosphorus and Sulfur. 4:285-286.

Weast, R. C. (ed.). 1980. Handbook of chemistry and physics. 60th ed. CRC Press, Cleveland, Ohio.

Weir, R. G. 1975. The oxidation of elemental sulphur and sulphides in soil. p. 40-49. In: K. D. McLachlan (ed.). Sulphur in Australasian Agriculture. Sidney Univ. Press, Sidney.

West, P. W. and G. C. Gaeke. 1956. Fixation of sulfur dioxide as disulfitomercurate(II) and subsequent colorimetric estimation. Anal. Chem. 28:1816-1819.

Whitehead, Alfred North. 1967. The aims of education. Macmillan, New York.

Whitfield, M. 1974. Thermodynamic limits on the use of the platinum electrode in Eh measurements. Limnol. Oceanogr. 19:857-865.

Wyckoff, R. W. G. 1948. Crystal structures. Interscience Publishers, New York.

APPENDICES

Appendix A

Solid Phase Analysis for Oxidized Iron

The oxidation of pyrite results in the formation a new solid phase of oxidized iron, either $Fe(OH)_3$ or a jarosite compound, depending on the solution pH and composition. In order to accurately evaluate the extent of pyrite oxidation, both the solution phase and solid phase iron products must be analyzed. The sodium citrate method of Jackson (1956) is a suitable method for dissolution of both jarosite and $Fe(OH)_3$ without appreciable degredation of the pyrite. Digestion of the sample with concentrated nitric acid on a steam plate, evaporation to dryness and redissolution in 3M HCl is a suitable method of analysis for total iron. Both the sodium citrate extract and $HCl-HNO_3$ digest may be analyzed for iron by standard flame atomic absorption (AA) techniques. Care must be taken to prepare iron standards in sodium citrate as the citrate may interfere with iron absorbance.

The simplest way to express the kinetics of pyrite oxidation is in terms of the conversion of pyritic Fe(II) to solution and solid phase Fe(III). The initial mass of Fe(III) in the system is assumed to be zero. At the end of the experiment, some of the pyritic Fe(II) has been oxidized to Fe(III), hence:

$$[Fe_T] = [Fe(II)] + [Fe(III)] \qquad [1]$$

where Fe_T represents the total iron in the system. Dividing equation [1] by [Fe(II)] results in equation [2]:

$$\frac{[Fe_T]}{[Fe(II)]} = 1 - \frac{[Fe(III)]}{[Fe(II)]} \qquad [2]$$

The ratio [Fe(III)]/[Fe(II)] can be calculated from the digest data:

$$\frac{[Fe(III)]}{[Fe(II)]} = \frac{[Fe_C]}{[Fe_N] - [Fe_C]} \qquad [3]$$

where $[Fe_C]$ represents the iron concentration on a mass basis in the citrate extract plus the total solution iron and Fe_N represents the concentration on a mass basis in the nitric acid extract. By rearrangement and substitution of equation [2] in equation [1], the amount of iron oxidized can be calculated:

$$[Fe(III)] = [Fe_T] - \frac{[Fe_T]}{1 + \frac{[Fe(III)]}{[Fe(II)]}} \qquad [4]$$

This calculation is independent of other sources of Fe(III) in the system, since the total iron concentration is measured. A correction must be made for iron in solution by adding both $[Fe^{3+}]$ and $[Fe^{2+}]$, or total solution iron to the Fe_C term. It is assumed that reduced iron in solution represents pyrite iron which has been oxidized, then reduced in the the autocatalytic, electrochemical oxidation of pyrite by solution iron(III) (Singer and Stumm, 1970).

Appendix B

Calibration of Platinum Redox Electrodes

Redox electrodes were constructed following the suggestions of Ponnamperuma (1972). They consisted of platinum wire fused in one end of a piece of glass tubing containing a mercury contact with copper wire. The electrodes were cleaned regularly with a mild silver polish and stored in an electrolyte solution similar to the experimental solution.

Orion double junction electrodes were used as the standard reference electrode. These electrodes consist of an inner Ag/AgCl electrode with a ceramic junction to an outer sleeve which functions as a salt bridge. The supporting electrolytes were prepared from deionized distilled water using analytical grade chemicals. The inner electrode solution was 3.5 M KCl saturated with Ag ($AgNO_3$ was used). The outer salt bridge solution was 10% KNO_3 (approximately 1 M). The inner electrode solution was replaced at least once each week and the outer salt bridge solution was replaced daily at least several hours before measurements. Most of the drift encountered in using the redox electrode-reference electrode pair could be eliminated by equilibrating the reference electrode with an electrolyte solution similar in ionic strength and composition to the experimental solution.

Ponnamperuma describes two methods for calibration of

the redox electrode-reference electrode pair. The first reference used was a solution 0.0033 M potassium ferrocyanide, 0.0033 M potassium ferricyanide and 0.1 M KCl. This solution contains the Fe(II)/Fe(III) redox couple, which was the same as the experimental redox couple. At 298 K the potential for this solution is 463 mV. This solution must be prepared fresh daily as the iron(II) oxidizes fairly rapidly.

The second reference solution used was a saturated "quinhydrone" suspension in 0.05 M potassium acid phthalate to maintain a pH of 4. Quinhydrone is a mixture of hydroquinone (1,4-dihydroxybenzene) and p-benzoquinone ($C_6H_4O_2$) which dissolves to form a 1:1 mixture in solution. The standard potential for this redox couple is 699.5 mV (vs. the hydrogen electrode, pH = 0). The redox reaction is:

$$\text{p-benzoquinone} + 2\ H^+ + 2\ e^- = \text{hydroquinone}.$$

The potential of the redox couple can be calculated for any pH based on the Nernst equation:

$$E = E^o - 59.2\ pH,$$

where E^o is the standard potential and E is the potential observed at the pH specified. The potentials calculated for pH 4 and 7 are 463 and 285 mV, respectively. Based on the difference between the potential measured in the standard solution using any specific pair of redox and reference electrodes and the potential calculated, the potentials measured in the experimental solutions may be corrected

relative to the standard hydrogen electrode.

The iron(II)/iron(III) reference solution was relatively unstable compared with the saturated quinhydrone suspension. This stability is documented for periods of up to a week in the data of Granger and Nelson (1921). The preparation in pH 4 buffer described here was observed to remain stable for many weeks. The pH dependence of the quinhydrone potential can also be calculated and standards of various acidities may be prepared. For these reasons the saturated quinhydrone suspension was used as the reference standard for most of these experiments.

Appendix C

Photometric Determination of Sulfate

The method of Nemeth (1963) was utilized in which sulfate is determined stoichiometrically as chromate after precipitation of barium sulfate from a barium chromate solution:

$$SO_4^{2-} + BaCrO_4 = BaSO_4(c) + CrO_4^{2-}$$

Barium sulfate is precipitated in the originally acidic solution. The excess barium chromate is then precipitated by raising the pH with ammonium hydroxide, leaving a quantity of chromate in solution stoichiometrically equivalent to the amount of sulfate precipitated as barium sulfate. The resulting solution is relatively stable and absorbance at 436 nm has been shown to obey the Beer-Lambert Law at total sulfate concentrations of 1.0 to 5.6 mmol/L (after dilution by reagents).

This method appears to work very well with sulfate concentrations between 1 and 50 mmol/L (as in gypsiferous soils). It works in the presence of iron(II) in solution, but other reducing agents such as thiosulfate may interfere by reduction of the chromium. It is very important to centrifuge or filter the samples carefully to remove fine

crystals of $BaCrO_4$ before the photometric measurement. Determination by photometric means gives a detection limit of between 0.1 and 1.0 mmol/L, while use of atomic absorption for chromium may extend the detection limit by an order of magnitude.

Reagents.

1. Barium chromate solution (0.1 N). Dissolve 12.66 g of $BaCrO_4$ in 150 ml of 25% HCl. Make to 1 L with distilled water. Note: it may take several hours for the barium chromate to dissolve.

2. Ammonium hydroxide solution. Make a 1:3 dilution of 25% ammonium hydroxide in distilled water.

3. Standards. Use sodium sulfate prepared in the same electrolyte solution used for extraction or distilled water.

Procedure.

1. Pipette 2 to 25 ml of sample into a 50 ml volumetric flask. Prepare standards similarly.

2. Add 10 ml barium chromate solution. Use less if sulfate concentrations are low (less than 1-5 mmol/L). Mix well.

3. Add 5 ml ammonium hydroxide solution. Make to volume with distilled water. Mix well.

4. Any one of three methods may be used to separate the fine, crystalline precipitate from the solution: (a) filter the sample with a fine filter, (b) centrifuge 5 minutes at 3000 rpm, (c) allow the contents of the flask to settle

overnight (followed by atomic absorption analysis of supernatant).

5. Chromium concentrations may be determined in either of two ways: (a) colorimetrically at 436 nm, or (b) measure chromium by atomic absorption.

Correction for thiosulfate and disulfane disulfonate. Thiosulfate will quantitatively reduce chromium(VI) to chromium(III) in this method. The reaction is very rapid, probably complete within an hour, oxidizing thiosulfate to sulfate after the addition of the ammonium hydroxide. An electron balance for the reduction of chromium(VI) by thiosulfate yields 2.67 moles of chromium(III) per mole of thiosulfate:

$$8\ Cr(VI) + 3\ S_2O_3^{2-} = 8\ Cr(III) + 6\ SO_4^{2-}.$$

A series of standard thiosulfate solutions analyzed as sulfate resulted in approximately 2.94 moles chromium (by atomic absorption) per mole of thiosulfate. Hence the 2.67 figure was adopted for correction of sulfate measurements in the presence of thiosulfate.

By analogy, the reduction of chromium(VI) by disulfane disulfonate would yield 4.67 moles of chromium(III) per mole of disulfane disulfonate:

$$14\ Cr(VI) + 3\ S_4O_6^{2-} = 14\ Cr(III) + 12\ SO_4^{2-}.$$

The formula for correction of sulfate measurements in the presence of thiosulfate and disulfane disulfonate is:

$$[SO_4^{2-}]_{corrected} =$$

$$[SO_4^{2-}]_{measured} - 2.6\ [S_2O_3^{2-}] - 4.6\ [S_4O_6^{2-}].$$

VITA

Aaron Donald Brown

Candidate for the Degree of

Doctor of Philosophy

Dissertation: Chemical Weathering of Pyrite in Soils

Major Field: Soil Science

Biographical Information:

Personal Data: Born in Binghamton, New York, on September 29, 1954 to Patricia Louise (Freshour) Brown and Donald Fredrick Brown.

Education: Graduated from Chenango Valley Junior-Senior High School, Binghamton, New York in 1972. Majored in Biology at Oberlin College, near Cleveland, Ohio, graduated with the A.B. degree in 1976. Attended a summer course on ecology at the Marine Biological Laboratory, Woods Hole, Massachusetts in 1976. Completed a Master of Science in Water Resources Science at the University of Michigan, Ann Arbor in the summer of 1977. Attended Utah State University from 1980 through 1984, completed requirements for the Doctor of Philosophy in Soil Science with emphasis in Soil Chemistry.

Professional Experience: Worked both as a research assistant and a teaching assistant in the Department of Soil Science and Biometeorology at Utah State University. Coauthored a laboratory manual Discovering Soils with G. Ashcroft in 1983. Taught English for Science Students and conducted research for the Soil Science and Conservation Department while on a Shansi Fellowship at Chiangmai University in Thailand. Worked as a teaching assistant and tutor in Biology at Oberlin College. Spent several summers as a nature instructor at a scout camp in upstate New York.

Professional Societies: Soil Science Society of America, Soil Chemistry Section; American Geophysical Union, Hydrology Section; American Association for the Advancement of Science, Agriculture Section.

Honors: Award for Excellence for a presentation at the 1984 meeting of the Western Society of Soil Science; Distinguished Service Award in 1983 from the Associated Students of Utah State University and Outstanding Young Man of America in 1983 from the U. S. Jaycees for work with the Graduate Student Association and various campus committees and organizations; President's Fellowship for study at Utah State University in 1981; Shansi Fellowship from the Oberlin Shansi Memorial Association for teaching, study and travel in Thailand from 1977 to 1980; Scholarship from the Biology Department at Oberlin College for summer study at the Marine Biological Laboratory, Woods Hole, 1976; New York State Regents Scholarship, 1972; American History Award from the Daughters of the American Revolution, 1972.